EQUATORIAL PACIFIC SEDIMENT DEPOSITION DURING THE EARLY TO MIDDLE MIOCENE:

CARBON CYCLING AND PROXIES FOR PRODUCTIVITY

A Thesis

by

CHRISTINE MARIE PIELA

Submitted to the Office of Graduate Studies of
Texas A&M University
in partial fulfillment of the requirements for the degree of

MASTER OF SCIENCE

December 2010

Major Subject: Oceanography

Equatorial Pacific Sediment Deposition during the Early to Middle Miocene:

Carbon Cycling and Proxies for Productivity

EQUATORIAL PACIFIC SEDIMENT DEPOSITION DURING THE EARLY TO MIDDLE MIOCENE:

CARBON CYCLING AND PROXIES FOR PRODUCTIVITY

A Thesis

by

CHRISTINE MARIE PIELA

Submitted to the Office of Graduate Studies of
Texas A&M University
in partial fulfillment of the requirements for the degree of

MASTER OF SCIENCE

Approved by:

Chair of Committee,	Mitchell Lyle
Committee Members,	Jack Baldauf
	Franco Marcantonio
	Annette Olivarez Lyle
Head of Department,	Piers Chapman

December 2010

Major Subject: Oceanography

ABSTRACT

Equatorial Pacific Sediment Deposition during the Early to Middle Miocene: Carbon Cycling and Proxies for Productivity. (December 2010)

Christine Marie Piela, B.S., University of Miami

Chair of Advisory Committee: Dr. Mitchell Lyle

The equatorial Pacific is a major region of biological production in the world oceans and an important part of the global carbon cycle. Changes in climate during the Cenozoic (65 Ma to present) have impacted the carbon cycle, and it is important to assess these impacts. This study focuses on the primary productivity of the equatorial Pacific during the early to middle Miocene (24 - 12 Ma) as recorded by Deep Sea Drilling Project (DSDP) Site 574, and investigates the sedimentary components potentially linked to productivity: bio-Ba, bio-SiO_2, C_{org}, $CaCO_3$, and uranium, as well as detrital thorium to estimate clay-bound barium. Within this time frame the plate beneath Site 574 traveled northwesterly across the equator and allows a unique opportunity to monitor changes in productivity and the carbon cycle in this region. It is difficult to determine directly primary productivity from the sedimentary record because the preservation of different proxies for this parameter - C_{org}, bio-$CaCO_3$, and bio-SiO_2, can be highly variable. The variability has many causes, including nutrient recycling in the water column and the depth of the *carbonate compensation depth* (CCD), which prevents the preservation and ultimate burial of plankton debris at the seafloor. To

interpret the production versus deposition rates during the early and middle Miocene, proxies were used in conjunction with direct measurements of biogenic remains. By determining the concentrations of biogenically produced barium (bio-Ba), which is less affected by degradation, it is evident that the mass of C_{org} produced was much greater than that preserved in the sediments. We observed higher deposition of bio-Ba and bio-SiO_2 as the site was transported over the equatorial divergence by plate tectonics, as expected. In contrast, $CaCO_3$, accumulation was low in the divergence region, and coincides with a dissolution event known from other site studies in the equatorial Pacific. The pattern of uranium deposition resembles $CaCO_3$ and C_{org}, and average U concentrations suggest that it was primarily deposited as a trace element in the shell material of biogenic carbonate. C_{org} also resembles $CaCO_3$ and appears to represent primarily a dissolution signal. Total uranium analysis proved to be a useful proxy for C_{org} and $CaCO_3$ preservation, and analysis of detrital thorium (^{232}Th) concentration suggests very limited terrigenous clay input. Comparison of the different proxies reveals carbonate preservation events, changes in C_{org} preservation, and changes in deposition as DSDP Site 574 migrated northwesterly across the equator.

ACKNOWLEDGEMENTS

I would like to thank my committee chair, Dr. Mitchell Lyle, and my committee members, Dr. Franco Marcantonio, Dr. Annette Olivarez Lyle, and Dr. Jack Baldauf for their guidance and for keeping me on track throughout the course of this research. I do tend to waiver along a windy road on the way to the destination.

I also want to extend my gratitude to the National Science Foundation, which provided monetary support for this project through grant OCE-0725301.

I want to thank my friend, Ajay Singh, for his inexhaustible help and facilitation with the HR-ICP-MS portion of my research. It would have been much less exciting by myself in the perchloric hood closet lab.

I want to thank my family for their support, keeping me grounded without limiting me, and always pretending to be interested in whatever project I am involved in, regardless of how boring it sounds when I am talking about it.

Lastly, I want to thank Hugh Keogh for always bringing the “cup half full” attitude.

NOMENCLATURE

Ba	Barium
Bio-SiO_2	Biogenic Silica
C_{org}	Organic Carbon
$CaCO_3$	Calcium Carbonate
CCD	Carbonate Compensation Depth *or* Calcite Compensation Depth
DIC	Dissolved Inorganic Carbon
DOC	Dissolved Organic Carbon
DSDP	Deep Sea Drilling Project
IC	Inorganic Carbon
IODP	Integrated Ocean Drilling Program
Ma	Million Years Ago
MAR	Mass Accumulation Rate
MBSF	Meters Below Sea Floor
PEAT	Pacific Equatorial Age Transect
Th	Thorium (232)
U	Uranium

TABLE OF CONTENTS

Page

LIST OF FIGURES

LIST OF TABLES

1. INTRODUCTION: PURPOSE OF RESEARCH

The primary objective of the research in this thesis is to contribute to the fundamental understanding of how the equatorial Pacific participated in large-scale earth systems between 24 and 12 million years ago. By analyzing sediment cores from the equatorial Pacific, this study provides a comprehensive dataset to clarify and refine the evolution of the carbon cycle and how it is affected by climate change. The dataset will serve as a component of a larger project that aims to improve the climate record during the Cenozoic Era (0-66 Ma).

Climate and carbon cycle shifts are recorded in particulate matter generated at the sea surface that can subsequently be preserved as sediment at the seafloor. The variability of preservation makes it difficult to interpret the surface paleo-productivity from the deep-sea sediment record, so the total flux of multiple independent sediment components must be taken into account to determine productivity trends. Analyses of calcium carbonate and organic carbon in core sediment samples confirm major changes in the Cenozoic carbon cycle through the migration of the *carbonate compensation depth* (CCD). The CCD is defined as the depth at which calcium carbonate ($CaCO_3$) dissolution exceeds $CaCO_3$ deposition, and where no calcium carbonate is preserved. Carbonate solubility increases as pressure increases and temperature decreases, and, if the ocean is deep enough, there is a depth where all carbonate plankton tests will dissolve before burial. Biogenic silica and terrestrial fractions are of interest to determine

---

This thesis follows the style of *Paleoceanography*.

surface productivity in sediments where the biogenic carbonate record is absent, as well as the strength and structure of major zonal winds during the Miocene. During 1982, on Deep Sea Drilling Project Leg 85, a series of 5 sites were drilled in the Central equatorial Pacific. DSDP Site 574 was studied for this thesis to augment the datasets published in the DSDP Initial Reports [Shipboard Scientific Party, Init. Repts. DSDP 574, 1985].

Publication of this DSDP Site 574 (Holes 574A and 574C) research provides a quantitative dataset to the scientific community including the biogenic sediment fraction (organic carbon, calcium carbonate, and biogenic silica, as well as biogenic barium), uranium, terrestrial input, and the climate and carbon cycle changes. Investigation of the biogenic sediment fraction shows how fluxes of biogenic material changed from the Early to Middle Miocene (Figure A1; 23-11.6 Ma) in the sediment record. This record is our primary venue for studying paleo-productivity changes in the equatorial region. In theory, the productivity of surface waters in the past can be inferred by compiling and comparing the accumulation rate values for the biogenic components. DSDP Site 574 data can then be used in comparative analyses with current and future studies in the equatorial Pacific region, including the 2009 Pacific Equatorial Age Transect (PEAT) expedition (IODP Expedition 320/321, [Pälike et al., 2010a, 2010b]), whose sites are located to the east of Site 574 (See IODP Expedition 320/321 Preliminary Report, http://iodp.tamu.edu/scienceops/expeditions/equatorial_pacific.html).

1.1. The Importance of the Carbon Cycle

The carbon cycle is defined as the flux of carbon between all of the earth's zones: the biosphere, pedosphere, geosphere, hydrosphere, and atmosphere. During the 19th and 20th centuries, rapid increase in atmospheric CO_2 has led to intensified research of the carbon cycle, including those specifically aimed at methods for storing carbon in long-term reservoirs. The ocean and the seafloor are major components in the storage of carbon and assimilation of CO_2 from the atmosphere (Figure A2, [Berner, 1999]). The equatorial Pacific is a high production region (Figure A3, [Behrenfeld and Falkowski, 1997]) that plays a major role in global carbon recycling. Highest productivity is confined to a zone within 2° of the equator. Chlorophyll *a* concentrations at the equator reach values > 0.25 mg/m^3 [NASA, 2010], concentrations that are only surpassed by coastal zones. Observations published by McClain [2009] of NASA also illustrate significantly higher concentrations of chlorophyll *a* in the equatorial Pacific, notably during La Nina, when higher winds drive upwelling and eolian transport of continental nutrients [NOAA, 2008].

A second indicator of production is dissolved organic carbon (DOC). DOC in marine and freshwater systems is one of the greatest cycled reservoirs of organic material on Earth. The equatorial Pacific has greater than 70 µmol/kg DOC in surface waters [Hansell et al., 2009], as compared to the Southern Ocean (~ 50 µmol/kg) and the central Pacific at 3,000 m depth (39 µmol/kg). The DOC functions as a food source and productivity indicator as it is leaked from the cells of plankton, and plays a major role in the recycling of global carbon, from absorption of atmospheric CO_2 at the ocean-

atmosphere interface to the deposition of carbon-rich sediments at the seafloor. High DOC at the equator implies high productivity, and it is generally accepted that increased productivity in the surface waters results in increased sequestration of CO_2 from the atmosphere. This relationship is caused by the formation of carbon-rich skeletal and tissue material in phytoplankton and zooplankton in the photic zone, and its sinking below the thermocline.

Sediment cores from Deep See Drilling Project (DSDP) Leg 85, Site 574 were sampled and analyzed to determine the biogenic sediment accumulation rates of the Miocene equatorial Pacific. Site 574 is now located at 04˚ 12.52'N, 133˚ 19.81'W (Figure A 4) in 4561 m of water, and provides a record from the Late Eocene to present. Because of plate tectonic movement of the Pacific plate, Site 574 has transited northwestward from more than 2˚S to its current position. This record of migration allows us to examine the depositional effects of an equatorial crossing during the Miocene.

The transition from the Late Oligocene to the Early Miocene is marked by a climatic shift from a warm late Oligocene to a cooler Miocene, coinciding with a deepened CCD and the Mi-1 glaciation. The climate shift (Figure A5) is evidenced by changes in atmospheric carbon (pCO_2) values, which decreased at the end of the Oligocene approximately 24 million years ago [Pagani et al., 2005]. The carbon cycle requires that a decrease in atmospheric pCO_2 must be mirrored by an increase in carbon in another reservoir, such as the deep ocean (high carbonate deposition). The low pCO_2 levels (260-190 ppmv [Pagani, et al., 1999]) experienced in the early to middle Miocene

signify a cooler climate, which corresponds to the rapid expansion of the East Antarctic ice sheet and organic carbon burial events [Pagani et al., 1999]. Recent work by Kürschner et al. [2008] using plant leaf stomata to estimate paleo-CO_2 in the atmosphere reports values in the Miocene of 300-500 ppmv, dropping slightly lower during the Early Miocene glaciation (Mi-1) and the expansion of the East Antarctic ice sheet (Mi-3/4).

Preservation of organic carbon, biogenic carbonate, and biogenic silica in the sediment serve as indicators for the past, showing the effects of tectonics, productivity, and degradation. However, incomplete preservation can result in a misinterpretation of the paleo-productivity of the equatorial Pacific region. Important marine sediment makers including siliceous diatoms and radiolarians, and calcareous nannofossils, coccolithophores and foraminifera are labile compounds, and may be recycled in the water column or completely dissolved prior to or upon reaching the seafloor [Dymond and Lyle, 1994]. Biogenic silica may be dissolved in the upper sediment layers because it is undersaturated throughout the ocean [Hurd, 1973; Ragueneau et al., 2000]. Carbonate dissolution results from its higher solubility in cold, high pressure, less alkaline water below the lysocline (depth of undersaturation), eventually reaching the *carbonate compensation depth* (CCD). When carbonate materials reach the lysocline they dissolve more rapidly, and eventually the rate of dissolution exceeds the particulate carbonate flux to dissolve all carbonate sediments before burial at the seafloor below the CCD water depth.

It was anticipated that there would be a decrease in organic carbon and calcium carbonate deposition during the early to middle Miocene due to a carbonate dissolution

event, as it has been previously published as a shoaling of the CCD [Lyle, 2003; Lyle et al., 1995]. The dissolution event is explained by shifts in the carbon cycle, as described in the following sections.

1.2. Study Site: DSDP Site 574

Site 574 was cored during DSDP Leg 85, which was the first to collect nearly complete and relatively undisturbed sedimentary records of the past 34 million years by using a hydraulic piston corer in the upper unconsolidated sediments and a rotary corer for the lower, consolidated layers [Mayer et al., 1986]. Site 574 was chosen as the focus of this study because the sediments preserved at this site record the site's migration from south of the equator into the high-productivity belt, and to the site's present location at 4° north of the equator (Figure A4). This sedimentary record provides insight to the productivity of the region from the Eocene through the present, including the equatorial crossing between 16 and 17 Ma. A total of 361 samples from holes 574A and 574C were used in this study, providing depositional data from 119.6 to 353.4 meters below seafloor (mbsf), which equates to approximately 12.2 through 24.3 Ma.

Deep Sea Drilling Project Site 574 was occupied in 1985 over an elongate basement trough [Shipboard Scientific Party, Init. Repts. DSDP 574, 1985]. Four holes were cored: Hole 574 cored from 0 – 206.5 mbsf, Hole 574A cored from 0 - 180.2 m in length (100% recovery) and Hole 574C cored from 194.5 to 525.5 mbsf (58% recovery); Hole B recovered only 9.5 m of core. Sediments from both Holes A and C are dominantly calcareous ooze. Siliceous microfossils are a typical component (2-30%,

Table 1) and make up the majority of the non-carbonate sediment fraction [Mayer et al., 1986].

The variability seen in the record has several causes; nutrient recycling in the water column, a shallow CCD, and inter-pore dissolution in the seafloor all result in the degradation and dissolution of carbonate plankton debris. This variability makes the carbonate sediment component problematic as paleo-productivity proxies. The exact depth of the CCD is determined by temperature, pressure, and seawater chemistry, the last of which is dominantly controlled by the amount of dissolved CO_2 in the water. The solubility of $CaCO_3$ can be explained using the following equation:

$$CaCO_3 + CO_2 + H_2O \rightleftharpoons Ca^{2+}(aq) + 2\ HCO_3^-(aq)$$

Increased CO_2 results in greater dissolution of $CaCO_3$, and increased production of free calcium ions and bicarbonate (HCO_3^-). Increased bicarbonate raises the alkality and works as a pH buffer in the ocean. As more biocarbonate is released into the water by dissolution of compounds like calcium carbonate, the pH value will increase to counteract the acidification caused by dissolved CO_2.

1.3. Hypotheses

Previous research [Rea and Leinen, 1992; Lyle, 2003] point in the direction of a carbonate dissolution event during the Miocene, which resulted in a large decline in the volume of carbonate preserved in the sediments.

The hypotheses of the research plan are as follows:

H_0: External factors affecting productivity have remained the same; therefore productivity remains the same; only tectonic plate movement through the equatorial zone of divergence is affecting the rates of sediment deposition.

- If the null hypothesis is true, the deposition at DSDP Site 574 will represent a pattern of surface production that reflects only the changes in longitude and latitude associated with plate migration.

H_1: The productivity is changing through time due to external factors such as climate change throughout the Cenozoic, Intertropical Convergence Zone migration, upwelling variations, and variable nutrient input levels. Sediment deposition reflects theses external factors as well as the plate movement beneath the equatorial divergence zone.

- If the alternate hypothesis is true, the productivity will illustrate shifts due to not only the migration of the Pacific Plate, but also the effects of air and sea temperature change, as well as wind and current dynamics, in the vicinity of DSDP Site 574.

H_2: Biogenic deposition is affected not only by productivity, but also by degradation and dissolution of organic carbon and carbonate on the seafloor. Therefore, carbonate sediment does not accurately represent productivity in the geologic record due to the shallow CCD during the Miocene [Rea and Leinen, 1992; Lyle, 2003], and microbial degradation.

- Proxies for organic and inorganic carbon will be investigated to provide a more accurate determination of carbonate sediment

deposition than the direct measurement of carbon in the core sediment samples.

2. MANUSCRIPT

2.1 Summary

The equatorial Pacific is a major region of biological productivity in the world oceans and an important part of the global carbon cycle. Changes in climate during the Cenozoic (65 Ma to present) have impacted the carbon cycle, and it is important to assess these impacts. This study focuses on the primary productivity of the equatorial Pacific during the early to middle Miocene (24 - 12 Ma) as recorded at Deep Sea Drilling Project (DSDP) Site 574. It is difficult to directly determine production because of the potential variability of preservation of organic carbon, biogenic carbonate, and biogenic silica in the geologic record. The variability has many causes, including nutrient recycling in the water column and the *carbonate compensation depth* (CCD), varying the preservation of plankton debris at the seafloor. To interpret the production versus deposition rates during the early and middle Miocene, proxies were used in conjunction with direct measurements of biogenic remains. Biogenic SiO_2 and biogenic barium are positively correlated and have higher rates of preservation than C_{org} or $CaCO_3$, and illustrate increased productivity in the equatorial Pacific region. By determining the concentrations of refractory bio-barium (bio-Ba), it is evident that the volume of C_{org} produced was much greater than that which was preserved in the geologic record. Total uranium analysis proved to be a useful proxy for $CaCO_3$ preservation, and analysis of thorium concentration illustrates very limited terrigenous clay input. Comparison of the proxies reveals carbonate and C_{org} preservation events,

changes in production, and changes in deposition as research site DSDP 574 migrated northwesterly across the equator.

2.2. Introduction

The global carbon cycle has been under intense investigation since the realization that atmospheric carbon dioxide (pCO_2) is a major underlying factor responsible for climate change throughout the Cenozoic (65 Ma to present) [Berner et al., 1983]. The equatorial Pacific is a high production region that plays a major role in global carbon recycling. Dissolved organic carbon (DOC) in marine and freshwater systems is one of the greatest cycled reservoirs of organic material on Earth, and serves as an energy source for microorganisms. The equatorial Pacific has greater than 70 μmol/kg DOC in surface waters [Hansell et al., 2009], as compared to the Southern Ocean (~ 50 μmol/kg) and the central Pacific at 3,000 m depth (39 μmol/kg). The DOC functions as a food source and productivity indicator and plays a major role in the recycling of global carbon, from absorption of atmospheric CO_2 at the ocean-atmosphere interface to the deposition of carbon-rich sediments at the seafloor. High DOC at the equator implies high productivity, and it is generally accepted that increased productivity in the surface waters results in increased sequestration of CO_2 from the atmosphere. This relationship is caused by the formation of carbon-rich skeletal material in phytoplankton and zooplankton in the oceans' photic zone.

According to Berner [1999], the export of carbon from the upper ocean currently transfers 4-5 gigatons of carbon to the deep ocean every year, where it may be stored in

the sediment record. However, it is difficult to determine past production and transfer because of the potential variability of preservation of organic carbon, biogenic carbonate, and biogenic silica in the geologic record, which is dominantly controlled by the rain rate of the component and its rate of dissolution. Dymond and Lyle [1994] estimate this relationship in a simple equation:

(1) Rain rate of any particulate component =

Burial rate of that component + Benthic flux

where rain rate is the amount of production that reaches the seafloor, burial rate is that which is preserved, and benthic flux is the dissolution and degradation that occurs at the sea floor but before burial.

The goal of the research presented is to determine to what extent we are able to estimate productivity, and establish how it changed through the early and middle Miocene.

2.3. Study Site

DSDP Site 574 was chosen as the focus of this study because it migrated from south of the equator into the high-productivity belt and sediment bulge, and to its present location at 4° north of the equator during the Miocene (Figure A1). Within the period studied in this paper (12-24 Ma) Site 574 was less than ± 2° of latitude from the equator, or within the equatorial zone proper. DSDP Site 574 was drilled in 1985 and is currently

located at 4°12.52'N, 133°19.81'W in 4561 m of water over an elongate basement trough [Shipboard Scientific Party, Init. Repts. DSDP 574, 1985]. Sediments at Site 574 range in age from Latest Eocene to Holocene. A total of 361 samples from Holes 574A and 574C were used in this study, providing depositional data from 119.6 to 353.4 meters below seafloor, which equates to approximately 12.2 through 24.3 Ma. Both Holes 574A and 574C are dominantly calcareous ooze chalk; siliceous microfossils are a common component (2-30%, Table 1).

The variability seen in the record has several potential causes; variations in productivity, nutrient recycling in the water column, dissolution rates (i.e., CCD depth), and inter-pore dissolution in the seafloor all result in the degradation and dissolution of plankton debris. This variability makes the biogenic sediment component potentially unreliable as paleo-productivity proxies, which is why more refractory sediment components were used as proxies for production in this study.

Several refractory elements have been used to estimate paleo-productivity. Biogenic barium has been used to estimate the carbon export based on findings of previous research [Dymond et al., 1992; Dymond and Collier, 1996; Eagle et al., 2003; Eagle Gonneea and Paytan, 2006; Paytan and Griffith, 2007] and was measured as a proxy for production in this research. Since DSDP Site 574 is geographically far from any terrigenous input, the fraction of barium under consideration is primarily autochthonous. To support this assumption, terrigenous input was calculated using the sediment thorium concentration, which is a proxy for the amount of windblown dust from the continent, or eolian transport (Appendix D). The eolian transport is very low

(dust flux = 0.85 wt. % of sediment sample), but the biogenic barium reaches 9,000 ug/g at the equator in the Middle Miocene, much higher concentrations than what was being deposited by wind. Background levels for barium in sediments normally range from 100 – 3,000 ug/g.

3. METHODS

3.1. Calcium Carbonate and Organic Carbon Analysis

The method for the inorganic and organic carbon analysis is described in Lyle et al., [2000] and is based on the 'difference' method (see below) to calculate $CaCO_3$. Samples were taken from the cores then ground, freeze-dried, and stored in Rubbermaid containers with desiccant to prevent hydration. Total carbon was measured using a UIC, Inc. CM5012 coulometer to measure the CO_2 released when the sediment sample is combusted (Figure A6). Organic carbon (C_{org}) is measured by acidifying samples prior to coulometric analysis to remove the carbonate fraction. The difference between the total and organic carbon fractions represents the inorganic carbon fraction (IC) that can be converted to $CaCO_3$ as the product of: IC *100/12 (assuming no dolomite). Data reported is on per/weight basis.

Organic carbon is measured by adding an excess volume of 10% hydrochloric acid (HCl) to a small known mass of sediment sample in fused quartz glass combustion boats, thereby dissolving the carbonates and releasing their CO_2 prior to analysis. The remainder of the sample is placed in the combustion furnace, providing a quantitative value of the remaining organic carbon through the coulometer.

Reproducibility and precision was confirmed by analyzing every fourth unknown sample in duplicate and by including two independent standards on each run. The average difference between replicates was 0.09 wt. % C for total carbon analyses and 0.002 wt. % C for organic carbon analyses, which is less than 1% and 4%, respectively,

of the average measured values (Avg. total carbon = 10.3 ± 0.94; Avg. C_{org} = 0.05 ± 0.01). Two standards were run prior to each unknown sample analysis: the "Midway in-house standard," and reagent-grade sucrose. The "Midway" standard is a homogenized marine sediment from "W8709A-5BC: 5-20 cm, with an average total carbon content of 2.64 ± 0.02 wt%, *n* = 523, and an average C_{org} value of 0.85 ± 0.01 wt%, *n* = 570. The average total carbon content of Midway measured during the Site 574 analyses was 2.61 ± 0.142 and C_{org} content was 0.84 ± 0.09. Outliers, peaks and troughs in the data were rerun to confirm reproducibility; the average difference between the C_{org} sample repeat runs that did not produce synonymous values was ~0.01 wt%; however, the majority of sample repeats produced synonymous values during analysis. This high level of precision for organic carbon determination is important because the total organic carbon is low in Site 574 sediments, averaging only 0.05 wt%.

3.2. Biogenic Silica Analysis

The Olivarez Lyle and Lyle [2002] method for biogenic silica analysis, modified after Mortlock and Froelich [1989], was used here to determine the concentration of bio-SiO_2 in the sediment samples. The method uses potassium hydroxide (KOH) to digest the biogenic silica of a known quantity of sample; this differs from the Mortlock and Froelich [1989] method, which used sodium carbonate (Na_2CO_3). Olivarez Lyle and Lyle [2002] found that Na_2CO_3 digestion is incomplete and underestimates biogenic silica in sediments because it does not dissolve resistant bio-SiO_2 forms. However, both

methods attack volcanic ash or glass so therefore, overestimate bio-SiO_2 if these components are present in significant quantity.

Using the Hach "Low Silica" Method 8186 and reagents (molybdate, citric acid, and amino acid), the digested biogenic silica in solution reacts, changing the light transparency of the solution by changing the color from clear to blue. Higher silica concentrations result in darker solutions and therefore lower transparency values; the light transparency can then be measured quantitatively using a spectrophotometer. The dataset provided in this research was compiled using a HACH DR/4000 Spectrophotometer.

Solutions of deionized water, potassium hydroxide, a reagent grade Silica standard, and a digested in-house marine sediment standard were analyzed with each set of samples to verify the purity of the water used in reagents, to establish a blank value for the KOH solution, and to check the accuracy of the run. The in-house standard represents a freeze-dried, homogenized marine sediment that is high is biogenic silica: either a radiolarian ooze from Site 1219A (IUPC 1219A) or a diatom ooze from Site 1098 (BSU Site 1098). Summary statistics were established from previous analyses using the HACH method. IUPC Site 1219A in-house standard (n = 52) has an average value of 65.0 SiO_2 by dry weight percent, and a standard deviation of 5.0. The BSU Site 1098 Standard, n = 118, averaged 28.1 SiO_2 weight percent with a standard deviation of 2.25. The average total bio-SiO_2 measured during the Site 574 analyses was 68.2 ± 4.9 for IUPC Site 1219A and 28.2 ± 2.51 for BSU Site 1098 standard. Every fourth unknown sample was run in duplicate to confirm precision and reproducibility; outliers

and peak and trough values were rerun for confirmation and correction. The average difference between unknown replicates was 0.22 wt. % bio-SiO_2, which is approximately 4.4% of the average measured values (Avg. bio-SiO_2 = 4.97 ± 3.3). This data is reported only as bio-SiO_2 and does not account for water content, which means the values reported effectively underestimate the amount present. Mortlock and Froelich [1989] estimate that diatomaceous silica is about 10% water.

3.3. HR-ICP-MS Element Concentration Analysis

Barium, thorium and uranium were analyzed by high-resolution inductively-coupled plasma mass spectrometry (HR-ICP-MS) on the *Element XR* at Texas A&M University. Sediment samples were weighed (approximately ~50 mg) into Savillex Teflon beakers and spiked with appropriate amounts of ^{135}Ba, ^{229}Th, and ^{236}U for isotope dilution analysis. Total sample dissolution was achieved by digestion using a variety of strong acids. First, 1 ml of concentrated trace metal grade perchloric acid ($HClO_4$) with 1 ml of trace metal grade 16M Nitric Acid (HNO_3) was added to the beaker. The beaker was heated to between 190-200˚C until the solution produced dense white fumes. At this point, the solution is covered for 30 minutes to reflux, then 1ml of concentrated trace metal grade hydrofluoric acid (HF) is added and the solution continues to be heated until dense white fumes reappear. The reflux and HF steps are repeated until the solution is clear and the sediment sample is completely dissolved. Once the sample is completely dissolved, 16 M trace metal grade HNO_3 is used to rinse the beaker walls and lid, and the remaining solution is dried to a gel-like state. 1 ml of 16 M HNO_3 is added and the

sample is volumetrically transferred to a 50 ml centrifuge tube and diluted to 50 ml with MilliQ water. The samples are centrifuged for 10 minutes at 1500 rpm to separate any suspended material (rare) from the solution. A second dilution (~1:50) was performed and the sample was ready for analysis by HR-ICP-MS.

Prior to each sample run the HR-ICP-MS was calibrated with a standard calibrating solution from Spex. Standards were not run during the element concentration analyses. Reproducibility was determined by duplicate runs of every fourth sample, and multiple reruns of peak and trough values. The samples representing the equatorial crossing were each analyzed at least three times on separate occasions to confirm that the bio-barium peak during the equatorial crossing was not an anomaly. Sample 574C 1:6, 10-11 cm, averaged 1,773 ug Ba per g sediment with a standard deviation of 144, n = 4; averaged 169 ng U per gram sediment with a standard deviation of 23, n = 3; and averaged 63.9 ng Th per gram sediment with a standard deviation of 5, n = 3.

3.4. Determination of Age Model, Mass Accumulation Rates, and Paleo-latitude

The age model used for this study is based on the chronostratigraphic model developed for the Pacific Equatorial Age Transect (PEAT) expeditions 320/321 using the Lourens [2004] time-scale. Specific magnetic events and biostratigraphic datums are based on the analysis of previous workers and can be referenced in Appendix 1. Only datums referenced specifically from Site 574 Holes A and C were used; datums referenced in other holes drilled at Site 574 were not used because of the offset between the Holes. The stratigraphic depth for each biostratigraphic event is based on the

following. Radiolarian events are from Nigrini [1985]; diatom events are from Barron [1985a], Barron (1985b], and Baldauf [1985]; calcareous nannofossil events are from Gartner and Chow [1985], and Pujos [1985]. The foraminiferal events are from Saito [1985], all published in the DSDP Initial Reports, Volume 85 [1985].

The age for each datum was determined based on the calibrations developed for the PEAT expeditions [Pälike et al., 2010a; Pälike et al., 2010b; Expedition 320/321 Scientists, 2010]. The reliability of each event was determined based on personal communications with B. Wade for foraminifera and J. Baldauf for diatoms. Datums cited from the Mediterranean or Caribbean, or markers without well-defined boundaries, were omitted from the biostratigraphic model due to lack of confidence in the datum and lack of simultaneous geographic occurrence with the same datum in Pacific.

Several biostratigraphic events were omitted from the model due to the lack of a Pacific reference; some datums may have been common in the Atlantic but absent from the Pacific record, most notably after the closing of the Isthmus of Panama at 3 Ma. Atlantic foraminifera references were used when available and if the ages were not obviously inaccurate according to the age vs. depth curve (example: base occurrence *Globiquadrina binaiensis*).

Magnetostratigraphy was determined from Weinreich and Theyer, (1985). A reasonable magnetostratigraphy was only available for the uppermost 10 cores of Hole 574A, from 1.66 Ma through 8.98 Ma due to the low paleomagnetic intensities of the lower sections (the lower record was incoherent).

The age model curve was developed by plotting the published depths of the biostratigraphic and magnetotratigraphic events against the ages referenced in the Integrated Ocean Drilling Program (IODP) Pacific Equatorial Age Transect (PEAT) timescale. Markers for each biostratigraphic group as well as the magnetostratigraphy were plotted separately to allow for discrimination between groups (Figure A7). For stratigraphic markers with a depth range, the average depth was plotted against the specified age.

The upper and lower limits (first and last occurrences) as well as the average depths were plotted to build an accurate age versus depth plot to use when determining the mass accumulation rates for Holes 574A and 574C. Several curves were tested prior to selecting the curve of best fit. Finally, a 9^{th} degree polynomial curve was fitted to the data and used to extrapolate ages from given depths in the cores. The interval of interest (12 -24 Ma) lies well within the bounds of the fitted age/depth model (0 - 30 Ma) so errors that often occur at the extreme limits of polynomial curves should not be present.

Determination of Mass Accumulation Rates

Formula: $MAR = SR \bullet D_{bulk}$

Sedimentation Rate (SR)

Dry Bulk Density (D_{bulk})

SR = depth/time [cm/kyr]

D_{bulk} = [$g/cm^2/kyr$]

Dry bulk density was determined using the wet bulk density measurements DSDP Leg 85 Site 574 shipboard Gamma Ray Attenuation (GRAPE) data, published online at the

National Geophysical Data Center (NGDC) website: http://www.ngdc.noaa.gov/mgg/geology/seadas.html [NOAA, 1985]. Dry bulk density was estimated by the linear correlation between wet and dry bulk density shown by the physical properties measurements [Shipboard Scientific Party, Init. Repts. DSDP 574, 1985].

The sedimentation rate is a linear relationship expressing the amount of sediment deposited (m) per unit time (yr). The sedimentation rate was determined using the biostratigraphic data previously discussed.

The mass accumulation rate (MAR) compensates for changes in porosity and grain density differences by calculating the mass of sediment deposited per unit area and unit time. The mass accumulation rate was averaged in 0.5 m.y. intervals to provide an average accumulation rate that is in line with the quantity of age determination and to expedite the interpretation of data for the reader (Table 1). The complete data set is available at the NCDC paleoclimatology site: http://www.ncdc.noaa.gov/paleo/paleo.html.

Paleo-latitude was determined by calculating a polynomial equation relating the reported latitude for specific core positions published by Lyle, [2003] to the core depths for Site 574, Holes 574A and 574C. Lyle [2003] calculated these positions based on the migration of the tectonic plate using fixed hot spot positions. These calculations were found to be relatively accurate for the Neogene based on the position of the equatorial sediment bulge.

4. RESULTS

The sum of each component measured, as listed in Appendix D, is not equal to 100%. This could be due to several factors, including partial dissolution of biogenic silica (resistant radiolarians and diatoms) resulting in the under-estimation of that sediment fraction. The bio-SiO_2 is consistently underestimated in the sediment fractions presented in this dataset. The salt fraction is also omitted from Appendix D, but since sediment samples were not washed, salt contributes to approximately 1% of the total sediment fraction. The clay faction represents a variable amount of each sample on average, and is discussed in greater detail in the thorium section of this paper.

4.1. Sedimentation and Mass Accumulation Rates

Site 574 sedimentation rates can be divided into 4 average sections: 0 – 5.5 Ma: 0.51 cm/kyr, 5.5 – 12 Ma: 1.29 cm/kyr; 12 – 22.4: 2.07 cm/kyr; and 22.4 – 30 Ma: 1.67 cm/kyr. The highest rates of sedimentation occur in the equatorial region, when the Site 574 paleoposition migrated between 1.75°S and 0.75°N (Figure A8; Appendix B). The higher rates of sediment accumulation in this zone imply higher productivity than at other latitudes. This illustrates that Site 574 did migrate through a high-productivity belt.

4.2. Thorium

Thorium in the sediment studied here is derived entirely from windblown crustal material (dust) that is delivered by upper-level winds. Concentrations in DSDP Site 574 cores range from 25 ppb to 350 ppb (Appendix D), with mass accumulation rates

peaking just below 400 ng/cm^2/kyr (Figure A9). It is possible to estimate the amount of alumnosilicate assuming that the average thorium concentration of the upper continental crust is 10.7 ppm [Taylor and McLennan, 1985]. By this estimate, the concentration of thorium in Site 574 samples ranges from about 0.02 ppm to 0.40 ppm; detrital crustally derived dust particles make up <1% up to 4.5% of the sample weight. Such low eolian fractions are typical of present-day sediments of the equatorial Pacific far from continental margins [e.g. Anderson, 2006; McGee et al., 2007]. There is a general pattern of higher dust flux after 18 Ma. The highest percentages of terrigenous input are recorded in a narrow equatorial zone (0.25°S to 0.75°N, Appendix D – Master Datalist), but the concentrations are highly variable, most likely due to variations in zonal wind strength. A weather pattern similar to modern La Nina may have been strengthening zonal winds, or thermal gradients from polar ice formation could intensify wind belts.

4.3. Barium

Biogenic barium is generally a reliable proxy for productivity because ≈ 30% of barium is preserved in the sediment record, as opposed to biogenic silica (≈ 5%) and organic carbon (<1%) [Dymond et al., 1992]. Barium is a reliable proxy for productivity in this region because there is little to no dilution from terrestrial input and the environment is not reducing. Sulfate (SO_4) is not being reduced and $BaSO_4$ (barite) is no being dissolved and remobilized in the sediment column.

Unfortunately the Leg 85 Shipboard Party did not measure pore water SO_4; however, we can estimate porewater SO_4 by comparing alkalinity profiles to those of the

PEAT drilling. The alkalinity concentration curve published in the Leg 85 shipboard data volume [Shipboard Scientific Party, Init. Repts. DSDP 574, 1985] shows that the sulfate concentration (as derived from the sediment alkalinity) was high enough throughout the core for barite to be preserved in the subsurface (Figure A10a). Sulfate can be inferred from the sulfate and similar alkalinity porewater profiles of the IODP equatorial Site U1337 at the same latitude to the east. Figure As 10b and 10c indicate similar alkalinity produced by reduction of C_{org}, and a sulfate-rich environment, with only a 10% reduction of porewater SO_4 from seawater.

The strong correlation between the total barium concentration and the calcium carbonate (Figure A11) shows the dissolution of calcium carbonate in relation to barium. The R^2 value (0.68) shows there is a direct negative correlation between $CaCO_3$ and barium concentration, and shows that much of the variation in $CaCO_3$ is caused by dissolution. Total barium concentration could potentially be used to estimate the dissolution of $CaCO_3$.

4.4. Biogenic Silica

Biogenic silica values show less variability of degradation than calcium carbonate and less total degradation than organic carbon. The non-carbonate component of the cores is almost entirely biogenic silica [Mayer et al., 1986]. Bio-SiO_2 values strongly correlate with total barium values ($R^2 = 0.5$, Figure A12), indicating high productivity in the surface waters, which is mostly attributed to Miocene diatom expansion [Falkowski et al., 2004; Kidder and Gierlowski-Kordesch., 2005; Rabosky

and Sorhannus, 2009]. The increase in biogenic silica in the world oceans coincides with increases in $\delta^{18}O$ values, noted as "Oi" and "Mi" events on Figure A 5. Progressive cooling during the Miocene led to a turnover in diatom assemblages, and the Monterey Event recorded near 17 Ma [Barron, 1992].

4.5. Calcium Carbonate and Organic Carbon

Appendix B contains the C_{org} and $CaCO_3$ total weight percentages and their mass accumulation rates (MAR) for Site 574. The high production in the equatorial region of the Pacific is evidenced by the high MARs of the components (Figure A12) between 1.25°S and 0.2°S, but at the equator there is a drastic drop in the MAR of both C_{org} and $CaCO_3$. The decline in carbon compounds is not mirrored by the SiO_2 and total barium mass accumulation rates, which follow changes expected of a traverse of the equatorial region. The decreases of C_{org} and $CaCO_3$ are assumed to be the artifact of a dissolution event, which selectively removed carbonate and organic carbon.

4.5.1. Sediment Dissolution

Carbonates are extremely susceptible to mineralogical and textural change, cementation, and dissolution, which can occur at any time from production to initial burial and then deep burial. The reduction of preservation of calcium carbonate and organic carbon as illustrated in Table 1 indicate either a) lack of production or b) lack of preservation. Modern estimates of equatorial Pacific production (~ 2 -3 g $CaCO_3/cm^2/kyr$] using sediment traps [Dymond and Lyle, 1994; Honjo et al., 1995] and chlorophyll concentration data indicate high surface production in the equatorial Pacific,

and, therefore, sediment deposition rates should follow suit. One factor potentially reducing the volume of calcium carbonate and organic carbon preserved includes dissolution by a shallow CCD. During the Miocene the lysocline in the South Pacific shoaled by 500 m, to an estimated depth of approximately 3,700 m [Rea and Leinen, 1992]. Data reported in this work suggests that the lysocline was even shallower in the equatorial region.

Estimated depth at the time of deposition based on models built by Sclater et al., [1985] for other DSDP Sites in the region indicate that Miocene water depth was shallower than present day. Site 77, located approximately 3° south of DSDP Site 574, was 559 m shallower than it is today, but still below the Miocene elevated CCD. Using the estimates from Sclater et al., [1985], Site 77 was 14% shallower, so Site 574 crust may have been approximately 3965 m below sea level when it crossed the equatorial region. Based on the Rea and Lyle [2005] method for depth backtracking, the depth for Site 574 would have been approximately 4170 m at 17 Ma, more than 400 m below the lysocline as estimated by Rea and Leinen [1992].

4.5.2. Sediment Degradation

Degradation throughout the water column and on the seafloor via consumption and recycling by plankton and benthic organisms including bacteria is a key factor in the rate of sediment degradation and remineralization. The rates of remineralization of C_{org} are dominantly controlled by the input rate; continental margins, for example, generally have higher rates of preservation than open ocean regions because of high production and very high sedimentation rates of clays, which can lead to anoxic porewaters and

occasionally anoxic bottom waters. Because the sediment in the open ocean is deposited on a particle-by-particle basis, the water-seafloor interface cannot be buried rapidly enough to become anoxic, and deep-sea circulation also prevents anoxia. The metabolic pathways in oxygenated versus anoxic environments play a role in the rate of C_{org} recycling [Canfield, 1994]. Anoxic seafloor environments preserve more C_{org} than oxic environments because they lack bioturbation and the faster oxic metabolic pathways. Organic carbon preservation is sensitive to sedimentation rate, C_{org} flux, and bottom water oxygen concentration [Rabouille and Gaillard, 1991], so several factors have to be taken into consideration. Site 574 experienced oxic bottom water conditions, which would promote multiple types of degradation through oxygen-metabolizing pathways. The oxic conditions are assumed from the presence of benthic foraminifers and reworked nannofossils, inferring burrowing and reworking of the sediment after deposition. A high proportion of nannofossils, specifically discoasters, were reported as being reworked at Site 574, including the lower Miocene [Shipboard Scientific Party, Init. Repts. DSDP 574, 1985].

4.6. Uranium

Uranium concentration [ng/g] and mass accumulation rates [ng/cm^2/kyr] strongly correlate with the calcium carbonate, and to a slightly lesser degree with the organic carbon. In McManus et al., [2004], uranium demonstrated a linear relationship with $CaCO_3$ rain rate in the Pacific. Mo et al. [1973] observed a direct proportionality

between the percentage of C_{org} and uranium in sediments deposited in several different environments, and the same for calcium and uranium in manganese nodules.

Organisms that form tests out of calcium carbonate incorporate the uranium, which sinks with the $CaCO_3$ when the organisms die. As they are recycled and dissolved through the water column or on the seafloor, the uranium is put back into the nutrient cycle rather than being preserved in the geologic record. This illustrates the potential for uranium accumulation rates to be used as a proxy for calcium carbonate processes (Figure A13).

Site 574 has uranium concentrations of less than 1000 ng/g, which are similar to data on foraminifera collected by Mo et al. [1973] (Figure A 14). Even though the dominant calcium carbonate producers in DSDP 574 sediment are calcareous nannofossils (discoasters are the most common [Shipboard Scientific Party, Init. Repts. DSDP 574, 1985]), foraminifers are also an important carbonate component. In several sections of Hole 574A, almost 100% of the sand-sized fraction (> 63 μm) is planktonic foraminifers [Shipboard Scientific Party, Init. Repts. DSDP 574, 1985]. The dissolution of sediment makers like foraminifera results in the release of uranium back into the seawater, rather than preservation in the deep-sea sediments. As mentioned in section 4.5.2., the oxic seafloor allows for the degradation of organic carbon at the seafloor. Where bioturbation or reworking are present, even buried material that would be preserved is remineralized and put back into the cycle.

5. DISCUSSION AND CONCLUSIONS

5.1. Discussion

The low preservation rates of C_{org} and $CaCO_3$ during the crossing of the equator in conjunction with the low uranium burial rates indicate that calcium carbonate and organic carbon were subjected to severe dissolution and degradation either throughout the water column, on the seafloor, post-burial in the bioturbation zone, or a combination of the three. An elevation of the CCD would have resulted in increased dissolution of carbonate skeletal material when DSDP Site 574 was located between approximately 0.25°S and 0.25°N. This interval has an age estimate between 15.5 Ma and 17.5 Ma, which corresponds with the warm mid-Miocene climatic optimum (Figure A 5), a period of high atmospheric pCO_2 levels and high dissolved CO_2 in the oceans.

A lack of surface production is not what is causing the $CaCO_3$ deficiency in the sediment record, as evidenced by the high deposition of bio-Ba and bio-SiO_2 across the equator. Calcareous production rates increase and decrease relative to bio-SiO_2 production, as observed in the modern equatorial region derived from sediment traps [Dymond and Collier, 1988] and satellite data [NOAA, 2010]. High modern productivity at the equator is clearly illustrated by the NOAA Aqua-MODIS satellite measurements for chlorophyll *a* peak in the equatorial Pacific region (Figure A15). It is expected that the majority of plankton should follow a similar high productivity pattern in normal environmental conditions; however, the early Miocene carbonate anomaly at 17 Ma remains even though the diatom population booms at the equator.

During modern periods of low nutrient input, like ENSO phases, competition for valuable nutrients in the photic zone between primary producers is high. Sediment trap data from Dymond and Collier [1988] illustrates the variability between euphotic producers. I am assuming that equatorial currents during the Miocene were similar to today's to make a comparison of production in the photic zone during nutrient-limited periods. Diatoms appear to be more successful than calcareous organisms in eutrophic environments [Dymond and Lyle, 1985] based on biogenic opal to calcium carbonate ratios determined from sediment trap data and plankton surveys. During the 1983-84 ENSO event, bio-SiO_2 production increases in a shear zone developed in oligotrophic waters at 10°N but calcareous production is higher at the equator, where upwelling is suppressed [Dymond and Collier, 1988]. Biogenic component sediment flux by weight is nearly cut in half during El Niño periods compared to normal meteorological conditions between 1883 m and 1895 m water depth. (This sediment trap depth was chosen for the productivity comparison because it is deep enough to be exempt from surface variability, but not deep enough to be affected by the lysocline or carbonate dissolution.) Diatoms may have out-competed the calcareous producers 16 million years ago, but that does not single-handedly account for the large removal of calcareous producers, the degradation of foraminifera in Site 574 cores, or the increase in bio-barium at the equatorial crossing.

Honjo et al. [1995] equatorial Pacific sediment trap data between 1992 and 1993 also supports the positive correlation between $CaCO_3$ and bio-SiO_2 (Figure A 16). Both $CaCO_3$ and bio-SiO_2 rain rates increase and decrease together. Assuming Miocene primary production followed the same pattern as modern primary production, the

increase in bio-SiO_2 at the equatorial crossing seen in Site 574 should have been mirrored by a $CaCO_3$ increase. If the siliceous plankton were displacing calcareous organisms, the expected relationship would be an inverse correlation between calcium carbonate and biogenic silica, not seen in the Honjo et al. [1995] dataset. is not true. If there were a drastic drop in calcareous production it should also be illustrated in the biogenic silica record.

The mid-Miocene climate optimum was a very warm period with high atmospheric CO_2 concentrations (>240 ppm [Pagani et al., 1999]). The high atmospheric pCO_2 resulted in higher dissolved CO_2 in the world oceans, leading to acidification, like the situation we see in the oceans today. The total concentration of the carbonate ion (CO_3) is equal to the total alkalinity (TA) of the ocean minus the dissolved inorganic carbon (DIC), or: $[CO_3] = TA - DIC$. The rate that inorganic carbon (DIC) is stored in reservoirs, like the seafloor, controls the concentration of carbonate ions and ocean pH. If more inorganic carbon, like dissolved CO_2, is introduced to the system, the alkalinity (TA) has to increase to keep the system in equilibrium, therefore the total concentration of carbonate $[CO_3]$ ions also increases. The result of higher dissolved CO_2 would have been a shoaling of the CCD to balance the increasingly acidic pH with bicarbonate (HCO_3), which is exactly what is illustrated by this dataset. The low carbonate relative to the increased biogenic silica dilute indicate a shoaling of the CCD at 17 Ma resulting in the poor preservation of $CaCO_3$ and C_{org} during the warm mid-Miocene climate optimum shown by this data. DSDP Leg 85 Initial Reports [1985] also notes the poor preservation of planktic foraminifers found in Site 574 during this time period relative to

the rest of the record. This proves that the production was taking place in surface waters, but preservation, even of larger consumers, was a problem for calcareous organisms.

Increased diatom productivity at approximately 17 to 17.5 Ma correlates with the Monterey Event Hypothesis (depending on which timescale is referenced). Increased zonal wind, as mentioned in section 4.2, would have increased upwelling [Ingle, 1981; Barron and Baldauf, 1989; Chang et al., 1998] and terrestrial input, since thorium and terrestrial input increase at 17 Ma (Figure A9). The terrestrial input would likely increase eolian silica deposition and iron concentration, increasing productivity in a silica and iron-limited ecosystem. More available nutrients and building material for siliceous microorganisms from upwelling and windblown deposits would increase overall productivity. The increased intensity of wind-driven currents must have increased throughout the Miocene, as evidenced by the increasing thorium concentration values that signify stronger winds, and the same is true for upwelling [Berger, 1981; Vincent and Berger, 1981]. Increased equatorial upwelling is reflected in the diatom and biogenic silica record in the data reported here as well as other research sites (DSDP Site 216 [Vincent et al., 1985]).

The end of mid-Miocene climatic optimum at 14 Ma is coincident with the increase in $\delta^{18}O$ values from 2‰ in the Lower Miocene to 3‰ in the Upper Miocene (Figure A 5), which was a result of the drop in atmospheric CO_2 values, average global temperature and the formation of Antarctic ice sheets [Savin et al., 1975; Shackleton and Kennett, 1975; Wright and Miller, 1992; Flower and Kennett, 1993]. The oxygen isotope change is measured benthic foraminifera, which may have been independently caused by

bottom-water cooling [Matthews and Poore, 1980]. The water was very cold (3‰ $\delta^{18}O$ is approximately equivalent to 5°C [Vincent and Killingsley, 1985] at the depth of DSDP Site 574 sediment deposition. The planktonic and deep-water foraminifera do not reflect such a drastic shift in $\delta^{18}O$ values, meaning deeper waters were colder than surface waters and infers a steepened equatorial Pacific thermocline. The growing Antarctic ice shelf was creating a more drastic thermal gradient between the poles and the equator, so a steeper thermocline in the water is not far-fetched. The atmospheric temperature gradient is most likely the driving force behind the changes zonal wind patterns, as illustrated by the changing clay fraction, which increased and was highly variable during the Miocene.

5.2. Conclusions

Direct measurement of organic carbon and carbonate in deep-sea sediments are not always reliable proxies for ocean productivity. Refractory compounds and elements, such as total barium, can be used as proxies to provide a more reliable estimate of productivity in the event that biogenic sediment is not preserved in the geologic record. Total uranium could potentially be used as a proxy for $CaCO_3$ burial. Determining the volume of terrestrial input by using proxies such as sediment thorium concentration can strengthen these productivity and preservation proxies.

Direct measurement of biogenic sediment components and refractory elements reflect a dissolution event that took place in combination with an increase in productivity during the time that DSDP Site 574 crossed the equator between 15 and 18 Ma. The

biogenic silica and barium signals confirm that the production was taking place in the surface waters, but the conditions were not favorable for preservation of $CaCO_3$ and C_{org}, were not entirely preserved (Figure A 17, A 18). This reduction of $CaCO_3$ preservation at Site 574, also found at other equatorial Pacific sites, signals that there was a significant dissolution event, most likely caused by increased atmospheric CO_2 penetration into the oceans. The higher pCO_2 values resulted in increased CO_2 sequestration, which lowered oceanic pH. Low oceanic pH values trigger a shoaling of the carbonate compensation depth, putting more carbonate, DOC, and DIC in solution in an effort to neutralize the pH. The shoaling of the CCD did not have an affect on bio-Ba or bio-SiO_2, which is why they illustrate a factor of 2 increase in production in the equatorial region during the Miocene at DSDP Site 574 while the C_{org} and $CaCO_3$ do not. Increase in biogenic silica and barium mass accumulation rates coupled with decreased C_{org} and $CaCO_3$ indicate equatorial Pacific production was affected by several variables including tectonicism, climate change, zonal wind and terrestrial nutrient fluxes, as well as intense dissolution.

REFERENCES

Anderson, N. J. (2006), Linking palaeoenvironmental data and models to understand the past and to predict the future, *Trends in Ecology & Evolution, 21*, 696-704, doi: 10.1016/j.tree.2006.09.005.

Baldauf, J. G. (1985), A high resolution late Miocene-Pliocene diatom biostratigraphy for the eastern equatorial Pacific, *DSDP Init. Repts*, *85*, 457-476, doi:10.2973/dsdp.proc.85.109.1985.

Barron, J. A. (1985a), Late Eocene to Holocene diatom biostratigraphy of the equatorial Pacific Ocean, Deep Sea Drilling Project Leg 85, *DSDP Init. Repts*, *85*, 413- 456, doi:10.2973/dsdp.proc.85.108.1985.

Barron, J. A. (1985b), Diatom paleoceanography and paleoclimatology of the central and eastern equatorial Pacific between 18 and 6.2 Ma, *Init. Repts. DSDP*, *85*, 935-946, doi:10.2973/dsdp.proc.85.131.1985.

Barron, J. A., and J. G. Baldauf (1989), Tertiary cooling steps and paleoproductivity as reflected by diatoms and biosiliceous sediments, *Productivity of the Ocean: Present and Past*, edited by W.H. Berger, V.S. Smetacek, and G. Wefer, pp. 341-354, John Wiley and Sons, New York.

Barron, J. A. (1992), Neogene diatom datum levels in the equatorial and north Pacific, in *Centenary of Japanese Micropaleontology*, edited by K. Ishizaki and T. Saito, pp. 413-425, Terra Scientific Publishing Company, Tokyo.

Behrenfeld, M.J. and P.G. Falkowski (1997), Photosynthetic rates derived from satellite-based chlorophyll concentration, *Limnology and Oceanography*, *42*, 1-20.

Berger, W. H. (1981), Paleoceanogrphy: The deep-sea record, *The Oceanic Lithosphere: The Sea*, 7, edited by C. Emiliani, pp. 1437-1519, Wiley Interscience, New York.

Berner, R. A., and A. D. Lasaga and R. M. Garrels (1983), The carbonate-silicate geochemical cycle and its effecton atmospheric carbon dioxide over the past 100 million years, *Am. J. Sci., 283*, 641-683.

Berner, R. A. (1999), A new look at the long-term carbon cycle, *GSA Today*, *9*, 1-6.

Canfield, D. (1994), Factors influencing organic carbon preservation in marine sediments, *Chemical Geology*, *114*, 315-329, doi:10.1016/0009-2541(94)90061-2.

Chang, A. S., K. A. Grimm, and L. D. White (1998), Diatomaceous sediments from the Miocene Monterey Formation, California: A lamina-scale investigation of biological, ecological, and sedimentary processes, *PALAIOS*, *13*, 439-458.

Dymond, J. and M. Lyle (1985), Flux comparisons between sediments and sediment traps in the eastern tropical Pacific: Implications for CO_2 variations during the Pleistocene, *Limnol*. *Oceanogr*., *30*, 699-712.

Dymond, J. and R. Collier (1988), Biogenic particle fluxes in the equatorial Pacific: Evidence for both high and low productivity during the 1982-1983 El Nino, *Global Biogeochemical Cycles*, *2*, 129 – 137.

Dymond, J., E. Suess, and M. Lyle (1992), Barium in deep-sea sediment: A geochemical proxy for paleoproductivity, *Paleoceanography*, *7*, 163-181.

Dymond, J. and M. Lyle (1994), Particle fluxes in the ocean and implications for sources and preservation of ocean sediments, in *Studies in Geophysics: Material Fluxes on the Surface of the Earth*, edited by The National Research Council, pp. 125-142, National Academy Press, Washington, D.C..

Dymond, J. and R. Collier (1996), Particulate barium fluxes and their relationships to biological productivity, *Deep-Sea Research* II, *43* (4-6), 1283-1308.

Eagle, M., A. Paytan, K.R. Arrigo, G. Dijken, R.W. Murray (2003), A comparison between excess barium and barite as indicators of carbon export, *Paleoceanogrpahy, 12*, 1021-1033, doi:10.1029/2002PA000793.

Eagle Gonneea, M. and A. Paytan (2006), Phase associations of barium in marine sediments, *Marine Chemistry*, *100*, 124-135, doi:10.1016/j.marchem.2005.12.003.

Expedition 320/321 Scientists, Methods (2010), *In* H. Pälike, M. Lyle, H. Nishi, I. Raffi, K. Gamage, A. Klaus, and the Expedition 320/321 Scientists, *Proc. IODP,* 320/321: Tokyo (Integrated Ocean Drilling Program Management International, Inc.), doi:10.2204/iodp.proc.320321.102.2010.

Falkowski, P.G., M.E. Katz, A.H. Knoll, A. Quigg, J.A. Raven, O. Schofield, and F.J.R. Taylor (2004), The evolution of modern eukaryotic phytoplankton, *Science, 305*, 354–360, doi:10.1126/science.1095964.

Flower, B. and J. P. Kennett (1993), Middle Miocene ocean-climate transition: High resolution oxygen and carbon isotopic records from Deep Sea Drilling Project Site 588A, *Paleoceanography*, *8*, 811-843.

Gartner, S. and T. J. Chow (1985), Calcareous nannofossil biostratigraphy, Deep Sea Drilling Project Leg 85, eastern equatorial Pacific, *Init. Repts. DSDP*, *85*, 609-619, doi:10.2973/dsdp.proc.85.115.

Hansell, D.A., C.A. Carlson, D.J. Repeta, and R. Schlitzer (2009), Dissolved organic matter in the ocean, *Oceanography*, *22*, 202-211.

Honjo, S., J. Dymond, R. Collier, and S. Manganini (1995), Export production of particles to the interior of the equatorial Pacific Ocean during the 1992 EqPac experiment, *Deep Sea Research II, 42,* 831-870.

Hurd, D. (1973), Interactions of biogenic opal, sediment and seawater in the central equatorial Pacific, *Geochemica et Cosmochimica Acta*, *37*, 2257-2266.

Ingle, J.C. (1981), Origin of Neogene diatomites around the north Pacific Rim, *The Monterey Formation and Related Siliceous Rocks of California*, edited by R. E. Garrison, R.G. Douglas, K.E. Pisciotto, C.M. Isaacs, J.C. and Ingle, pp. 159-179, Society of Economic Paleontologists and Mineralogists, Pacific Section, Special Publication No. 15, Los Angeles, California.

Kidder, D.L., and E.H. Gierlowski-Kordesch (2005), Impact of grassland radiation on the nonmarine silica cycle and Miocene diatomite, *Palaios*, *20*, 198–206, doi:10.2110/palo.2003.p03-108.

Kürschner W.M., Z. Kvaček, and D. L. Dilcher (2008), The impact of Miocene atmospheric carbon dioxide fluctuation on climate and the evolution of terrestrial ecosystems, *PNAS*, *105*(2), 449-453, doi: 10.1073/pnas.0708588105.

Lourens, L.J. (2004), Revised tuning of ocean drilling program Site 964 and KC01B (Mediterranean) and implication for the ^{18}O, tephra, calcareous nannofossil, and geomagnetic chronologies of the past 1.1 MYR, *Paleoceanography, 19*, 3010-3029, 10.1029/2003PA000997.

Lyle, M., K. Dadey, and J. Farrell (1995), The Late Miocene (11-8 Ma) eastern Pacific carbonate crash: Evidence for reorganization of deep water circulation by the closure of the Panama Gateway, edited by N. G. Pisias, et al., pp. 821-837, *Proc. of the ODP, Sci. Results, 138*.

Lyle, M., A. Mix, A. C. Ravelo, D. Andreasen, L. Heusser, and A. Olivarez (2000), Kyr-scale $CaCO_3$ and C_{org} events along the northern and central California margin: Stratigraphy and origins, edited by M. Lyle, pp. 163-182, *Proc. of the ODP, Sci. Results, 16*.

Lyle, M. (2003), Neogene carbonate burial in the Pacific Ocean, *Paleoceanography*, *18*, 1059-1077, doi:10.1029/2002PA000777.

Matthews, R. K. and R. Z. Poore (1980), Tertiary ∂^{18}O record and glacio-eustatic sea-level fluctuations, *Geology*, *8*, 501-504.

Mayer, L. A., T. H. Shipley, and E. L. Winterer (1986), Equatorial Pacific seismic reflectors as indicators of global oceanographic events, *Science*, *233*, 761-764.

McClain, C.R. (2009), A decade of satellite ocean color observations, *Annual Review of Marine Science*, *1*, 19- 32, doi:10.1146/annurev.marine.010908.163650.

McGee, D., F. Marcantonio, and J. Lynch-Stieglitz (2007), Deglacial changes in dust flux in the eastern equatorial Pacific, *Earth and Plantetary Science Letters*, *257*, 215-230.

McManus, J., W.M. Berelson, G.P. Klinkhammer, D.E. Hammond, and C. Holm (2004), Authigenic uranium: Relationship to oxygen penetration depth and organic carbon rain, *Geochimica et Cosmochimica Acta*, *69*, 95-108, doi:10.1016/j.gca.2004.06.023.

Mo, T., A. D. Suttle, W. M. Sackett (1973), Uranium concentrations in marine sediments, *Geochimica et Cosmochimica Acta*, *37*, 35-51.

Mortlock, R.A. and P.N. Froelich (1989), A simple method for the rapid determination of biogenic opal in pelagic marine sediments, *Deep-Sea Res., Part A*, *36*, 1415-1426.

NASA, OceanColor home page, 2010, http://oceancolor.gsfc.nasa.gov/, accessed on (May 2, 2010).

Nigrini, C. A. (1985), Radiolarian biostratigraphy in the central equatorial Pacific, Deep Sea Drilling Project Leg 85, *DSDP Init. Repts*, *85*, doi:10.2973/dsdp.proc.85.112.1985.

NOAA (2008), Tropical atmosphere ocean project, "What is La Niña?", Pacific Marine Environmental Laboratory, 03-24-2008, http://www.pmel.noaa.gov/tao/elnino/la-nina-story.html, accessed on (March 10, 2010).

NOAA (2010), Aqua Modis satellite data, http://coastwatch.pfeg.noaa.gov/erddap/griddap/erdMWchla8day.html, accessed on (May 11, 2010).

NOAA National Environmental Satellite, Data and Information Service, National Geophysical Data Center (NGDC), Marine Geology and Geophysics Division, Geology, DSDP Site 574 (1985), http://www.ngdc.noaa.gov/mgg/geology/seadas.html.

Olivarez Lyle, A. and M. W. Lyle (2002), Determination of biogenic opal in pelagic marine sediment: A simple method revisited. *Proc. ODP Init. Repts.*, *199*, 1-21, doi:10.2973/odp.proc.ir.199.106.2002.

Pagani, M., M. Arthur, and K.H. Freeman (1999), Miocene evolution of atmospheric carbon dioxide, *Paleoceanography*, *14*, 273-292.

Pagani, M., J.C. Zachos, K.H. Freeman, B. Tipple, and S. Bohaty (2005), Marked decline in atmospheric carbon dioxide concentrations during the Paleogene, *Science*, *309*, 600-603.

Pälike, H., H. Nishi, M. Lyle, I. Raffi, K. Gamage, A. Klaus, and the Expedition 320/321 Scientists (2010a), *Proc. IODP,* 320/321: Tokyo (Integrated Ocean Drilling Program Management International, Inc.), doi:10.2204/iodp.proc.320321.2010.

Pälike, H., H. Nishi, M. Lyle, I. Raffi, K. Gamage, A. Klaus, and the Expedition 320/321 Scientists (2010b), Expedition 320/321 summary, *In* H. Pälike, M. Lyle, H. Nishi, I. Raffi, K. Gamage, A. Klaus, and the Expedition 320/321 Scientists, *Proc. IODP*, 320/321: Tokyo (Integrated Ocean Drilling Program Management International, Inc.), doi:10.2204/iodp.proc.320321.101.2010.

Paytan, A. and E. Griffith (2007), Marine barite: Recorder of variations in ocean export productivity, *Deep-Sea Research* II, *54*, 687-705.

Rabosky, D.L. and U. Sorhannus (2009), Diversity dynamics of marine planktonic diatoms across the Cenozoic, *Nature*, *457*, 183–186, doi:10.1038/nature07435.

Rabouille, C. and J. F. Gaillard (1991), A coupled model representing the deep□sea organic carbon mineralization and oxygen consumption in surficial sediments, *J. Geophys. Res., 96*, 2761-2776.

Ragueneau, O., P. Tréguer, A. Leynaert, R.F. Anderson, M.A. Brzezinksi, D.J. DeMaster, R.C. Dugdale, F. Dymond, G. Fischer, R. Francois, C. Heinze, E. Maier-Reimer, V. Martin-Jézéquel, D.M. Nelson, and B. Quéguiner (2000), A review of the Si cycle in the modern ocean: Recent progress and missing gaps in the application of biogenic opal as a paleoproductivity proxy, *Global and Planetary Change*, *26*, 317-365.

Rea, D. and M. Leinen (1992), Crustal subsidence and calcite deposition in the South Pacific Ocean. *Init. Reports, DSDP, Leg 92*, 299-303.

Rea, D. and M. Lyle (2005), Paleogene calcite compensation depth in the eastern subtropical Pacific: Anwers and questions, *Paleoceanography*, *20*, PA1012, doi:10.1029/2004PA001064.

Saito, T. (1985), Planktonic foraminiferal biostratigraphy of eastern equatorial Pacific sediments, Deep Sea Drilling Project Leg 85, *DSDP Init. Repts*, *85*, 621-653, doi:10.2973/dsdp.proc.85.116.1985.

Savin, S. M., R.G. Douglas, and F.G. Stehli (1975), Tertiarymarine paleo-temperatures, *Geological Society of America Bulletin*, *86*, 1499-1510.

Sclater, J.G., L. Meinke, A. Bennett, and C. Murphy (1985), The depth of the ocean through the Neogene, *Geological Society of America, Memior 163*, 1-19.

Shackleton, N. J. and J. P. Kennett (1975), Paleotemperature history of the Cenozoic and the initiation of Antarctic glaciation: Oxygen and carbon isotope analyses in DSDP Site 277, 279, and 281, *Init. Repts. DSDP*, *29*, 743-756.

Shipboard Scientific Party (1985), Site 574, *Init. Repts. DSDP*, *85*, 225-244.

Taylor, S.R. and S.M. McLennan (1985), *The Continental Crust: its Composition and Evolution: An examination of the geochemical record preserved in sedimentary rocks*, edited by A. Hallam, Blackwell, Oxford, UK.

Vincent, E. and W. H. Berger (1981), Planktonic foraminifera and their use in paleoceanography, *The Oceanic Lithosephere: The Sea*, edited by D. Emiliani, pp. 1025-1119, 7, Wiley Interscience, New York.

Vincent, E. and J. S. Killingley (1985), Oxygen and carbon isotope record for the early and middle Miocene in the central equatorial Pacific (DSDP Leg 85) and paleoceanographic implications, *Init. Repts. DSDP*, *85*, 749-769.

Walker, J.D. and J. W. Geissman (2009), Geologic time scale: Geological Society of America, doi: 10.1130/2009.CTS004R2C http://www.geosociety.org/science/timescale/.

Weinreich, N. and F. Theyer (1985), Paleomagnetism of deep sea drilling project Leg 85 sediments: Neogene magnetostratigraphy and tectonic history of the central equatorial Pacific, *Init. Repts. DSDP*, *85*, 849-901.

Wright, J.D., and K G. Miller (1992), Miocene stable isotope stratigraphy, Site 747, Kerguelen Plateau. *In* S.W. Wise Jr., R. Schlich et al., *Proc. ODP, Sci. Results, 120*, pp. 855–866. doi:10.2973.odp.proc.sr.120.193.1992.

Zachos, R. C., G. R. Dickens, R. E. Zeebe (2008), An early Cenozoic perspective on greenhouse warming and carbon-cycle dynamics, *Nature*, *451*, 279-283, doi:10.1038/nature06588.

APPENDIX A

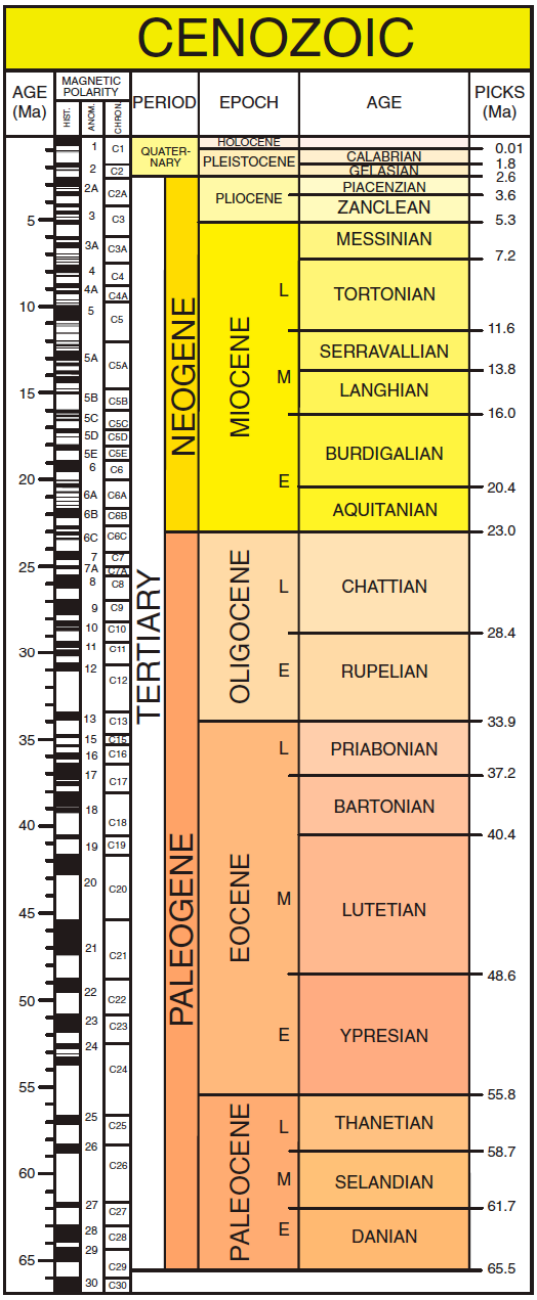

Figure A1. Geologic time scale. The Early to Middle Miocene spans from about 23 Ma to 11.6 Ma. Walker, J.D., and J. W. Geissman, (2009), Geologic Time Scale: Geological Society of America. http://3dparks.wr.usgs.gov/coloradoplateau/timescale.htm.

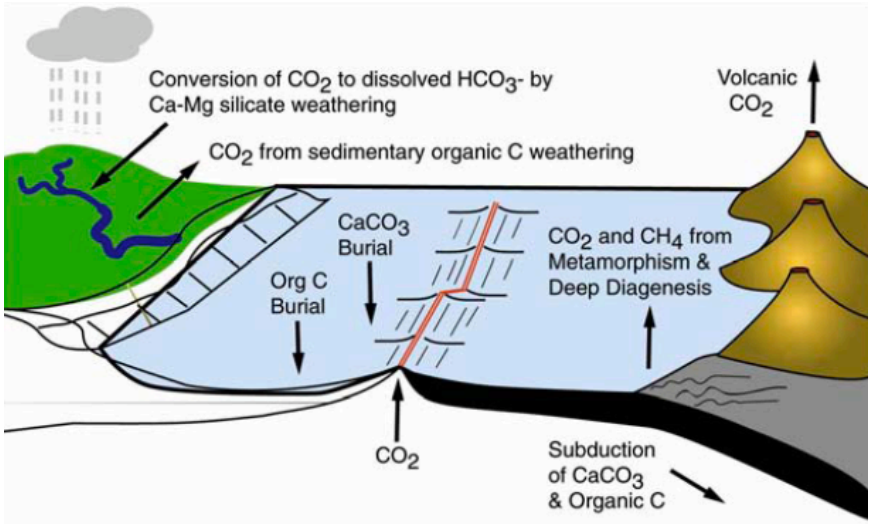

Figure A2. The long-term carbon cycle. The carbon cycle (>100,000 years) regulates the carbon in each reservoir. *R. Berner, (1999), GSA Today, 9.*

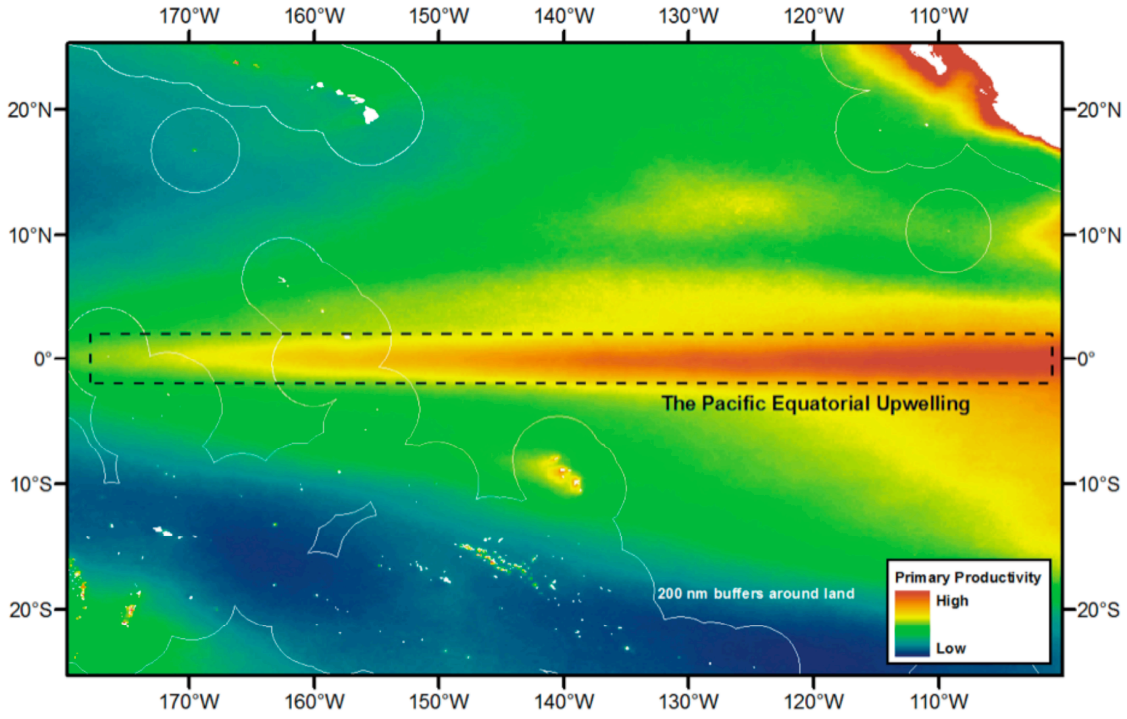

Figure A3. Modern Equatorial Pacific Primary Production. The modern high productivity band on the equatorial Pacific based on the mean annual values of primary production, derived from the Vertically Generalized Productivity Model (VGPM) [Behrenfeld and Falkowski, 1997.] Factors taken into account include surface chlorophyll concentration, surface temperature, day length, flux of photosynthetically active radiation, and the depth of the euphotic zone.

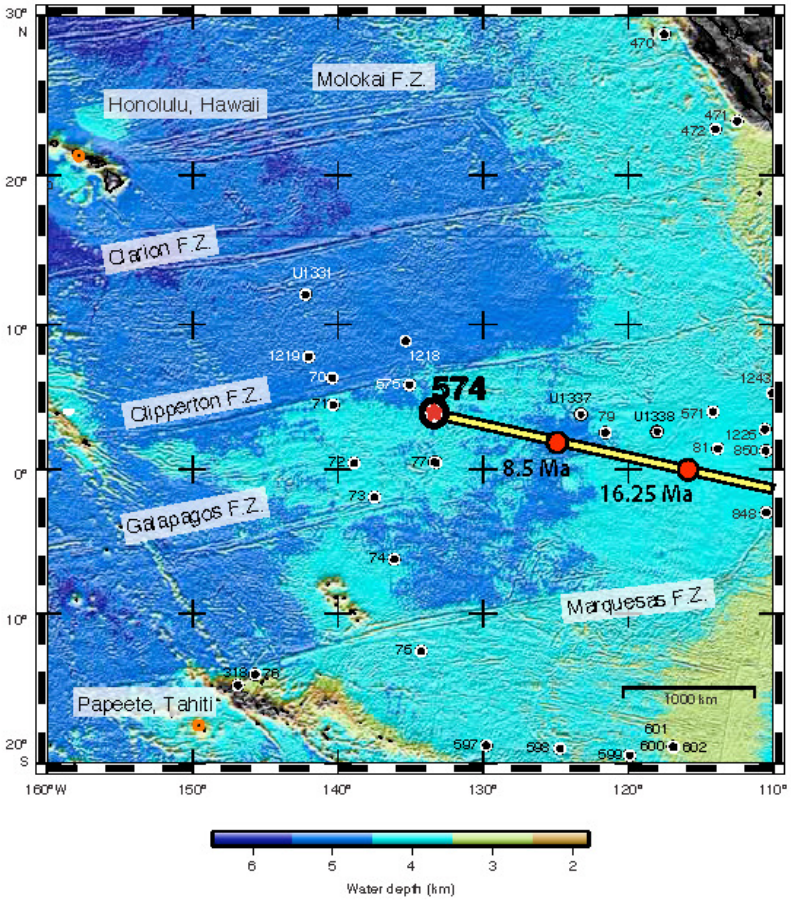

Figure A4. DSDP Site 574 Map. The current location of DSDP Site 574; note the modern water depth. The yellow line illustrates the path of migration from the Eocene to present. DSDP Site 574 crossed the equator (0°) at approximately 16.2 Ma, based on the polynomial fit used in this research. Red circles indicate approximate site location at that time.

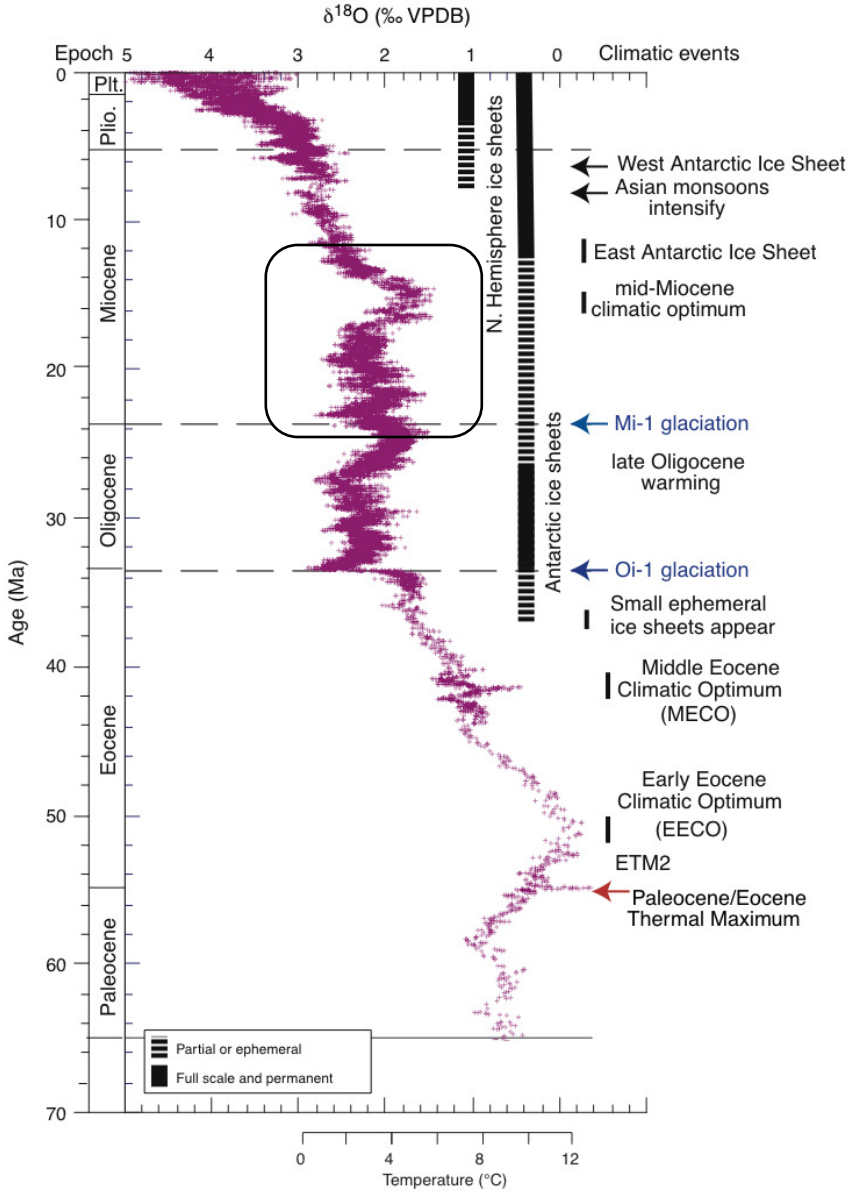

Figure A5. $\partial^{18}O$ values and Cenozoic Temperature Flux. The $\partial^{18}O$ values shifted multiple times between the late and middle Miocene. High $\partial^{18}O$ values infer lower temperatures; note the warm mid-Miocene climatic optimum between 16 and 14 million years ago, which correlates with the high equatorial productivity values presented. Zachos et al., 2008. Proc. IODP Init. Results, 321, 2009.

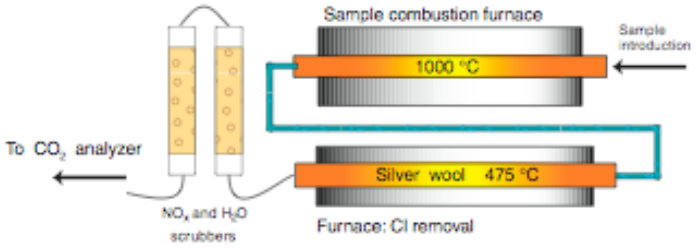

Figure A6. Coulometric Method Illustration. The figure illustrates the furnaces and method used in coulometric method for determining CO_2. From *Lyle et al., 2000*.

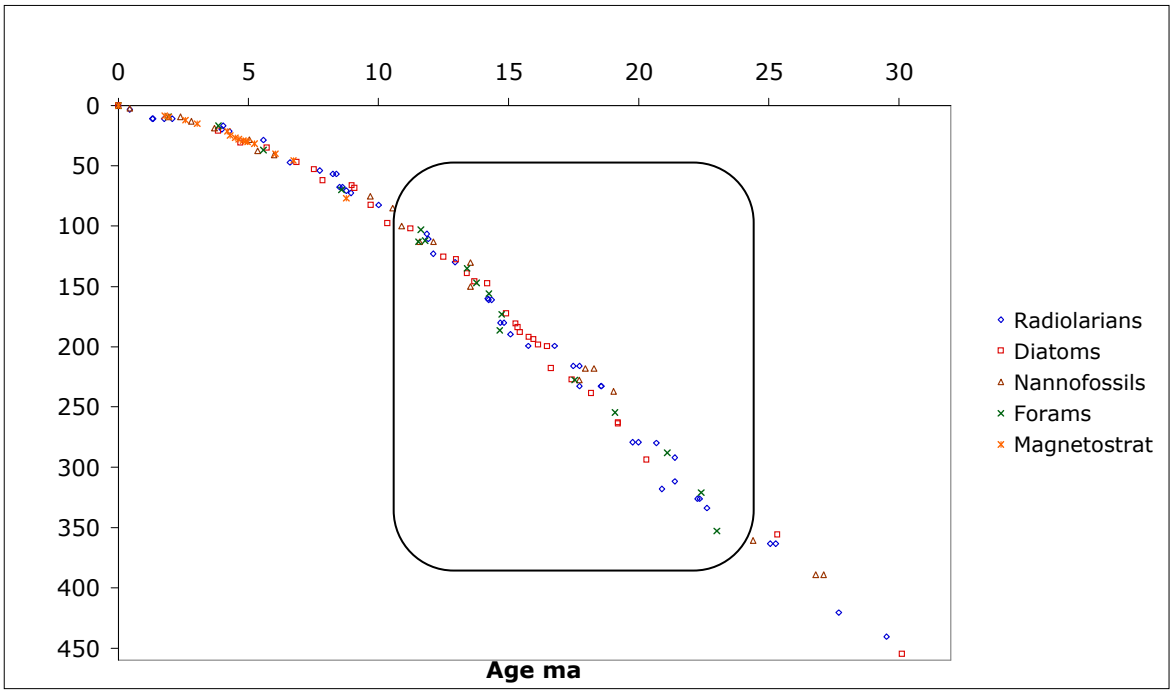

Figure A7. Stratigraphic Plot with Polynomial Equation. Biostratigraphy and Magnetic Stratigraphy for DSDP Site 574, Holes A and C, as determined from Init. Repts. of DSDP [1985], and IODP Legs 320/321 [2009]. The boxed area illustrates the focus area of this study: 12 to 24 Ma.
Polynomial Age = -0.140026 + (Depth * 0.2692) - ($Depth^2$ * 0.005302) + ($Depth^3$ * 0.000093981) - ($Depth^4$ * 0.0000010264) + ($Depth^5$ * 0.000000006683) - ($Depth^6$ * 0.000000000026002) + ($Depth^7$ * 0.000000000000059169) - ($Depth^8$ * 7.2497E-17) + ($Depth^9$*3.6885E-20).

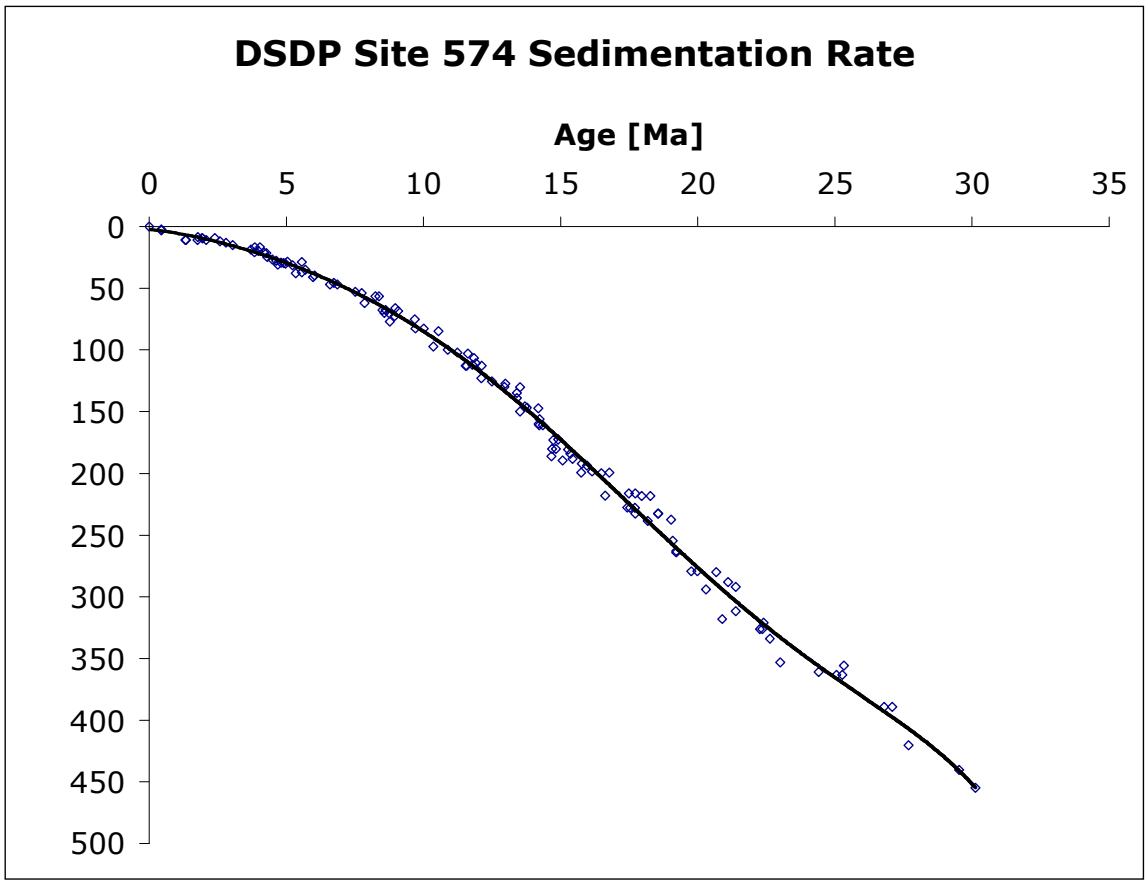

Figure A8. DSDP Site 574 Sedimentation Rates Plot. The highest rates were recorded during the crossing of the equatorial "high productivity belt" and during the mid-Miocene climatic optimum.

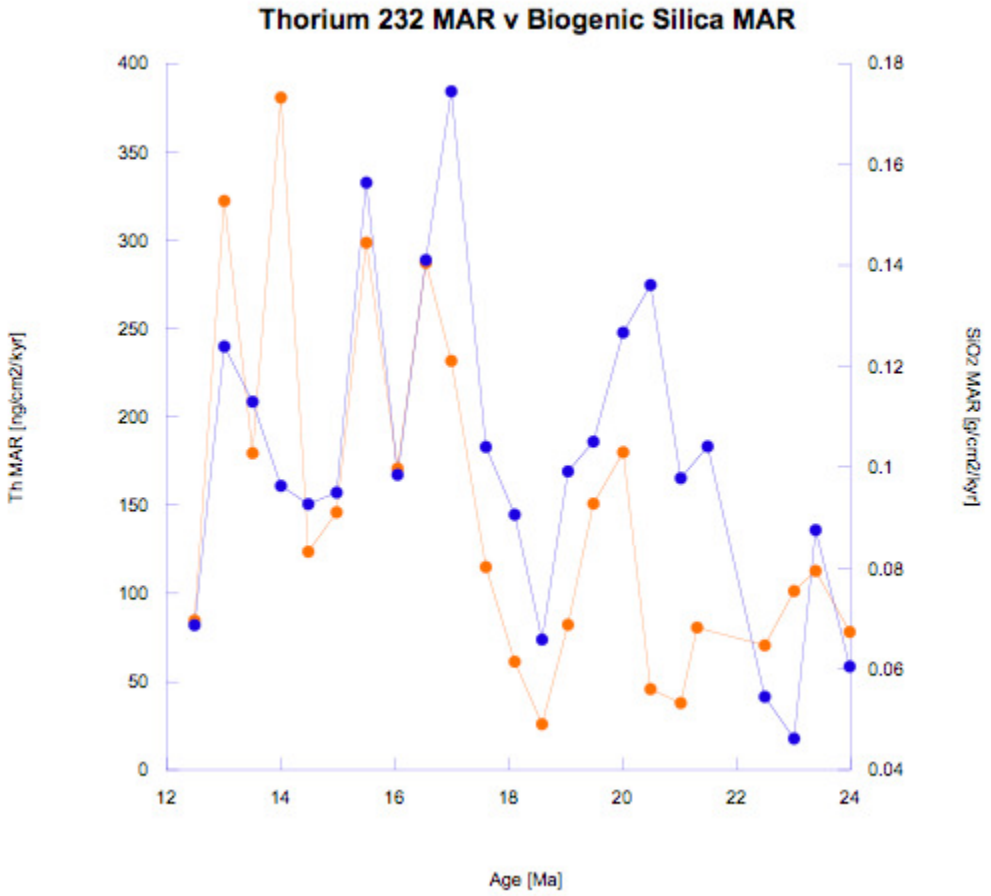

Figure A9. Thorium and Bio-SiO_2 MAR Plot. Thorium (orange) mass accumulation rates increases at approximately 17 Ma, following the biogenic silica curve (blue), and again at 14 Ma at the end of the Mid-Miocene Climatic Optimum.

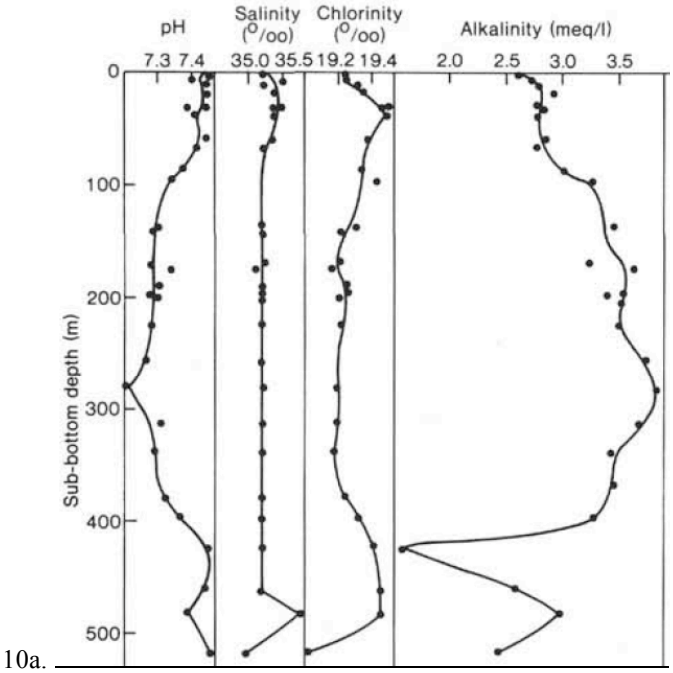

10a.

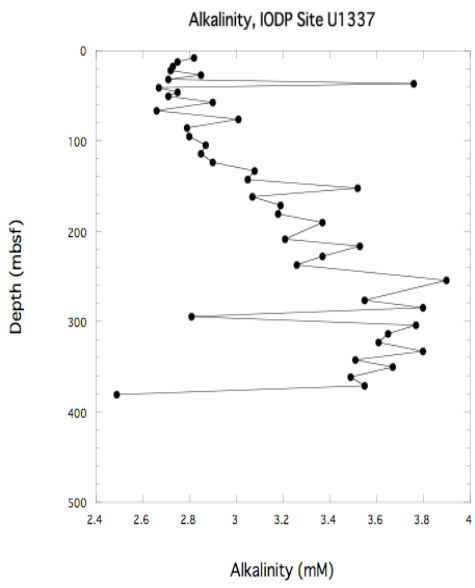

10b.

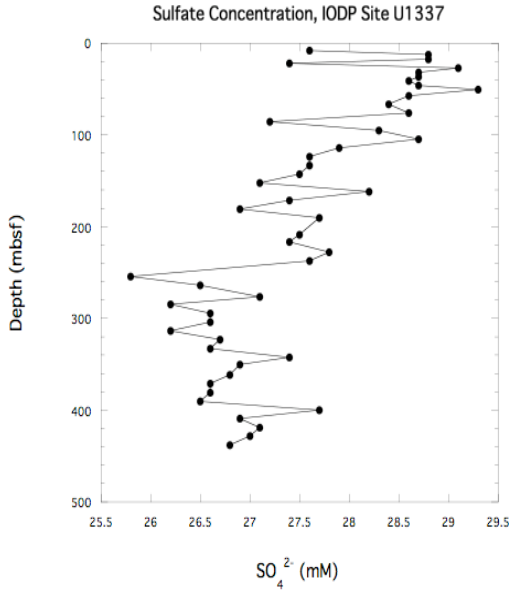

10c.

Figure A10 a. DSDP Site 574 Alkalinity, b. IODP U1337 Alkalinity, c. IODP U1337 Sulfate Concentration. a. Low alkalinity and low pH values are indicative of a sulfur-containing environment. b, c: The 2009 IODP U1337 Site, also located at 4°N, closely resembles the alkalinity profile of DSDP Site 574. The sulfate concentration curve shows that the environment is not reducing.

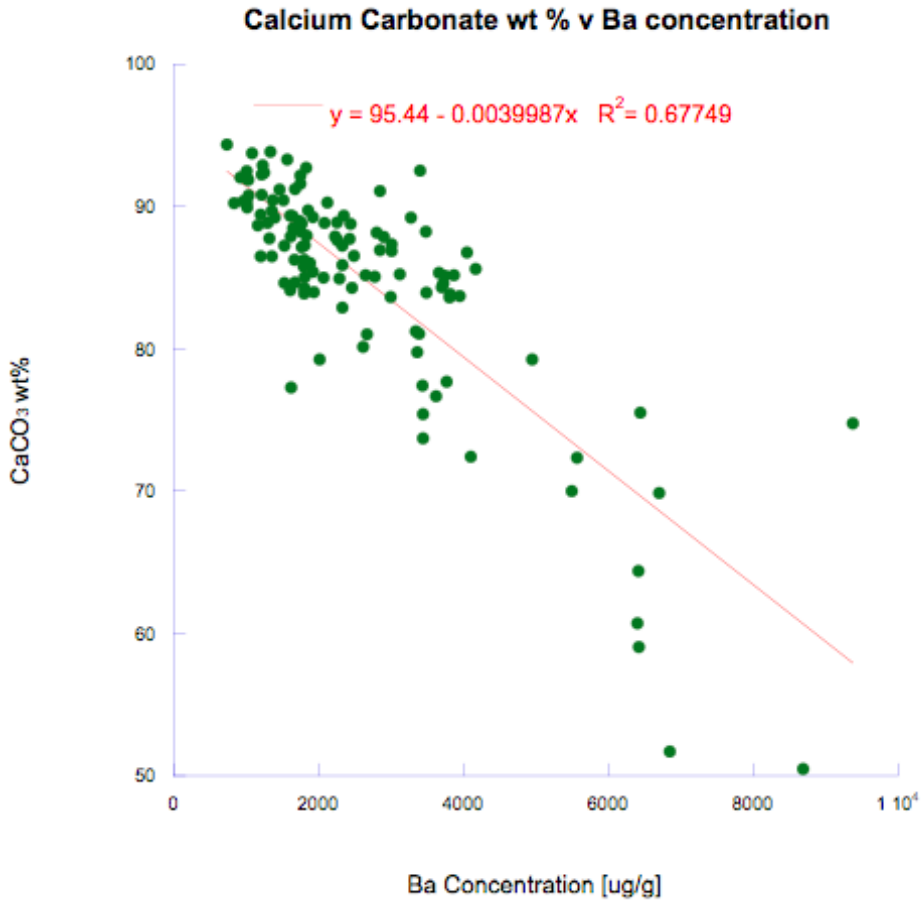

Figure A11. $CaCO_3$ and Ba wt% Correlation Plot. Correlation between total barium concentration and calcium carbonate weight percent. R^2 value of 0.68 illustrates a good correlation between the two components; barium could potentially be used to estimate $CaCO_3$ weight percent.

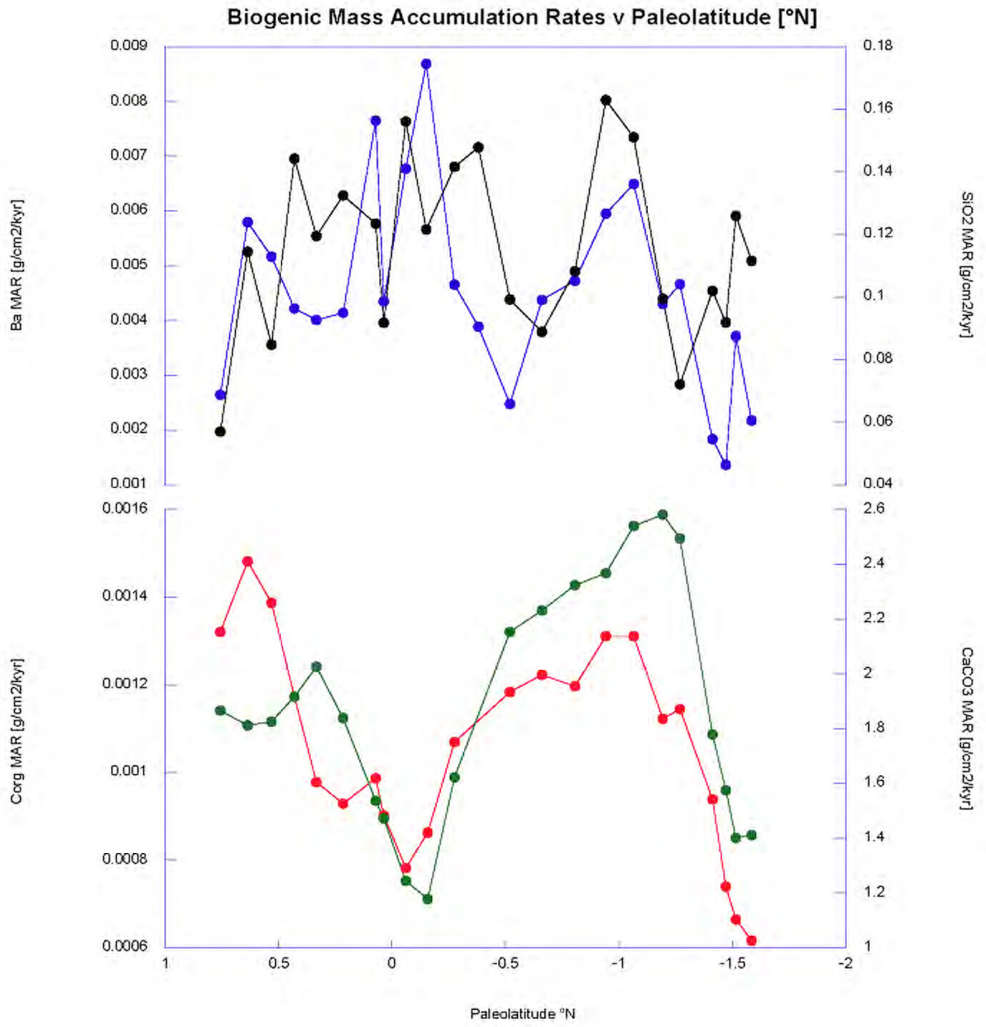

Figure A12. Biogenic MAR v Paleolatitude. The decrease in C_{org} and $CaCO_3$ at the equatorial crossing does not support modern sediment trap data, which illustrates the equatorial zone as a high productivity area. (**Black – ^{135}Ba, blue – SiO_2, red – C_{org}, green – $CaCO_3$**). In this plot, the ^{135}Ba and SiO_2 are unaffected or increase near the equator, while the carbon-based compounds are either a) not produced or b) not preserved.

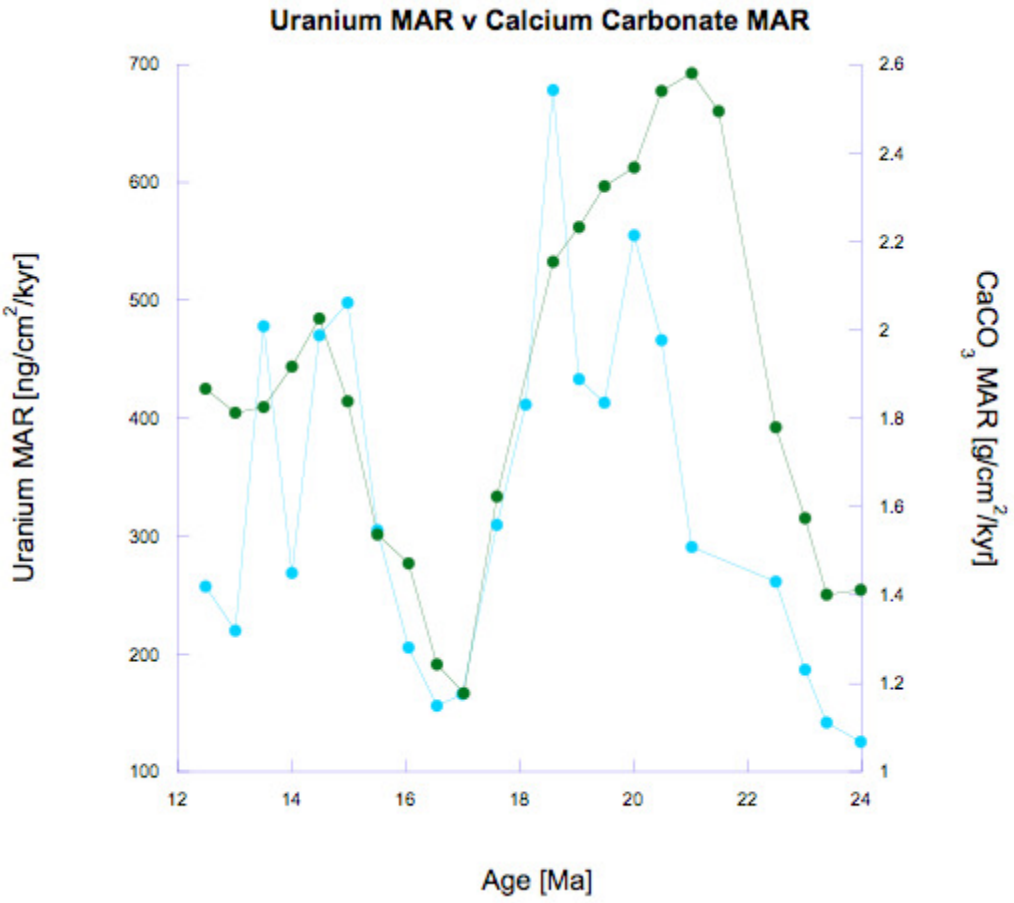

Figure A13. Uranium and $CaCO_3$ MAR Plot. Uranium (light blue) concentration decreases at the equator with the calcium carbonate (green). The decrease at 16.5 Ma coincides with the equator crossing, illustrating the decrease in carbonate accumulation and the resulting decrease in uranium in the sediments.

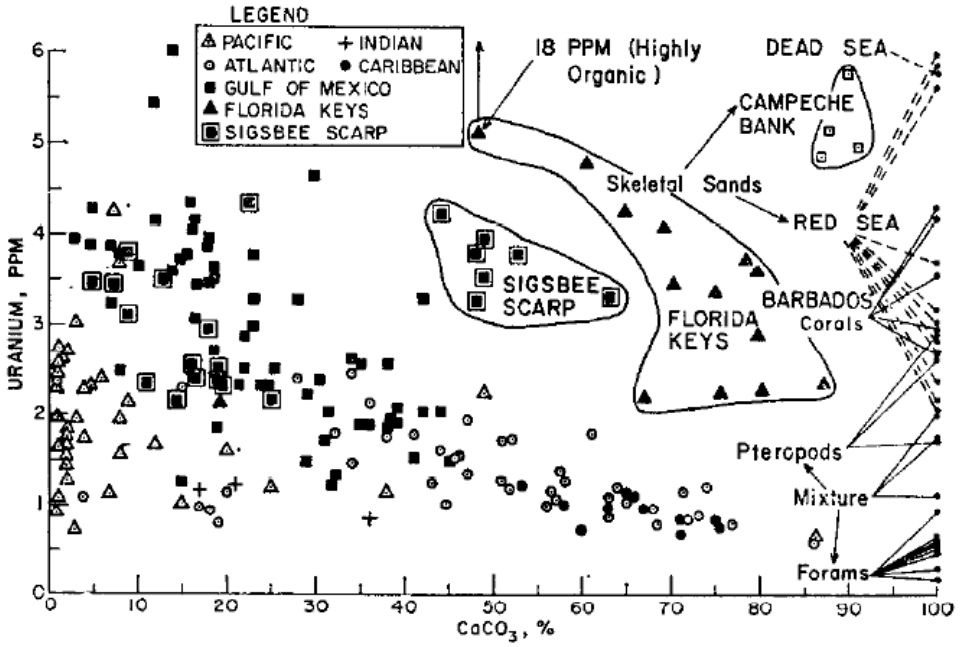

Figure A14. Uranium Concentration in Various Marine Components. The Uranium concentration of foraminifera coincides with the data presented by this research. (Note unit change: data in the plot is presented in PPM, while data presented in this research is in PPB). [Mo et al., 1973].

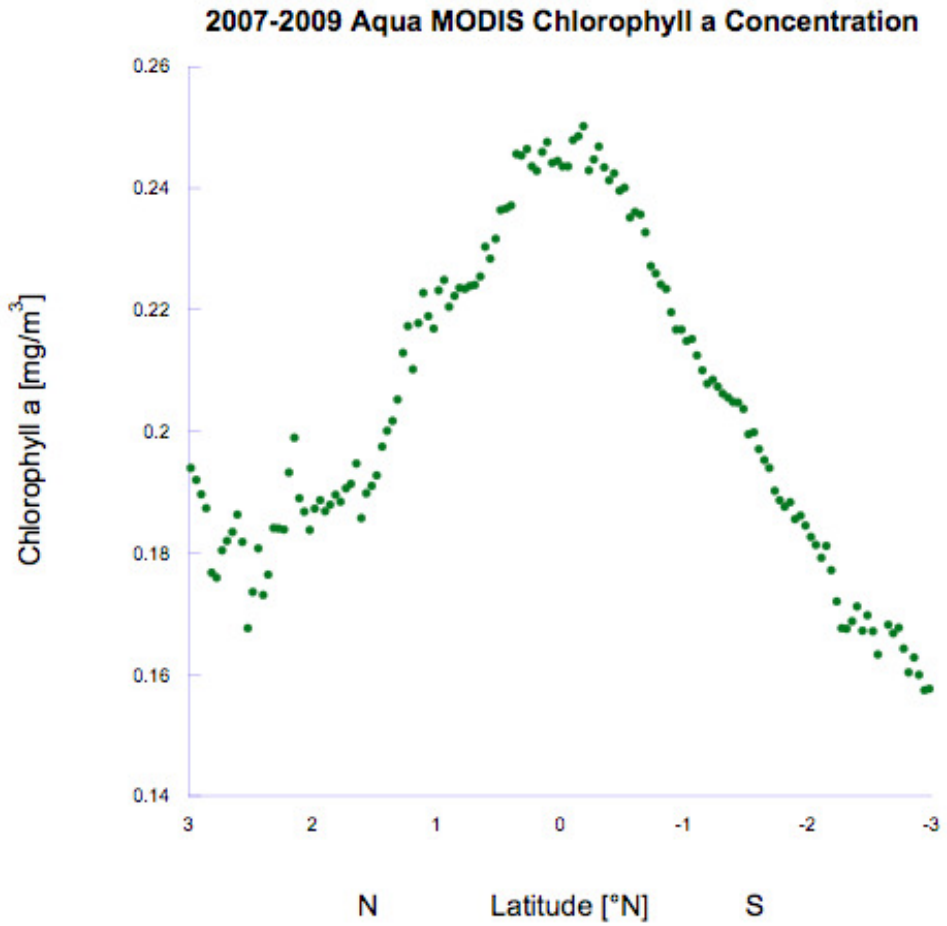

Figure A15. Modern Chlorophyll a Concentration Plot. Aqua MODIS satellite data collected between 2007 and 2009 for 110°W. Chlorophyll a data presented in monthly increments and units are mg/m^3. [NOAA, 2010].

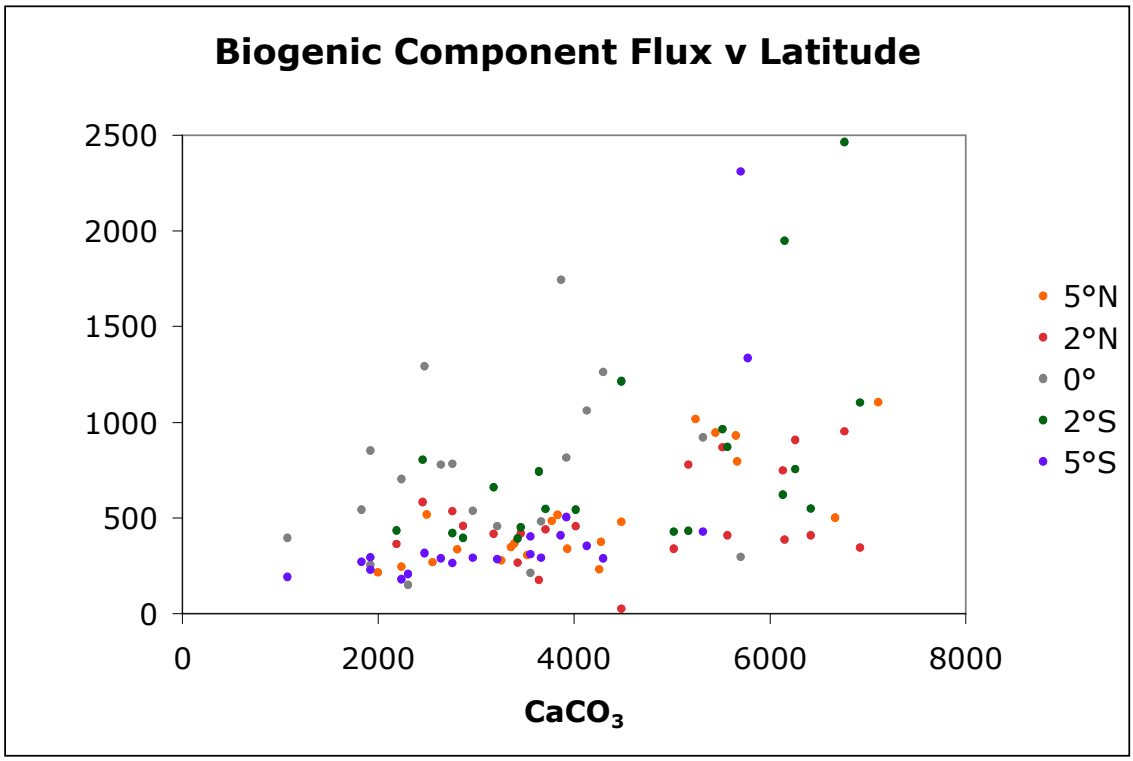

Figure A16. Modern Bio-SiO_2 and $CaCO_3$ Sediment Trap Flux. Based on sediment trap data from Honjo et al., [1995] illustrating the positive correlation between biogenic silica flux and calcium carbonate flux in the equatorial Pacific from January 1992 to February 1993. This data supports the carbonate dissolution hypothesis at 17 Ma because the high biogenic silica production should correlate with high calcium carbonate production.

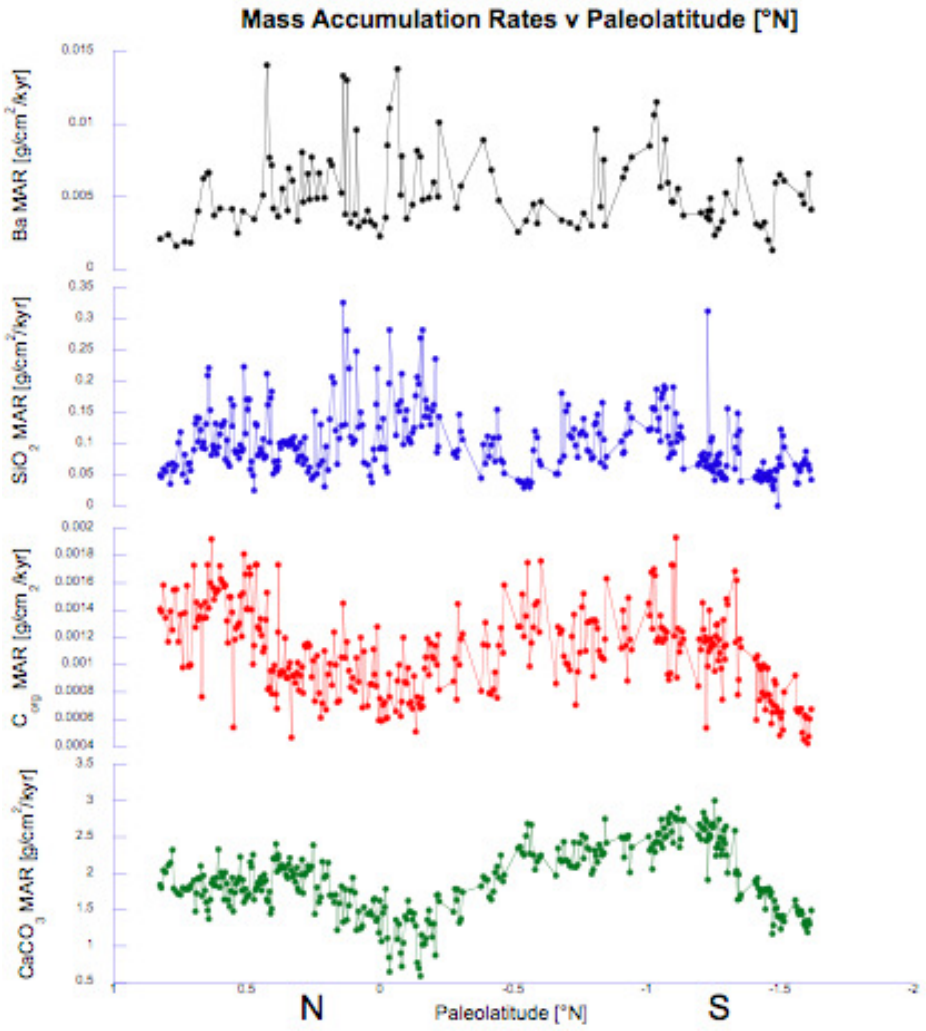

Figure A17. Component MAR v Paleolatitude Plot. Organic carbon and calcium carbonate (bottom two plots) mass accumulation rates follow a similar trend and decrease at the high productivity equator, while barium and biogenic silica, which are not affected by the CCD, peak during the equatorial crossing.

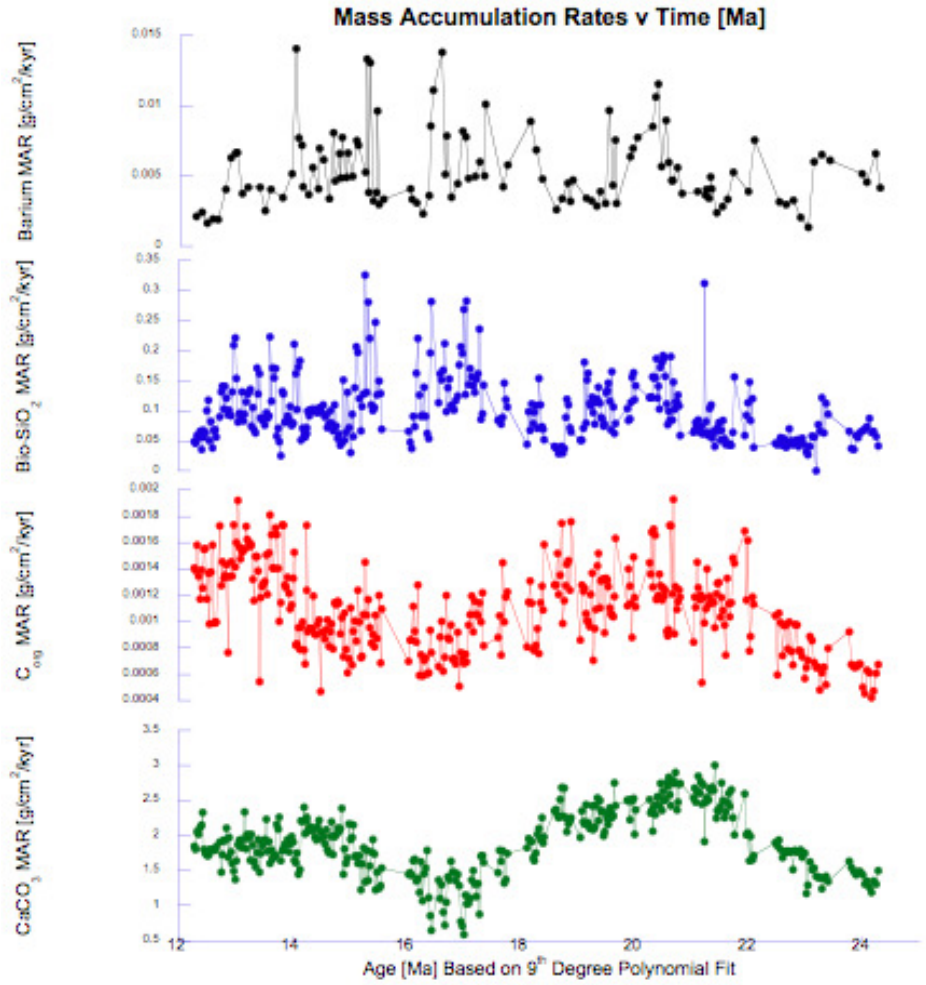

Figure A18. Component MAR v Age Plot. Same mass accumulation data as Figure A 16 plotted against the estimated age. Note the increase in bio-SiO2 at 17 Ma and the corresponding decrease in organic carbon and carbonate.

APPENDIX B

Table B1- 500 kyr DSDP Site 574 Sediment Components

Mean Age [Ma]	Age Top [Ma]	Age Bottom [Ma]	# of Samples in Interval	Site 574 Sample Interval			mbsf Top	mbsf Bottom	Paleo LAT°N
				Hole-Core-Section-Depth [cm]					
12.5	12.25	12.75	18	A-16-1-90	to	A-17-1-94	118.90	128.73	0.76
13.0	12.75	13.25	21	A-17-1-93	to	A-18-5-141	128.73	139.20	0.64
13.5	13.25	13.75	21	A-18-5-140	to	A-19-6-91	139.20	149.80	0.53
14.0	13.75	14.25	22	A-19-6-90	to	A-21-1-41	149.80	160.30	0.43
14.5	14.25	14.75	21	A-21-1-40	to	A-22-2-41	160.30	170.40	0.33
15.0	14.75	15.25	19	A-22-2-90	to	A-23-2-91	170.40	180.30	0.22
15.5	15.25	15.75	13	A-23-2-90	to	C-1-1-41	180.30	189.70	0.07
16.1	15.75	16.25	9	C-1-1-40	to	C-1-3-141	189.70	198.80	0.04
16.5	16.25	16.75	15	C-1-3-140	to	C-2-3-91	198.80	207.90	-0.06
17.0	16.75	17.25	18	C-2-3-90	to	C-3-3-37	207.90	216.86	-0.15
17.5	17.25	17.75	10	C-2-3-36	to	C-4-2-139	216.86	226.00	-0.28
18.1	17.75	18.25	7	C-4-2-138	to	C-5-2-141	226.00	235.40	-0.38
18.5	18.25	18.75	14	C-5-2-140	to	C-6-3-40	235.40	245.50	-0.52
19.0	18.75	19.25	16	C-6-3-39	to	C-7-4-41	245.50	256.30	-0.66
19.5	19.25	19.75	20	C-7-4-40	to	C-9-1-41	256.30	267.80	-0.80
20.0	19.75	20.25	9	C-9-1-40	to	C-10-1-91	267.80	280.20	-0.94
20.5	20.25	20.75	23	C-10-1-90	to	C-11-2-141	280.20	292.50	-1.07
21.1	20.75	21.25	13	C-11-3-40	to	C-12-4-91	292.50	304.40	-1.19
21.5	21.25	21.75	21	C-12-4-90	to	C-13-5-36	304.40	314.85	-1.27
22.0	21.75	22.25	7	C-13-5-35	to	C-14-3-36	314.85	324.20	-1.34
22.6	22.25	22.75	9	C-15-1-40	to	C-15-4-41	324.20	332.40	-1.41
23.0	22.75	23.25	15	C-15-4-40	to	C-16-2-138	332.40	339.87	-1.47
23.4	23.25	23.75	5	C-16-2-137	to	C-17-1-41	339.87	346.70	-1.52
24.0	23.75	24.25	13	C-17-1-40	to	C-17-5-91	346.70	353.10	-1.58

n/a- Data for the interval is not reliable

Table B1 Continued

Paleo LONG°W	LSR [cm/kyr]	MAR [g/cm²/kyr]	Avg C_{org} Wt%	C_{org} MAR [g/cm²/kyr]	Avg $CaCO_3$ wt%	$CaCO_3$ MAR [g/cm²/kyr]	Avg Bio-SiO_2 wt%	Bio-SiO_2 MAR [g/cm²/kyr]
123.37	1.97	2.07	0.06	0.00132	90.17	1.87	3.38	0.07
123.01	2.08	2.14	0.08	0.00160	85.22	1.83	5.90	0.12
122.67	2.13	2.12	0.06	0.00131	85.80	1.82	5.35	0.11
122.34	2.10	2.22	0.06	0.00133	85.79	1.91	4.51	0.10
122.01	2.04	2.30	0.02	0.00047	87.54	2.01	4.09	0.09
121.61	1.95	2.12	0.03	0.00072	86.38	1.84	4.61	0.09
121.13	1.89	1.93	0.07	0.00120	78.65	1.52	8.70	0.17
120.84	1.82	1.75	0.05	0.00086	83.51	1.46	5.86	0.10
120.60	1.80	1.59	0.04	0.00066	72.92	1.18	9.49	0.14
120.38	1.80	1.59	0.06	0.00068	74.55	1.20	10.67	0.16
119.96	1.84	1.88	0.05	0.00088	81.69	1.55	6.45	0.12
119.61	1.92	2.11	0.04	0.00081	85.93	1.81	4.10	0.09
119.11	2.01	2.48	0.05	0.00128	89.34	2.22	2.57	0.06
118.62	2.16	2.48	0.04	0.00086	88.65	2.20	4.15	0.10
118.10	2.32	2.61	0.05	0.00133	88.47	2.31	4.03	0.11
117.61	2.46	2.77	0.04	0.00111	86.66	2.40	4.36	0.12
117.17	2.49	2.94	0.04	0.00126	86.24	2.54	4.66	0.14
116.71	2.32	2.88	0.03	0.00084	89.22	2.57	3.41	0.10
116.43	2.10	2.71	0.04	0.00103	91.73	2.49	2.51	0.07
116.17	1.84	2.21	0.04	0.00078	87.86	1.95	4.37	0.09
115.91	1.61	1.98	0.03	0.00060	90.67	1.80	2.49	0.05
115.68	1.48	1.73	0.05	0.00065	89.97	1.56	2.84	0.05
115.52	1.39	1.66	0.05	0.00080	84.46	1.40	5.33	0.09
115.26	1.28	1.62	0.03	0.00050	87.14	1.41	3.77	0.06

Table B1 Continued

Avg Ba [ug/g]	Ba MAR [mg/cm^2/kyr]	# of Ba Samples in Interval	Avg Th [ng/g]	Th MAR [ng/cm^2/kyr]	Avg U [ng/g]	U MAR [ng/cm^2/kyr]	# of Th/U Samples in Interval
959.15	1.98	5	41.12	85.02	125.20	258.83	5
2591.65	5.55	6	165.48	354.21	110.63	236.82	4
1604.81	3.41	3	80.80	171.47	217.91	462.47	3
3022.36	6.70	7	162.18	359.56	121.32	268.97	6
2300.46	5.29	8	61.46	141.39	211.56	486.72	6
2873.01	6.09	9	67.24	142.57	231.61	491.11	4
3317.61	6.40	9	144.67	278.91	144.24	278.08	9
1785.22	3.13	5	101.04	176.91	114.63	200.71	5
5424.82	8.65	7	200.62	319.78	106.37	169.55	5
4242.91	6.74	6	163.89	260.47	108.19	171.95	6
3269.69	6.15	4	74.13	139.33	100.25	188.43	4
3587.06	7.56	4	30.67	64.66	201.61	425.01	4
1956.20	4.86	4	10.79	26.79	282.04	700.02	4
1522.48	3.78	5	33.05	82.10	174.59	433.77	5
1902.52	4.97	7	58.81	153.69	169.26	442.31	6
2869.09	7.95	5	64.38	178.47	198.11	549.18	5
2536.56	7.47	9	29.65	87.27	160.61	472.80	9
1452.41	4.18	5	11.95	34.41	91.89	264.65	1
1333.34	3.62	7	27.05	73.39	n/a	n/a	1
2743.48	6.06	2	n/a	n/a	n/a	n/a	0
2147.00	4.26	4	34.69	68.82	133.82	265.51	3
2257.53	3.91	5	55.21	95.72	114.11	197.84	4
3936.64	6.52	2	84.47	139.94	88.64	146.84	2
3164.11	5.12	4	48.70	78.80	77.83	125.93	4

APPENDIX C

AGE-PEAT 320/321	MICRO GROUP	DSDP Leg 85, Site 574 DATUM NAME	Depths [1] Site 574	Magnetostrat	AGE- Diatoms	AGE- Rads	AGE- Nannos	AGE- Forams	Avg Rad Depth [mbsf]	Avg Diatom Depth [mbsf]	Avg Nanno Depth [mbsf]	Avg Foram Depth [mbsf]
0.000		top of core	0.00	0.000	0.00	0	0.00	0.00	0			
0.440	N	top *Pseudoemiliania lacunosa*	2.25				0.44				2.25	
0.443	R	top *Stylatractus universus*	3.15			0.443			3.15			
1.308	R	base *Lamprocyrtis nigriniae (haysi)*	10.88			1.308			10.875			
1.332	R	top *Theocorythium vetulum*	10.88			1.332			10.875			
1.778	M	top Olduvai (C2n)	8.58	1.778								
1.757	R	base *Theocorythium trachelium*	10.88			1.757			10.875			
1.920	D	top *Rhizosolenia praebergonii*	9.25		1.92					9.25		
1.930	N	top *Discoaster brouweri*	9.25				1.93				9.25	
1.945	M	base Olduvai (C2n)	9.59	1.945								
2.077	R	top *Pterocanium prismatium*	10.88			2.077			10.875			
2.390	N	top *Discoaster pentaradiatus*	9.25				2.39					
2.581	M	top Gauss (C2An.1n)	12.10	2.581								
2.800	N	top *Discoaster tamalis*	13.00				2.80					
3.032	F	base C2An.1n (top Kaena)	15.02	3.032								
3.700	N	top *Reticulfenestra pseudoumbilicus*	18.75				3.70				18.75	
3.840	D	base *Thalassiosira convexa var. convexa*	21.00		3.84					21		
3.850	F	top *Globorotalia (Hirsutella) margaritae*	16.64					3.85				16.635
3.977	R	top *Spongaster pentas*	19.69			3.977			19.685			
4.032	R	top *Phormostichoartus doliolum*	16.64			4.032			19.685			
4.187	M	top C3n.1n (top Cochiti)	21.28	4.187								
4.264	R	base *Spongaster tetras*	21.34			4.264			19.685			
4.300	M	base C3n.1n (base Cochiti)	24.83	4.300								
4.493	M	top C3n.2n (top Nunivak)	26.82	4.493								
4.631	M	base C3n.2n (base Nunivak)	27.83	4.631								
4.799	M	top C3n.3n (top Sidufjall)	29.08	4.799								
4.690	D	top *Fragilariopsis (Nitzschia) cylindrica*	31.00		4.69							
4.896	M	base C3n.3n (base Sidufjall)	29.57	4.896								
4.997	M	top C3n.4n (top Thvera)	30.12	4.960								
5.040	N	top *Ceratolithus acutus*	28.25				5.04				28.25	
5.235	M	base C3n.4n (base Thvera)	31.57	5.235								
5.350	N	base *Ceratolithus acutus*	37.75				5.35				37.75	
5.570	F	base *Globborotalia tumida*	37.00					5.57				
5.573	R	top *Spongaster berminghami*	28.53			5.573			28.525			
5.700	D	base *Thalassiosira oestrupii*	35.00		5.70							
5.980	N	top *Nicklithus amplificus*	41.00				5.98					
6.033	M	top C3An.1n	39.90	6.033								
6.280	D	top *Fragilariopsis (Nitzchia) miocenica*	41.00		6.28							
6.599	R	top *Calocycletta caepa*	47.13			6.599			47.13			
6.733	M	base C3An.2n	45.50	6.733								
6.860	D	base *Thalassiosira miocenica*	47.00		6.86							
6.910	D	base *Thalassiosira convexa*	46.00		6.91							
7.530	D	top *Nitzschia porteri*	53.00		7.53							
7.750	R	Trans: *Stichocorys delmontensis to S. peregi*	54.00			7.75			54			
7.860	D	top *Thalassiosira burckliana*	62.00		7.86					62		
8.250	R	base *Solenosphaera omnitubus*	56.59			8.25			56.59			
8.392	R	top *Diartus hughesi*	56.59			8.392			56.59			
8.508	R	base *Didymocyrtis penultima*	67.50			8.508			67.5			
8.580	F	base *Globoratalia plesiotumida*	70.00					8.58				
8.629	R	top *Diartus petterssoni*	67.50			8.629			67.5			
8.760	R	Trans: *D. petterssoni > D. hughesi*	70.57			8.76			70.565			
8.769	M	top C4An	76.94	8.769								

AGE-PEAT 320/321	MICRO GROUP	DSDP Leg 85, Site 574 DATUM NAME	Depths[1] Site 574	Magnetostrat	AGE- Diatoms	AGE- Rads	AGE- Nannos	AGE- Forams	Avg Rad Depth [mbsf]	Avg Diatom Depth [mbsf]	Avg Nanno Depth [mbsf]	Avg Foram Depth [mbsf]
8.950	R	top *Stichocorys wolffii*	72.50			8.95			72.5			
8.980	D	base *Nitzschia fossiis*	66.25		8.98					66.25		
9.090	D	base *Thalassiosira burkliana*	68.50		9.09					68.5		
9.690	N	top *Discoaster hamatus*	75.25				9.69				75.25	
9.930	D	top *Actinocylus moronensis*	82.50		9.930					82.5		
10.010	R	base *Didymocyrtis antepenultima*	82.50			10.01			82.5			
10.550	N	base *Discoaster hamatus*	85.00				10.55					
10.890	N	base *Catinaster coalitus*	100.00				10.89					
11.160	D	top *Crasepedodicus coscinodiscus*	97.50		11.160					97.5		
11.340	D	base *Hemidiscus cuneiformis*	102.00		11.34					102		
11.540	F	top *Globigerinoides subquadratus*	112.85					11.54				112.85
11.580	N	first common occur. *Discoaster kugleri*	112.85				11.58				112.85	
11.630	F	base *Globigerina nepenthes*	103.00					11.63				
11.790	F	top *Globoratalia fohsi s.l.*	112.00					11.79				
11.855	R	top *Cyrtocapsella cornuta*	106.50			11.855			106.5			
11.912	R	top *Cyrtocapsella tetrapera*	110.63			11.912			110.625			
11.912	R	top *Lithopera renzae*	110.63			11.912			110.625			
12.111	R	base *Diartus petterssoni*	123.00			12.111			123			
12.120	N	top *Coronocyclus nitescens*	112.85				12.12				112.85	
12.500	D	top *Crucidenticula (Denticulopsis) nicobari*	125.45		12.50					125.45		
12.949	R	base *Lithopera neotera*	129.87			12.949			129.87			
12.990	D	top *Coscinodiscus lewisianus*	127.50		12.99					127.5		
13.410	F	base *Globoratalia fohsi s.l.*	135.00					13.41				
13.410	D	top *Thalassiosira tappanae*	139.10		13.41					139.1		
13.520	D	base *Triceratium cinnamomeum*	145.80		13.70					145.8		
13.530	N	top *Sphenolithus heteromorphus*	130.10				13.53				130.1	
13.530	N	top *Sphenolithus heteromorphus*	150.05				13.53				150.05	
13.770	F	base *Globoratalia praefohsi*	147.00					13.77				
14.190	D	top *Cestodiscus peplum*	147.50		14.19					147.5		
14.199	R	top *Didymocyrtis violina*	160.00			14.199			160			
14.229	R	top *Calocycletta costata*	161.00			14.229			161			
14.240	F	base *Globoratalia peripheroacuta*	156.00					14.24				
14.348	R	top *Didymocyrtis tubaria*	161.00			14.348			161			
14.660	F	top *Globigerinatella insueta*	186.25					14.66				186.25
14.683	R	top *Dorcadospyris forcipata*	180.00			14.683			180			
14.740	F	base *Orbulina spp*	173.00					14.74				
14.826	R	top *Liriospyris stauropora*	180.00			14.826			180			
14.910	D	top *Annellus californicus*	172.50		14.91					172.5		
15.075	R	base *Dorcadospyris alata*	189.50			15.075			189.5			
15.270	D	top *Azpeitiea (Coscinodiscus) praenodulife*	180.65		15.27					180.65		
15.360	D	base *Actinocyclus ingens*	183.80		15.36					183.8		
15.440	D	top *Nitzschia maleinterpretaria*	188.00		15.44							
15.753	R	base *Acrocubus octopylus*	199.32			15.753			199.315			
15.780	D	top *Crucidenticula kanayae*	192.00		15.78							
15.960	D	top *Thalassiosira fraga*	193.70		15.96					193.7		
16.150	D	base *Cestodiscus peplum*	198.50		16.15					198.5		
16.490	D	top *Raphidodiscus marylandicus*	199.70		16.49					199.7		
16.630	D	base *Crucidenticula kanayae*	218.00		16.63							
16.771	R	base *Lithopera renzae*	199.32			16.771			199.315			
17.430	D	bottom *Crucidenticula nicobarica*	227.50		17.43					227.5		
17.490	R	base *Calocycletta costata*	216.08			17.49			216.08			
17.540	F	top *Catapsydrax dissimilis*	227.75					17.54				227.75
17.710	N	base *Sphenolithus heteromorphus*	227.75				17.71				227.75	

AGE-PEAT 320/321	MICRO GROUP	DSDP Leg 85, Site 574 DATUM NAME	Depths [1] Site 574	Magnetostrat	AGE- Diatoms	AGE- Rads	AGE- Nannos	AGE- Forams	Avg Rad Depth [mbsf]	Avg Diatom Depth [mbsf]	Avg Nanno Depth [mbsf]	Avg Foram Depth [mbsf]
17.724	R	base *Liriospyris stauropora*	232.73			17.724			232.73			
17.724	R	base *Dorcadospyris dentata*	216.08			17.724			216.08			
17.950	N	top *Sphenolithus belemnos*	218.25				17.95				218.25	
18.180	D	top *Craspedodiscus elegans*	238.50		18.18					238.5		
18.280	N	top *Triquertrorhabdulus carinatus*	218.25				18.28				218.25	
18.547	R	top *Dorcadospyris ateuchus*	232.73			18.547			232.73			
18.567	R	base *Stichocorys wolffii*	232.73			18.567			232.73			
19.030	N	base *Sphenolithus belemnos*	237.25				19.03				237.25	
19.090	F	top *Globiquadrina binaiensis*	254.62					19.09				254.62
19.210	D	base *Thalassiosira fraga*	264.00		19.21							
19.210	D	top *Bogorovia veniamini*	263.00		19.210					263		
19.766	R	base *Didymocyrtis violina*	279.35			19.766			279.35			
19.992	R	base *Didymocyrtis tubaria*	279.35			19.992			279.35			
20.300	D	base *Actinocyclus radionovae*	294.00		20.30					294		
20.677	R	base *Stichocorys delmontensis*	280.00			20.677			280			
20.889	R	top *Lophocyrtis (Cyclampterium) pegetrum*	318.16			20.889			318.16			
21.100	F	top *Paragloborotalia kugleri*	288.00					21.10				
21.384	R	top *Theocyrtis annosa*	292.00			21.384			292			
21.391	R	base *Calocycletta virginis*	311.67			21.391			311.665			
22.260	R	base *Cyrtocapsella cornuta*	326.15			22.26			326.15			
22.347	R	base *Cyrtocapsella tetrapera*	326.15			22.347			326.15			
22.400	F	base *Globoquadrina dehiscens*	321.00					22.40				
22.619	R	top *Artophormis gracilis*	333.89			22.619			333.885			
23.000	F	base *Paragloborotalia kugleri*	353.00					23.00				
24.400	N	top *Sphenolithus ciperoensis*	360.75				24.40				360.75	
25.051	R	base *Lychnocanoma elongata*	363.33			25.051			363.325			
25.266	R	base *Calocycletta robusta*	363.33			25.266			363.325			
25.330	D	base *Rocella gelida*	356.00		25.33					356		
26.800	N	top *Sphenolithus distentus*	389.25				26.80				389.25	
27.100	N	base *Sphenolithus ciperoensis*	389.25				27.10				389.25	
27.685	R	top *Lithocyclia angusta*	420.50			27.685			420.5			
29.534	R	top *Lophocyrtis (Cyclampterium) milowi*	440.50			29.534			440.5			
30.130	R	top *Theocyrtis tuberosa*	455.00		30.13				455			

1- Depths (mbsf) were compiled from data published in the DSDP Leg 85 Volume.
2- Diatom biohorizons are from J. A. Barron, Init. Reports, DSDP Leg 85, 413-457, especially Table 3; and J. Baldauf, Init. Reports, DSDP Leg 85,457-477.
3- Radiolarian biohorizons are from C. A. Nigrini, Init. Reports, DSDP Leg 85, 511-552, especially Table 3.
4- Calcareous Nannofossil biohorizons are from Gartner and Chow, Init. Report, DSDP Leg 85, 609-621; and Pujos, Init. Report, DSDP Leg 85, 581-609.
5- Planktonic Foraminifera biohorizons are from Bridget Wade (personal correspondence) and T. Saito, Init. Report, DSDP Leg 85, 621-655
6- Magnetostatigraphy from N. Weinreich and F. Theyer, Init. Report, DSDP Leg 85,849-904, especially Table 3.

APPENDIX D

Leg	Site	Hole	Core	Section	Sample ID	Interval Top (cm)	Interval Bottom (cm)	mbsf Top	Age Ma: 9th Degree Polynomial	Binned Average Age: 0.5 My Increments	*n (Samples per Interval)*	Paleo LAT°N	Paleo LONG°E	Ba [ug/g]	Avg. Ba [ug/g]: Binned Interval	Th [ng/g]	Avg. Th [ng/g]: Binned Interval	U [ng/g]	Avg. U [ng/g]: Binned Interval	Wet Bulk Density g/cc	Dry Bulk Density g/cc	LSR [cm/kyr]	Avg LSR: Binned Interval	MAR [g/(cm2 *kyr)]	Avg MAR: Binned Interval	Avg. Total-Carbon Wt%	Corg Wt%	Corg MAR	Avg Corg MAR: Binned Interval	CaCO3 Wt%	CaCO3 MAR	Avg CaCO3 MAR: Binned Interval	Avg Bio-SiO2 Wt%	Bio-SiO2 MAR	Avg Bio-SiO2 MAR: Binned Interval	Bio-SiO2 Notes	Dust Wt% [Th/10.7]	Sum of Major Sediment Components Wt%
85	574	A	15	2	1706563	10.00	11.00	119.60	12.28636			0.83	-123.51	1036.36		44.14		168.63		1.66	1.05	1.909		2.010		11.09	0.07	0.0014		91.85	1.85		2.47	0.05		2M KOH	0.41	94.80
85	574	A	15	2	1706566	40.00	41.00	119.90	12.30208			0.82	-123.50							1.65	1.04	1.913		1.984		10.97	0.07	0.0014		90.89	1.80		2.33	0.05		2M KOH		
85	574	A	15	2	1706567	90.00	91.00	120.40	12.32819			0.81	-123.48							1.74	1.18	1.919		2.260		10.94	0.07	0.0016		90.66	2.05		2.61	0.06		2M KOH		
85	574	A	15	2	1706568	140.00	141.00	120.90	12.35419			0.80	-123.47							1.73	1.16	1.926		2.239		10.85	0.06	0.0013		89.92	2.01		2.46	0.06		2M KOH		
85	574	A	15	3	1706574	40.00	41.00	121.40	12.38010			0.79	-123.45	1015.98		45.62		124.19		1.76	1.21	1.934		2.339		10.88	0.05	0.0012		90.30	2.11		2.83	0.07		2M KOH	0.43	93.60
85	574	A	15	3	1706575	90.00	91.00	121.90	12.40590			0.79	-123.43							1.75	1.19	1.941		2.317		11.20	0.06	0.0014		92.78	2.15		1.53	0.04		2M KOH		
85	574	A	15	3	1706576	140.00	141.00	122.40	12.43161			0.78	-123.41							1.81	1.29	1.947		2.506		11.20	0.05	0.0013		92.85	2.33		2.72	0.07		2M KOH		
85	574	A	15	4	1706789	10.00	11.00	122.60	12.44186			0.77	-123.41							1.62	0.99	1.955		1.936		11.23	0.08	0.0015		92.93	1.80		2.91	0.06		2M KOH		
85	574	A	16	1	1706790	45.00	46.00	123.25	12.47509			0.76	-123.38	842.14		34.69		108.97		1.62	0.99	1.960		1.940		10.91	0.08	0.0016		90.25	1.75		3.32	0.06		2M KOH	0.32	93.98
85	574	A	16	1	1706791	90.00	91.00	123.70	12.49800	12.50	19.00	0.76	-123.37		959.15		41.12		125.20	1.62	0.99	1.968	1.97	1.948	2.07	10.64	0.06	0.0012	0.001321	88.11	1.72	1.87	5.17	0.10	0.07	2M KOH		
85	574	A	16	1	1706792	140.00	141.00	124.20	12.52337			0.75	-123.35							1.62	0.99	1.974		1.955		10.57	0.07	0.0014		87.52	1.71		6.03	0.12		2M KOH		
85	574	A	16	2	1706793	40.00	41.00	124.70	12.54865			0.74	-123.33							1.62	0.99	1.981		1.961		11.07	0.05	0.0010		91.86	1.80		2.57	0.05		2M KOH		
85	574	A	16	2	1706794	90.00	91.00	125.20	12.57385			0.73	-123.32	971.24		38.54		116.16		1.62	0.99	1.988		1.968		10.92	0.07	0.0014		90.39	1.78		4.17	0.08		2M KOH	0.36	94.99
85	574	A	16	2	1706795	140.00	141.00	125.70	12.59896			0.72	-123.30							1.62	0.99	1.994		1.975		10.99	0.08	0.0016		90.90	1.79		1.96	0.04		2M KOH		
85	574	A	16	3	1706796	40.00	41.00	126.20	12.62399			0.72	-123.28							1.62	0.99	2.001		1.981		10.87	0.05	0.0010		90.21	1.79		3.41	0.07		2M KOH		
85	574	A	16	3	1706797	90.00	91.00	126.70	12.64894			0.71	-123.27							1.62	0.99	2.006		1.986		10.89	0.05	0.0010		90.40	1.80		3.44	0.07		2M KOH		
85	574	A	16	3	1706798	120.00	121.00	127.00	12.66387			0.71	-123.26	930.03		42.62		108.04		1.62	0.99	2.016		1.996		11.10	0.05	0.0010		92.04	1.84		2.81	0.06		2M KOH	0.40	95.30
85	574	A	17	1	1706799	40.00	41.00	128.20	12.72333			0.70	-123.22							1.67	1.07	2.021		2.159		10.66	0.08	0.0017		88.19	1.90		4.17	0.09		2M KOH		
85	574	A	17	1	1706800	93.00	94.00	128.73	12.74946			0.69	-123.20							1.56	0.90	2.031		1.820		9.80	0.07	0.0013		81.10	1.48		7.24	0.13		2M KOH		
85	574	A	17	1	1706801	140.00	141.00	129.20	12.77257			0.69	-123.18							1.64	1.02	2.037		2.080		10.04	0.07	0.0015		83.08	1.73		6.78	0.14		2M KOH		
85	574	A	17	2	1706802	40.00	41.00	129.70	12.79709			0.68	-123.16	1812.78		106.30		102.23		1.68	1.08	2.042		2.214		10.53	0.06	0.0013		87.29	1.93		4.65	0.10		2M KOH	0.99	92.99
85	574	A	17	2	1706803	90.00	91.00	130.20	12.82154			0.68	-123.15							1.69	1.10	2.047		2.252		10.33	0.06	0.0014		85.64	1.93		6.25	0.14		2M KOH		
85	574	A	17	2	1706804	140.00	141.00	130.70	12.84593			0.67	-123.13							1.73	1.16	2.053		2.386		10.63	0.06	0.0014		88.10	2.10		5.10	0.12		2M KOH		
85	574	A	17	3	1706805	40.00	41.00	131.20	12.87026			0.67	-123.11							1.58	0.93	2.058		1.908		10.67	0.04	0.0008		88.61	1.69		4.90	0.09		2M KOH		
85	574	A	17	3	1706806	90.00	91.00	131.70	12.89453			0.66	-123.10	2806.89						1.68	1.08	2.063		2.236		10.64	0.06	0.0013		88.17	1.97		4.55	0.10		2M KOH		
85	574	A	18	1	1706807	40.00	41.00	132.30	12.92358			0.66	-123.08							1.63	1.01	2.068		2.080		10.25	0.07	0.0015		84.89	1.77		4.40	0.09		2M KOH		
85	574	A	18	1	1706808	90.00	91.00	132.80	12.94772			0.65	-123.06							1.58	0.93	2.073		1.922		10.07	0.07	0.0013		83.33	1.60		6.83	0.13		2M KOH		
85	574	A	18	1	1706809	140.00	141.00	133.30	12.97182			0.65	-123.05	3441.63		197.30		112.51		1.58	0.93	2.077		1.926		9.38	0.09	0.0017		77.41	1.49		10.85	0.21		2M KOH	1.84	90.19
85	574	A	18	2	1706810	38.00	39.00	133.78	12.99491			0.64	-123.03	3772.34		239.70		129.71		1.53	0.85	2.081		1.768		9.41	0.08	0.0014		77.71	1.37		12.53	0.22		2M KOH	2.24	92.56
85	574	A	18	2	1706811	92.00	93.00	134.32	13.02083	13.01	20.00	0.64	-123.01		2591.65		165.48		110.63	1.60	0.96	2.085	2.08	1.999	2.14	9.91	0.08	0.0016	0.001492	81.94	1.64	1.83	7.69	0.15	0.12	2M KOH		
85	574	A	18	2	1706812	140.00	141.00	134.80	13.04382			0.63	-123.00							1.64	1.02	2.089		2.134		10.60	0.09	0.0019		87.62	1.87		3.81	0.08		2M KOH		
85	574	A	18	3	1706813	40.00	41.00	135.30	13.06774			0.63	-122.98							1.67	1.07	2.093		2.236		10.44	0.07	0.0016		86.38	1.93		4.32	0.10		2M KOH		
85	574	A	18	3	1706814	90.00	91.00	135.80	13.09161			0.62	-122.96	1772.72		118.60		98.08		1.63	1.01	2.096		2.108		10.53	0.07	0.0015		87.14	1.84		4.28	0.09		2M KOH	1.11	92.60
85	574	A	18	3	1706815	140.00	141.00	136.30	13.11544			0.62	-122.95							1.65	1.04	2.100		2.178		10.17	0.07	0.0015		84.10	1.83		6.05	0.13		2M KOH		
85	574	A	18	4	1706864	40.00	41.00	136.80	13.13923			0.61	-122.93							1.66	1.05	2.103		2.214		10.62	0.07	0.0015		87.93	1.95		3.74	0.08		2M KOH		
85	574	A	18	4	1706865	91.00	92.00	137.31	13.16346			0.61	-122.91							1.77	1.22	2.106		2.580		10.91	0.06	0.0015		90.41	2.33		3.65	0.09		2M KOH		
85	574	A	18	4	1706866	141.00	142.00	137.81	13.18719			0.60	-122.90	1943.52						1.64	1.02	2.109		2.154		10.16	0.08	0.0017		83.99	1.81		5.35	0.12		2M KOH		
85	574	A	18	5	1706867	40.00	41.00	138.30	13.21041			0.60	-122.88							1.69	1.10	2.111		2.322		10.49	0.07	0.0016		86.87	2.02		5.54	0.13		2M KOH		
85	574	A	18	5	1706868	90.00	91.00	138.80	13.23408			0.59	-122.86							1.68	1.08	2.114		2.292		10.30	0.07	0.0016		85.26	1.95		5.66	0.13		2M KOH		
85	574	A	18	5	1706869	140.00	141.00	139.30	13.25772			0.59	-122.85							1.58	0.93	2.116		1.963		10.18	0.08	0.0016		83.80	1.64		6.92	0.14		2M KOH		
85	574	A	18	6	1706870	40.00	41.00	139.80	13.28133			0.58	-122.83							1.67	1.07	2.118		2.263		10.76	0.07	0.0016		89.11	2.02		3.28	0.07		2M KOH		
85	574	A	18	6	1706871	90.00	91.00	140.30	13.30492			0.58	-122.82							1.65	1.04	2.120		2.199		10.22	0.06	0.0013		84.69	1.86		4.80	0.11		2M KOH		
85	574	A	18	6	1706872	137.00	138.00	140.77	13.32708			0.57	-122.80							1.57	0.91	2.122		1.935		10.18	0.06	0.0012		84.31	1.63		3.52	0.07		2M KOH		
85	574	A	18	7	1706873	40.00	41.00	141.30	13.35204			0.57	-122.78							1.55	0.88	2.124		1.870		10.01	0.08	0.0015		82.78	1.55		3.38	0.06		2M KOH		
85	574	A	19	1	1706874	40.00	41.00	141.80	13.37558			0.56	-122.77							1.63	1.01	2.125		2.138		9.93	0.07	0.0015		82.23	1.76		8.01	0.17		2M KOH		
85	574	A	19	1	1706875	90.00	91.00	142.30	13.39910			0.55	-122.75	1806.39		97.58		176.87		1.68	1.08	2.127		2.305		10.17	0.06	0.0014		84.28	1.94		5.55	0.13		2M KOH	0.91	90.80
85	574	A	19	1	1706876	140.00	141.00	142.80	13.42260			0.55	-122.74							1.53	0.85	2.128		1.807		9.84	0.03	0.0005		81.71	1.48		8.93	0.16		2M KOH		
85	574	A	19	2	1706877	40.00	41.00	143.30	13.44610			0.54	-122.72							1.58	0.93	2.129		1.974		10.63	0.06	0.0012		88.08	1.74		4.49	0.09		2M KOH		
85	574	A	19	2	1706878	90.00	91.00	143.80	13.46958			0.54	-122.70							1.62	0.99	2.129		2.108		10.61	0.06	0.0013		87.89	1.85		4.01	0.08		2M KOH		
85	574	A	19	2	1706879	140.00	141.00	144.30	13.49306			0.53	-122.69	1167.41		57.33		344.96		1.63	1.01	2.130	2.13	2.142	2.12	10.70	0.06	0.0013	0.001396	88.67	1.90	1.82	4.07	0.09	0.11	2M KOH	0.54	93.34
85	574	A	19	3	1706880	40.00	41.00	144.80	13.51653	13.50	22.00	0.53	-122.67		1604.81		80.80		217.91	1.64	1.02	2.130		2.176		10.79	0.06	0.0013		89.38	1.95		3.49	0.08		2M KOH		
85	574	A	19	3	1706881	90.00	91.00	145.30	13.54000			0.52	-122.66							1.74	1.18	2.131		2.510		10.72	0.06	0.0015		88.86	2.23		3.88	0.10		2M KOH		
85	574	A	19	3	1706882	140.00	141.00	145.80	13.56346			0.52	-122.64							1.59	0.94	2.131		2.010		10.62	0.06	0.0012		88.03	1.77		4.35	0.09		2M KOH		
85	574	A	19	4	1706883	40.00	41.00	146.30	13.58692			0.51	-122.62	1840.63		87.48		131.91		1.64	1.02	2.131		2.176		10.62	0.07	0.0015		87.94	1.91		4.20	0.09		2M KOH	0.82	93.03
85	574	A	19	4	1706884	90.00	91.00	146.80	13.61039			0.51	-122.61							1.59	0.94	2.131		2.010		9.65	0.09	0.0018		79.67	1.60		11.10	0.22		2M KOH		
85	574	A	19	4	1706885	140.00	141.00	147.30	13.63386			0.50	-122.59							1.61	0.97	2.130		2.076		10.43	0.08	0.0017		86.30	1.79		5.57	0.12		2M KOH		
85	574	A	19	5	1706886	40.00	41.00	147.80	13.65733			0.50	-122.56							1.59	0.94	2.130		2.009		10.02	0.07	0.0014		82.99	1.67		8.50	0.17		2M KOH		
85	574	A	19	5	1706887	90.00	91.00	148.30	13.68081			0.50	-122.56							1.59	0.94	2.129		2.008		10.18	0.07	0.0014		84.28	1.69		7.69	0.15		2M KOH		
85	574	A	19	5	1706888	140.00	141.00	148.80	13.70430			0.49	-122.54							1.63	1.01	2.128		2.141		9.71	0.08	0.0017		80.27	1.72		7.96	0.17		2M KOH		
85	574	A	19	6	1706889	40.00	41.00	149.30	13.72779			0.49	-122.53							1.70	1.12	2.127		2.373		10.99	0.07	0.0017		91.02	2.16		2.44	0.06		2M KOH		
85	574	A	19	6	1706890	90.00	91.00	149.80	13.75130			0.48	-122.51							1.69	1.10	2.126		2.338		10.77	0.06	0.0014		89.27	2.09		3.05	0.07		2M KOH		
85	574	A	19	6	1706891	140.00	141.00	150.30	13.77482			0.48	-122.50							1.74	1.18	2.125		2.503		10.88	0.04	0.0010		90.28	2.26		1.96	0.05		2M KOH		
85	574	A	19	7	1706892	40.00	41.00	150.80	13.79836			0.47	-122.48	1809.78		101.59		86.47		1.56	0.90	2.124		1.903		10.41	0.06	0.0011		86.26	1.64		1.32	0.03		2M KOH	0.95	88.59
85	574	A	20	1	1706893	53.00	54.00	151.43	13.82804			0.47	-122.46							1.64	1.02	2.122		2.168		9.92	0.08	0.0017		81.96	1.78		6.11	0.13		2M KOH		
85	574	A	20	1	1706894	90.00	91.00	151.80	13.84548			0.46	-122.45							1.64	1.02	2.120		2.166		10.10	0.08	0.0017		83.54	1.81		5.92	0.13		2M KOH		
85	574	A	20	1	1706895	140.00	141.00	152.30	13.86907			0.46	-122.43							1.63	1.01	2.119		2.131		10.64	0.06	0.0013		88.11	1.88		3.78	0.08		2M KOH		
85	574	A	20	2	1706898	40.00	41.00	152.80	13.89267			0.45	-122.42							1.62	0.99	2.117		2.096		10.73	0.06	0.0013		88.96	1.86		3.98	0.08		2M KOH		
85	574	A	20	2	1706897	90.00	91.00	153.30	13.91630			0.45	-122.40							1.66	1.05	2.115		2.226		10.54	0.06	0.0013		87.36	1.95		4.13	0.09		2M KOH		
85	574	A	20	2	1706896	140.00	141.00	153.80	13.93995			0.44	-122.38							1.60	0.96	2.113		2.026		10.52	0.06	0.0012		87.16	1.77		4.20	0.09		2M KOH		
85	574	A	20	3	1706967	40.00	41.00	154.30	13.96363			0.44	-122.37	2337.53		186.30		120.81		1.65	1.04	2.111		2.189		10.36	0.05	0.0011		85.89	1.88		4.90	0.11		2M KOH	1.74	92.58
85	574	A	20	3	1706966	90.00	91.00	154.80	13.98733			0.43	-122.35							1.67	1.07	2.108		2.252		10.65	0.05	0.0011		88.31	1.99		3.37	0.08		2M KOH		
85	574	A	20	3	1706965	140.00	141.00	155.30	14.01106	14.01	23.00	0.43	-122.34		3022.36		162.18		121.32	1.66	1.05	2.106	2.10	2.217	2.22	10.37	0.06	0.0013	0.001162	85.95	1.91	1.91	3.58	0.08	0.10	2M KOH		
85	574	A	20	4	1706968	40.00	41.00	155.80	14.03482			0.42	-122.32	6449.50		218.58		174.18		1.65	1.04	2.103		2.181		9.13	0.07	0.0015		75.52	1.65		9.69	0.21		2M KOH	2.04	87.32
85	574	A	20	4	1706969	90.00	91.00	156.30	14.05861			0.42	-122.30							1.61	0.97	2.101		2.047		9.49	0.04	0.0008		78.67	1.61		7.90	0.16		2M KOH		
85	574	A	20	4	1706970	140.00	141.00	156.80	14.08243			0.41	-122.29	3707.14		281.12		118.19		1.62	0.99	2.098		2.077		10.16	0.04	0.0008		84.32	1.75		4.92	0.10		2M KOH	2.63	91.91
85	574	A	20	5	1706973	40.00	41.00	157.30	14.10628			0.41	-122.27							1.57	0.91	2.095		1.910		9.14	0.05	0.0010		75.76	1.45		9.07	0.17		2M KOH		
85	574	A	20	5	1706972	90.00	91.00	157.80	14.13017			0.41	-122.26	3631.01						1.59	0.94	2.092		1.973		9.24	0.04	0.0008		76.67	1.51		9.29	0.18		2M KOH		
85	574	A	20	5	1706971	140.00	141.00	158.30	14.15409			0.40	-122.24	1753.45		100.99		87.94		1.72	1.15	2.089		2.395		re-run	0.04	0.0010		92.16	2.21		2.14	0.05		2M KOH	0.94	95.28
85	574	A	20	6	1706974	40.00	41.00	158.80	14.17804			0.40	-122.22							1.75	1.19	2.086		2.489		10.66	0.04	0.0010		88.53	2.20		2.86	0.07		switched ti		
85	574	A	20	6	1706975	90.00	91.00	159.30	14.20203			0.39	-122.21							1.79	1.26	2.082		2.616		11.05	0.03	0.0008		91.86	2.40		2.28	0.06		1M KOH		
85	574	A	20	6	1706976	140.00	141.00	159.80	14.22606			0.39	-122.19							1.68	1.08	2.079		2.254		10.81	0.03	0.0007		89.77	2.02		2.51	0.06		1M KOH		
85	574	A	20	7	1706977	40.00	41.00	160.30	14.25013			0.38	-122.17	1468.09		84.47		140.32		1.75	1.19	2.077		2.480		10.99	0.05	0.0012		91.19	2.26		2.54	0.06		1M KOH	0.79	94.56
85	574	A	21	1	1706978	40.00	41.00	160.30	14.25013			0.38	-122.17							1.75	1.19	2.074		2.476		10.76	0.07	0.0017		89.15	2.21		2.89	0.07		1M KOH		
85	574	A	21	1	1706979	90.00	91.00	160.80	14.27424			0.38	-122.16							1.70	1.12	2.072		2.311		10.75	0.04	0.0009		89.26	2.06		4.32	0.10		1M KOH		
85	574	A	21	1	1706980	140.00	141.00	161.30	14.29839			0.37	-122.14							1.72	1.15	2.069		2.372		10.70	0.04	0.0009		88.80	2.11		3.89	0.09		1M KOH		
85	574	A	21	2	1706983	40.00	41.00	161.80	14.32258			0.37	-122.12	2351.72		52.97		117.75		1.72	1.15	2.065		2.368		10.76	0.04	0.0009		89.36	2.12		4.33	0.10		1M KOH	0.50	94.22
85	574	A	21	2	1706982	90.00	91.00	162.30	14.34681			0.36	-122.11							1.72	1.15	2.062		2.364		10.56	0.04	0.0009		87.65	2.07		4.27	0.10		1M KOH		
85	574	A	21	2	1706981	140.00	141.00	162.80	14.37108			0.36	-122.09							1.73	1.16	2.058		2.392		10.48	0.05	0.0012		86.90	2.08		4.31	0.10		1M KOH		
85	574	A	21	3	1706984	40.00	41.00	163.30	14.39540			0.35	-122.08							1.69	1.10	2.054		2.259		10.56	0.04	0.0009		87.62	1.98		4.40	0.10		1M KOH		
85	574	A	21	3	1706985	90.00	91.00	163.80	14.41977			0.35	-122.06	1801.87		64.14		187.72		1.69	1.10	2.050		2.255		10.33	0.04	0.0009		85.76	1.93		4.38	0.10		1M KOH	0.60	90.78
85	574	A	21	3	1706986	140.00	141.00	164.30	14.44418			0.34	-122.04	2851.93						1.75	1.19	2.046		2.443		10.47	0.04	0.0010		86.93	2.12		3.97	0.10		1M KOH		
85	574	A	21	4	1706989	40.00	41.00	164.80	14.46864			0.34	-122.03							1.78	1.24	2.042		2.534		10.53	0.04	0.0010		87.45	2.22		4.14	0.10		1M KOH		
85	574	A	21	4	1706988	90.00	91.00	165.30	14.49314	14.48	22.00	0.33	-122.01		2300.46		61.46		211.56	1.72	1.15	2.038	2.04	2.337	2.30	10.55	0.02	0.0005	0.000965	87.69	2.05	2.01	4.50	0.11	0.09	1M KOH		

Leg	Site	Hole	Core	Section	Sample ID	Interval Top (cm)	Interval Bottom (cm)	mbsf Top	Age Ma: 9th Degree Polynomial	Binned Average Age: 0.5 My Increments	*n (Samples per Interval)*	Paleo LAT°N	Paleo LONG°E	Ba [ug/g]	Avg. Ba [ug/g]: Binned Interval	Th [ng/g]	Avg. Th [ng/g]: Binned Interval	U [ng/g]	Avg. U [ng/g]: Binned Interval	Wet Bulk Density g/cc	Dry Bulk Density g/cc	LSR [cm/kyr]	Avg LSR: Binned Interval	MAR [g/(cm2 *kyr)]	Avg MAR: Binned Interval	Avg. Total-Carbon Wt%	Corg Wt%	Corg MAR	Avg Corg MAR: Binned Interval	CaCO3 Wt%	CaCO3 MAR	Avg CaCO3 MAR: Binned Interval	Avg Bio-SiO2 Wt%	Bio-SiO2 MAR	Avg Bio-SiO2 MAR: Binned Interval	Bio-SiO2 Notes	Dust Wt% [Th/10.7]	Sum of Major Sediment Components Wt%
85	574	A	21	4	1706987	140.00	141.00	165.80	14.51769			0.33	-121.99	2658.42		44.58		378.22		1.71	1.13	2.034		2.301		10.26	0.04	0.0009		85.17	1.96		4.26	0.10		1M KOH	0.42	89.89
85	574	A	21	5	1706990	40.00	41.00	166.30	14.54230			0.32	-121.98							1.71	1.13	2.030		2.296		10.47	0.04	0.0009		86.94	2.00		4.80	0.11		1M KOH		
85	574	A	21	5	1706991	90.00	91.00	166.80	14.56695			0.32	-121.96							1.67	1.07	2.026		2.165		10.48	0.04	0.0009		86.92	1.88		4.18	0.09		1M KOH		
85	574	A	21	5	1706992	140.00	141.00	167.30	14.59164			0.31	-121.94							1.73	1.16	2.022		2.351		10.68	0.04	0.0009		88.67	2.08		3.99	0.09		1M KOH		
85	574	A	21	6	1707129	40.00	41.00	167.80	14.61639			0.31	-121.93	1656.58		45.45		378.15		1.63	1.01	2.019		2.030		10.43	0.05	0.0010		88.47	1.80		3.54	0.07		1M KOH	0.42	92.48
85	574	A	21	6	1707130	80.00	81.00	168.20	14.63623			0.30	-121.91							1.63	1.01	2.014		2.026		10.40	0.04	0.0008		86.33	1.75		3.89	0.08		1M KOH		
85	574	A	22	1	1707131	40.00	41.00	168.80	14.66605			0.30	-121.89							1.72	1.15	2.010		2.305		10.40	0.04	0.0009		86.27	1.99		4.38	0.10		1M KOH		
85	574	A	22	1	1707132	90.00	91.00	169.30	14.69095			0.29	-121.88	3279.00						1.77	1.22	2.006		2.457		10.75	0.04	0.0010		89.23	2.19		3.25	0.08		1M KOH		
85	574	A	22	1	1707133	140.00	141.00	169.80	14.71590			0.29	-121.86	2336.06		77.15		67.21		1.62	0.99	2.001		1.982		10.52	0.04	0.0008		87.24	1.73		3.37	0.07		1M KOH	0.72	91.37
85	574	A	22	2	1707136	40.00	41.00	170.30	14.74091			0.28	-121.84							1.72	1.15	1.997		2.290		10.43	0.05	0.0011		86.50	1.98		4.80	0.11		1M KOH		
85	574	A	22	2	1707135	90.00	91.00	170.80	14.76597			0.28	-121.83							1.71	1.13	1.993		2.254		10.76	0.05	0.0011		89.30	2.01		3.31	0.07		1M KOH		
85	574	A	22	2	1707134	140.00	141.00	171.30	14.79109			0.27	-121.80	2852.17						1.73	1.16	1.989		2.312		10.98	0.05	0.0012		91.10	2.11		2.35	0.05		1M KOH		
85	574	A	22	3	1707137	40.00	41.00	171.80	14.81625			0.26	-121.77	2126.43		62.61		84.61		1.72	1.15	1.985		2.276		10.88	0.05	0.0011		90.29	2.05		2.70	0.06		1M KOH	0.59	93.63
85	574	A	22	3	1707138	90.00	91.00	172.30	14.84147			0.26	-121.75	3409.34						1.72	1.15	1.980		2.271		11.14	0.04	0.0009		92.50	2.10		1.87	0.04		1M KOH		
85	574	A	22	3	1707139	140.00	141.00	172.80	14.86675			0.25	-121.73							1.82	1.30	1.976		2.575		11.17	0.04	0.0010		92.76	2.39		1.82	0.05		1M KOH		
85	574	A	22	4	1707142	40.00	41.00	173.30	14.89207			0.24	-121.70							1.58	0.93	1.972		1.829		9.52	0.04	0.0007		78.99	1.44		8.29	0.15		1M KOH		
85	574	A	22	4	1707141	90.00	91.00	173.80	14.91746			0.24	-121.68	2293.70		112.27		155.63		1.68	1.08	1.968		2.133		10.24	0.05	0.0011		84.93	1.81		2.41	0.05		1M KOH	1.05	88.44
85	574	A	22	4	1707140	140.00	141.00	174.30	14.94289			0.23	-121.66	3349.71						1.63	1.01	1.964		1.975		9.79	0.04	0.0008		81.22	1.60		3.27	0.06		1M KOH		
85	574	A	22	5	1707143	40.00	41.00	174.80	14.96838			0.22	-121.63							1.65	1.04	1.959		2.032		9.94	0.03	0.0006		82.55	1.68		6.42	0.13		1M KOH		
85	574	A	22	5	1707144	90.00	91.00	175.30	14.99393	15.01	20.00	0.22	-121.61		2873.01		67.24		231.61	1.77	1.22	1.955		2.395		10.87	0.03	0.0007		90.29	2.16		3.01	0.07		1M KOH		
85	574	A	22	5	1707145	140.00	141.00	175.80	15.01953			0.21	-121.59	2235.77		24.80		102.96		1.71	1.13	1.951	1.95	2.207	2.12	10.59	0.05	0.0011	0.000929	87.89	1.94	1.84	1.39	0.03	0.09	1M KOH	0.23	89.57
85	574	A	22	6	1707148	40.00	41.00	176.30	15.04518			0.20	-121.56							1.72	1.15	1.947		2.233		10.65	0.03	0.0007		88.44	1.97		4.24	0.09		1M KOH		
85	574	A	22	6	1707147	90.00	91.00	176.80	15.07089			0.19	-121.54							1.75	1.19	1.943		2.319		11.14	0.04	0.0009		92.55	2.15		2.47	0.06		1M KOH		
85	574	A	22	6	1707146	140.00	141.00	177.30	15.09665			0.19	-121.52	3728.21						1.65	1.04	1.939		2.011		10.20	0.05	0.0010		84.59	1.70		6.90	0.14		1M KOH		
85	574	A	22	7	1707149	40.00	41.00	177.80	15.12247			0.18	-121.49	3368.63		69.27		583.23		1.69	1.10	1.935		2.128		9.61	0.04	0.0009		79.77	1.70		9.72	0.21		1M KOH	0.65	90.18
85	574	A	23	1	1707150	40.00	41.00	178.30	15.14834			0.17	-121.47							1.67	1.07	1.931		2.063		9.39	0.06	0.0012		77.71	1.60		9.55	0.20		1M KOH		
85	574	A	23	1	1707151	90.00	91.00	178.80	15.17426			0.17	-121.44							1.65	1.04	1.927		1.998		10.31	0.05	0.0010		85.54	1.71		6.03	0.12		1M KOH		
85	574	A	23	1	1707152	140.00	141.00	179.30	15.20024			0.16	-121.42							1.47	0.76	1.923		1.452		10.15	0.05	0.0007		84.13	1.22		4.58	0.07		1M KOH		
85	574	A	23	2	1707155	40.00	41.00	179.80	15.22627			0.15	-121.40							1.60	0.96	1.919		1.840		10.42	0.04	0.0007		86.44	1.59		5.86	0.11		1M KOH		
85	574	A	23	2	1707154	90.00	91.00	180.30	15.25235			0.15	-121.37	2493.12						1.69	1.10	1.915		2.106		10.43	0.05	0.0011		86.54	1.82		6.09	0.13		1M KOH		
85	574	A	23	2	1707153	140.00	141.00	180.80	15.27849			0.14	-121.35	6423.28		500.60		204.82		1.68	1.08	1.911		2.072		7.80	0.07	0.0015		64.40	1.33		15.72	0.33		1M KOH	4.68	84.87
85	574	A	23	3	1707156	40.00	41.00	181.30	15.30467			0.13	-121.32	1817.54		88.02		68.98		1.69	1.10	1.907		2.098		10.26	0.05	0.0010		85.03	1.78		6.23	0.13		1M KOH	0.82	92.13
85	574	A	23	3	1707157	90.00	91.00	181.80	15.33091			0.12	-121.30	6709.45		292.10		124.36		1.64	1.02	1.904		1.944		8.45	0.06	0.0012		69.88	1.36		14.45	0.28		1M KOH	2.73	87.12
85	574	A	23	3	1707158	140.00	141.00	182.30	15.35721			0.12	-121.28							1.63	1.01	1.900		1.911		9.85	0.05	0.0010		81.66	1.56		11.55	0.22		1M KOH		
85	574	A	23	4	1707161	40.00	41.00	182.80	15.38355			0.11	-121.25	1535.53		81.61		91.01		1.69	1.10	1.896		2.085		10.19	0.04	0.0008		84.62	1.76		5.29	0.11		1M KOH	0.76	90.71
85	574	A	23	4	1707160	90.00	91.00	183.30	15.40994			0.10	-121.23							1.75	1.19	1.893		2.259		10.35	0.04	0.0009		85.93	1.94		4.44	0.10		1M KOH		
85	574	A	23	4	1707159	140.00	141.00	183.80	15.43639			0.09	-121.20	1885.75		83.27		155.71		1.67	1.07	1.889		2.018		10.36	0.04	0.0008		86.01	1.74		5.23	0.11		1M KOH	0.78	92.06
85	574	A	23	5	1707162	40.00	41.00	184.30	15.46288			0.09	-121.18	5504.34		100.58		234.32		1.58	0.93	1.885		1.749		8.45	0.06	0.0010		69.99	1.22		14.14	0.25		1M KOH	0.94	85.13
85	574	A	23	5	1707163	90.00	91.00	184.80	15.48942			0.08	-121.15	1681.62		84.71		278.58		1.58	0.93	1.882		1.746		10.21	0.05	0.0009		84.65	1.48		7.22	0.13		1M KOH	0.79	92.71
85	574	A	23	5	1707164	140.00	141.00	185.30	15.51602	15.45	14.00	0.07	-121.13		3317.61		175.84		165.40	1.57	0.91	1.879	1.89	1.713	1.93	8.80	0.07	0.0012	0.001006	72.78	1.25	1.52	8.75	0.15	0.17	1M KOH		
85	574	A	23	6	1707165	40.00	41.00	185.80	15.54266			0.07	-121.10							1.57	0.91	1.876		1.710		9.03	0.04	0.0007		74.93	1.28		7.55	0.13		1M KOH		
85	574	A	23	6	1707166	77.00	78.00	186.17	15.56240			0.06	-121.09	1807.89		113.72		117.69		1.62	0.99	1.848		1.830		10.12	0.06	0.0011		83.89	1.54		3.78	0.07		1M KOH	1.06	88.79
85	574	C	1	1	1707187	40.00	41.00	194.90	16.03505			0.05	-120.86	2331.75		127.70		183.76		1.59	0.94	1.846	1.82	1.741	1.75	9.98	0.04	0.0007	0.000880	82.88	1.44	1.46	3.78	0.07	0.10	1M KOH	1.19	87.89
85	574	C	1	1	1707188	90.00	91.00	195.40	16.06247	16.09	10.00	0.04	-120.84	1930.62	1785.22	73.86	101.04	96.20	114.63	1.59	0.94	1.823		1.719		10.30	0.05	0.0009		85.40	1.47		2.78	0.05		1M KOH	0.69	88.92
85	574	C	1	1	1707189	140.00	141.00	195.90	16.08991			0.03	-120.83							1.59	0.94	1.821		1.717		10.19	0.05	0.0009		83.35	1.43		2.17	0.04		1M KOH		
85	574	C	1	2	1707192	40.00	41.00	196.40	16.11738			0.03	-120.82							1.64	1.02	1.819		1.858		10.64	0.06	0.0011		88.11	1.64		4.89	0.09		1M KOH		
85	574	C	1	2	1707191	90.00	91.00	196.90	16.14489			0.02	-120.80	1644.37		98.76		101.76		1.64	1.02	1.817		1.856		10.77	0.05	0.0009		89.31	1.66		4.00	0.07		1M KOH	0.92	94.28
85	574	C	1	2	1707190	140.00	141.00	197.40	16.17242			0.02	-120.79							1.58	0.93	1.815		1.684		9.66	0.05	0.0008		80.06	1.35		9.65	0.16		1M KOH		
85	574	C	1	3	1707373	40.00	41.00	197.90	16.19997			0.01	-120.78							1.63	1.01	1.814		1.824		9.19	0.07	0.0013		75.97	1.39		12.10	0.22		1M KOH		
85	574	C	1	3	1707374	90.00	91.00	198.40	16.22756			0.00	-120.76							1.51	0.82	1.812		1.482		9.64	0.04	0.0006		80.00	1.19		8.50	0.13		1M KOH		
85	574	C	1	3	1707375	140.00	141.00	198.90	16.25516			0.00	-120.75	1211.46		91.15		73.73		1.65	1.04	1.810		1.878		10.42	0.04	0.0008		86.51	1.62		4.86	0.09		1M KOH	0.85	92.26
85	574	C	1	4	1707380	40.00	41.00	199.40	16.28279			-0.01	-120.73							1.68	1.08	1.809		1.961		6.57	0.03	0.0006		54.49	1.07		4.75	0.09		1M KOH		
85	574	C	1	4	1707381	90.00	91.00	199.90	16.31044			-0.01	-120.72							1.61	0.97	1.808		1.761		9.94	0.04	0.0007		82.55	1.45		7.92	0.14		1M KOH		
85	574	C	1	4	1707382	140.00	141.00	200.40	16.33811			-0.02	-120.71							1.63	1.01	1.806		1.817		10.19	0.04	0.0007		84.60	1.54		5.02	0.09		1M KOH		
85	574	C	1	5	1707387	40.00	41.00	200.90	16.36580			-0.02	-120.69	1773.29				63.89		1.70	1.12	1.805		2.013		10.69	0.03	0.0006		88.82	1.79		3.10	0.06		1M KOH		
85	574	C	1	5	1707388	90.00	91.00	201.40	16.39351			-0.03	-120.68	5572.19		147.36		85.35		1.53	0.85	1.804		1.532		8.72	0.04	0.0006		72.34	1.11		3.50	0.05		1M KOH	1.38	77.26
85	574	C	1	5	1707389	140.00	141.00	201.90	16.42123			-0.03	-120.67							1.46	0.74	1.803		1.334		7.71	0.07	0.0009		63.69	0.85		14.70	0.20		1M KOH		
85	574	C	1	6	1707390	10.00	11.00	202.10	16.43233			-0.03	-120.66	8692.77		400.63		158.18		1.44	0.71	1.801		1.276		6.12	0.06	0.0008		50.48	0.64		22.10	0.28		1M KOH	3.74	76.38
85	574	C	2	1	1707395	40.00	41.00	204.40	16.56006	16.50	16.00	-0.06	-120.60		5424.82		200.62		106.37	1.57	0.91	1.800	1.80	1.642	1.59	10.02	0.04	0.0007	0.000784	83.16	1.37	1.18	6.90	0.11	0.14	1M KOH		
85	574	C	2	1	1707396	90.00	91.00	204.90	16.58786			-0.07	-120.58	9382.56		188.09		158.58		1.51	0.82	1.799		1.471		9.03	0.06	0.0009		74.76	1.10		11.00	0.16		1M KOH	1.76	87.58
85	574	C	2	1	1707397	140.00	141.00	205.40	16.61566			-0.07	-120.57							1.58	0.93	1.798		1.668		9.42	0.06	0.0010		77.99	1.30		9.10	0.15		1M KOH		
85	574	C	2	2	1707398	40.00	41.00	205.90	16.64347			-0.08	-120.56	4105.62		191.70		117.33		1.43	0.69	1.798		1.245		8.74	0.05	0.0006		72.43	0.90		13.50	0.17		1M KOH	1.79	87.77
85	574	C	2	2	1707399	90.00	91.00	206.40	16.67129			-0.08	-120.54	6426.42						1.42	0.68	1.797		1.217		7.15	0.06	0.0007		59.04	0.72		17.40	0.21		1M KOH		
85	574	C	2	2	1707400	142.00	143.00	206.92	16.70022			-0.09	-120.53							1.52	0.83	1.797		1.498		8.45	0.08	0.0012		69.69	1.04		6.60	0.10		1M KOH		
85	574	C	2	3	1707401	40.00	41.00	207.40	16.72692			-0.09	-120.52							1.61	0.97	1.797		1.751		9.71	0.05	0.0009		80.50	1.41		7.90	0.14		1M KOH		
85	574	C	2	3	1707402	90.00	91.00	207.90	16.75474			-0.10	-120.50	2020.88		75.35		54.89		1.60	0.96	1.797		1.723		n/a	0.05	0.0009		79.24	1.37		8.90	0.15		1M KOH	0.70	88.89
85	574	C	2	3	1707403	140.00	141.00	208.40	16.78256			-0.10	-120.49							1.68	1.08	1.797		1.948		10.08	0.05	0.0010		83.59	1.63		5.60	0.11		1M KOH		
85	574	C	2	4	1707404	40.00	41.00	208.90	16.81038			-0.11	-120.47							1.62	0.99	1.798		1.780		9.97	0.04	0.0007		82.77	1.47		5.90	0.11		1M KOH		
85	574	C	2	4	1707405	90.00	91.00	209.40	16.83820			-0.12	-120.46							1.63	1.01	1.798		1.808		9.84	0.04	0.0007		81.61	1.48		5.60	0.10		1M KOH		
85	574	C	2	4	1707406	140.00	141.00	209.90	16.86600			-0.12	-120.45	2623.33		154.30		64.72		1.59	0.94	1.798		1.696		9.66	0.04	0.0007		80.13	1.36		6.90	0.12		1M KOH	1.44	88.51
85	574	C	2	5	1707408	46.00	47.00	210.46	16.89714			-0.13	-120.43							1.64	1.02	1.799		1.837		9.51	0.05	0.0009		78.84	1.45		6.80	0.12		1M KOH		
85	574	C	2	5	1707409	92.00	93.00	210.92	16.92271			-0.13	-120.42							1.59	0.94	1.799		1.697		9.09	0.03	0.0005		75.47	1.28		10.40	0.18		1M KOH		
85	574	C	2	5	1707410	143.00	144.00	211.43	16.95105			-0.14	-120.40	6409.28		264.00		202.32		1.44	0.71	1.800		1.275		7.35	0.06	0.0008		60.71	0.77		16.20	0.21		1M KOH	2.47	79.44
85	574	C	2	6	1707411	40.00	41.00	211.90	16.97716			-0.14	-120.39							1.41	0.66	1.801		1.191		7.14	0.06	0.0007		59.01	0.70		16.40	0.20		1M KOH		
85	574	C	2	6	1707412	93.00	94.00	212.43	17.00659	17.00	19.00	-0.15	-120.38	6853.98	4242.91		163.89		108.19	1.39	0.63	1.801	1.80	1.135	1.59	6.27	0.06	0.0007	0.000862	51.72	0.59	1.20	23.70	0.27	0.16	1M KOH		
85	574	C	2	6	1707413	140.00	141.00	212.90	17.03267			-0.16	-120.36							1.52	0.83	1.802		1.502		9.25	0.05	0.0008		76.73	1.15		8.50	0.13		1M KOH		
85	574	C	2	7	1707414	36.00	37.00	213.36	17.05819			-0.16	-120.35	3449.46		133.70		69.67		1.48	0.77	1.803		1.390		8.90	0.05	0.0007		73.71	1.02		20.30	0.28		1M KOH	1.25	95.31
85	574	C	3	1	1707415	40.00	41.00	213.90	17.08812			-0.17	-120.32							1.48	0.77	1.804		1.391		8.97	0.07	0.0010		74.14	1.03		10.30	0.14		1M KOH		
85	574	C	3	1	1707416	90.00	91.00	214.40	17.11582			-0.17	-120.31							1.52	0.83	1.806		1.505		8.86	0.07	0.0011		73.22	1.10		11.30	0.17		1M KOH		
85	574	C	3	1	1707417	140.00	141.00	214.90	17.14350			-0.18	-120.29							1.59	0.94	1.807		1.704		9.66	0.07	0.0012		79.92	1.36		9.20	0.16		1M KOH		
85	574	C	3	2	1707418	40.00	41.00	215.40	17.17116			-0.18	-120.27	2674.32		91.87		82.14		1.64	1.02	1.808		1.847		9.78	0.05	0.0009		81.02	1.50		7.70	0.14		1M KOH	0.86	89.63
85	574	C	3	2	1707419	91.00	92.00	215.91	17.19935			-0.19	-120.25							1.57	0.91	1.810		1.650		9.57	0.07	0.0012		79.20	1.31		7.90	0.13		1M KOH		
85	574	C	3	2	1707420	140.00	141.00	216.40	17.22641			-0.20	-120.23							1.52	0.83	1.811		1.510		9.02	0.07	0.0011		74.64	1.13		10.10	0.15		1M KOH		
85	574	C	3	3	1707421	36.00	37.00	216.86	17.25179			-0.20	-120.21	3447.11		175.60		122.12		1.60	0.96	1.813		1.739		9.11	0.06	0.0010		75.41	1.31		9.30	0.16		1M KOH	1.64	86.41
85	574	C	3	3	1707422	90.00	91.00	217.40	17.28156			-0.21	-120.19							1.49	0.79	1.815		1.428		7.46	0.08	0.0011		61.53	0.88		16.50	0.24		1M KOH		
85	574	C	3	3	1707423	140.00	141.00	217.90	17.30909			-0.21	-120.17							1.69	1.10	1.817		1.998		10.27	0.05	0.0010		85.17	1.70		4.30	0.09		1M KOH		
85	574	C	3	4	1707424	40.00	41.00	218.40	17.33660			-0.22	-120.15	2465.21		17.34		156.99		1.70	1.12	1.818		2.028		10.18	0.06	0.0012		84.28	1.71		4.70	0.10		1M KOH	0.16	89.20
85	574	C	3	4	1707425	72.00	73.00	218.72	17.35419			-0.22	-120.14	4953.69		186.80		77.84		1.70	1.12	1.831		2.042		9.55	0.04	0.0008		79.25	1.62		7.00	0.14		1M KOH	1.75	88.04
85	574	C	4	1	1707429	40.00	41.00	223.40	17.60974	17.51	11.00	-0.28	-119.96		3269.69		74.13		100.25	1.60	0.96	1.833	1.84	1.757	1.88	10.09	0.05	0.0009	0.001064	83.60	1.47	1.55	4.80	0.08	0.12	1M KOH		
85	574	C	4	1	1707430	90.00	91.00	223.90	17.63683			-0.28	-119.94							1.71	1.13	1.847		2.089		10.31	0.05	0.0010		85.52	1.79		4.10	0.09		1M KOH		
85	574	C	4	1	1707431	143.00	144.00	224.43	17.66550			-0.29	-119.92	2268.28		47.97		77.52		1.63	1.01	1.850		1.861		10.56	0.04	0.0007		87.62	1.63		4.20	0.08		1M KOH	0.45	92.31
85	574	C	4	2	1707432	37.00	38.00	224.87	17.68927			-0.29	-119.90							1.70	1.12	1.853		2.067		10.40	0.07	0.0014		86.05	1.78		4.30	0.09		1M KOH		
85	574	C	4	2	1707433	88.00	89.00	225.38	17.71676			-0.30	-119.88							1.56	0.90	1.857		1.664		9.60	0.06	0.0010		79.44	1.32		8.80	0.15		1M KOH		

Leg	Site	Hole	Core	Section	Sample ID	Interval Top (cm)	Interval Bottom (cm)	mbsf Top	Age Ma: 9th Degree Polynomial	Binned Average Age: 0.5 My Increments	*n (Samples per Interval)*	Paleo LAT°N	Paleo LONG°E	Ba [ug/g]	Avg. Ba [ug/g]: Binned Interval	Th [ng/g]	Avg. Th [ng/g]: Binned Interval	U [ng/g]	Avg. U [ng/g]: Binned Interval	Wet Bulk Density g/cc	Dry Bulk Density g/cc	LSR [cm/kyr]	Avg LSR: Binned Interval	MAR [g/(cm2 *kyr)]	Avg MAR: Binned Interval	Avg. Total-Carbon Wt%	Corg Wt%	Corg MAR	Avg Corg MAR: Binned Interval	CaCO3 Wt%	CaCO3 MAR	Avg CaCO3 MAR: Binned Interval	Avg Bio-SiO2 Wt%	Bio-SiO2 MAR	Avg Bio-SiO2 MAR: Binned Interval	Bio-SiO2 Notes	Dust Wt% [Th/10.7]	Sum of Major Sediment Components Wt%
85	574	C	4	2	1707434	138.00	139.00	225.88	17.74367			-0.30	-119.87	3391.59		44.41		88.64		1.57	0.91	1.860		1.696		9.80	0.07	0.0012		81.04	1.37		7.00	0.12		1M KOH	0.42	88.53
85	574	C	4	3	1707439	40.00	41.00	226.40	17.77160			-0.31	-119.85							1.68	1.08	1.887		2.046		10.27	0.06	0.0012		85.08	1.74		5.20	0.11		1M KOH		
85	574	C	5	1	1707440	39.00	40.00	232.89	18.11507	18.07	8.00	-0.38	-119.61		3587.06		30.67		201.61	1.67	1.07	1.892	1.92	2.021	2.11	10.88	0.04	0.0008	0.001029	90.34	1.83	1.81	2.20	0.04	0.09	1M KOH		
85	574	C	5	1	1707441	90.00	91.00	233.40	18.14162			-0.39	-119.58	3872.63		45.25		221.08		1.75	1.19	1.923		2.296		10.27	0.05	0.0011		85.18	1.96		4.30	0.10		1M KOH	0.42	89.95
85	574	C	5	1	1707442	142.00	143.00	233.92	18.16862			-0.40	-119.55							1.71	1.13	1.928		2.181		10.64	0.06	0.0013		88.12	1.92		3.10	0.07		1M KOH		
85	574	C	5	2	1707443	39.00	40.00	234.39	18.19296			-0.40	-119.53							1.74	1.18	1.934		2.278		10.14	0.05	0.0011		84.07	1.91		4.90	0.11		1M KOH		
85	574	C	5	2	1707444	92.00	93.00	234.92	18.22033			-0.41	-119.50							1.64	1.02	1.939		1.980		10.21	0.04	0.0008		84.80	1.68		4.00	0.08		1M KOH		
85	574	C	5	2	1707445	140.00	141.00	235.40	18.24506			-0.42	-119.48	3496.97		2.36		295.10		1.63	1.01	1.944		1.955		10.11	0.04	0.0008		83.94	1.64		5.00	0.10		1M KOH	0.02	89.00
85	574	C	5	3	1707446	37.00	38.00	235.87	18.26921			-0.42	-119.45							1.66	1.05	1.949		2.052		10.27	0.04	0.0008		85.23	1.75		5.30	0.11		1M KOH		
85	574	C	5	3	1707447	90.00	91.00	236.40	18.29636			-0.43	-119.42							1.76	1.21	1.954		2.364		10.28	0.04	0.0009		85.33	2.02		3.00	0.07		1M KOH		
85	574	C	5	3	1707448	140.00	141.00	236.90	18.32191			-0.44	-119.40							1.81	1.29	1.960		2.524		10.01	0.03	0.0008		83.17	2.10		6.10	0.15		1M KOH		
85	574	C	5	4	1707453	39.00	40.00	237.39	18.34687			-0.45	-119.37	2077.69		24.67		187.92		1.73	1.16	1.966		2.285		10.24	0.05	0.0011		84.99	1.94		4.80	0.11		1M KOH	0.23	90.07
85	574	C	5	4	1707454	90.00	91.00	237.90	18.37278			-0.45	-119.34							1.81	1.29	1.971		2.538		10.69	0.05	0.0013		88.63	2.25		2.90	0.07		1M KOH		
85	574	C	5	4	1707455	138.00	139.00	238.38	18.39709			-0.46	-119.32							1.69	1.10	1.976		2.173		10.49	0.05	0.0011		87.03	1.89		3.20	0.07		1M KOH		
85	574	C	5	5	1707456	20.00	21.00	238.70	18.41326			-0.47	-119.30							1.71	1.13	2.001		2.263		10.57	0.07	0.0016		87.52	1.98		2.30	0.05		1M KOH		
85	574	C	6	1	1707457	38.00	39.00	242.38	18.59697	18.49	15.00	-0.52	-119.11	1016.16	1956.20	6.17	10.79	258.95	282.04	1.80	1.27	2.006	2.01	2.552	2.48	11.09	0.05	0.0013	0.001209	91.98	2.35	2.22	1.60	0.04	0.06	1M KOH	0.06	93.69
85	574	C	6	1	1707458	90.00	91.00	242.90	18.62258			-0.53	-119.09							1.79	1.26	2.033		2.554		11.19	0.05	0.0013		92.84	2.37		1.50	0.04		1M KOH		
85	574	C	6	1	1707459	140.00	141.00	243.40	18.64713			-0.53	-119.06							1.78	1.24	2.040		2.531		10.92	0.06	0.0015		90.51	2.29		1.50	0.04		1M KOH		
85	574	C	6	2	1707460	38.00	39.00	243.88	18.67063			-0.54	-119.04							1.74	1.18	2.047		2.411		11.26	0.05	0.0012		93.43	2.25		1.20	0.03		1M KOH		
85	574	C	6	2	1707461	91.00	92.00	244.41	18.69648			-0.55	-119.01	1233.97		9.97		386.17		1.83	1.32	2.053		2.708		11.19	0.05	0.0014		92.88	2.52		1.30	0.04		1M KOH	0.09	94.32
85	574	C	6	2	1707462	139.00	140.00	244.89	18.71982			-0.55	-118.99							1.89	1.41	2.060		2.911		11.13	0.06	0.0017		92.27	2.69		1.40	0.04		1M KOH		
85	574	C	6	3	1707463	39.00	40.00	245.39	18.74405			-0.56	-118.96							1.75	1.19	2.067		2.468		11.10	0.04	0.0010		92.10	2.27		1.20	0.03		1M KOH		
85	574	C	6	3	1707464	92.00	93.00	245.92	18.76964			-0.57	-118.94							1.88	1.40	2.074		2.898		11.11	0.04	0.0012		92.25	2.67		1.30	0.04		1M KOH		
85	574	C	6	3	1707465	137.00	138.00	246.37	18.79130			-0.57	-118.91	1758.24		30.25		172.32		1.77	1.22	2.081		2.550		10.64	0.05	0.0013		88.22	2.25		3.50	0.09		1M KOH	0.28	92.05
85	574	C	6	4	1707470	40.00	41.00	246.90	18.81673			-0.58	-118.89							1.72	1.15	2.088		2.394		10.35	0.06	0.0014		85.75	2.05		5.00	0.12		1M KOH		
85	574	C	6	4	1707471	90.00	91.00	247.40	18.84063			-0.59	-118.87	1305.14		21.59		141.67		1.73	1.16	2.095		2.436		10.71	0.06	0.0015		88.84	2.16		4.50	0.11		1M KOH	0.20	93.60
85	574	C	6	4	1707472	140.00	141.00	247.90	18.86445			-0.60	-118.84							1.74	1.18	2.102		2.476		10.78	0.05	0.0012		89.40	2.21		2.90	0.07		1M KOH		
85	574	C	6	5	1707473	34.00	35.00	248.34	18.88534			-0.60	-118.81	1860.49		31.46		169.75		1.74	1.18	2.132		2.512		10.83	0.07	0.0018		89.72	2.25		2.60	0.07		1M KOH	0.29	92.68
85	574	C	7	1	1707821	40.00	41.00	251.90	19.05205	19.02	17.00	-0.66	-118.62		1522.48		33.05		174.59	1.63	1.01	2.139	2.16	2.152	2.48	11.04	0.04	0.0009	0.001226	91.67	1.97	2.20	2.40	0.05	0.10	1M KOH		
85	574	C	7	1	1707822	90.00	91.00	252.40	19.07513			-0.67	-118.59							1.74	1.18	2.170		2.556		11.09	0.05	0.0013		91.97	2.35		2.00	0.05		1M KOH		
85	574	C	7	1	1707823	140.00	141.00	252.90	19.09813			-0.67	-118.56							1.71	1.13	2.178		2.463		10.74	0.05	0.0012		89.09	2.19		2.90	0.07		1M KOH		
85	574	C	7	2	1707826	40.00	41.00	253.40	19.12105			-0.68	-118.54	1359.03		52.46		187.58		1.72	1.15	2.185		2.506		10.42	0.05	0.0013		86.48	2.17		7.20	0.18		1M KOH	0.49	94.22
85	574	C	7	2	1707825	90.00	91.00	253.90	19.14389			-0.69	-118.51							1.76	1.21	2.193		2.652		11.07	0.04	0.0011		91.92	2.44		3.00	0.08		1M KOH		
85	574	C	7	2	1707824	140.00	141.00	254.40	19.16665			-0.70	-118.48							1.72	1.15	2.201		2.524		10.44	0.04	0.0010		86.64	2.19		6.00	0.15		1M KOH		
85	574	C	7	3	1707827	40.00	41.00	254.90	19.18932			-0.71	-118.46							1.71	1.13	2.209		2.498		10.42	0.04	0.0010		86.50	2.16		6.50	0.16		1M KOH		
85	574	C	7	3	1707828	90.00	91.00	255.40	19.21192			-0.71	-118.43	1329.52		29.47		201.65		1.68	1.08	2.216		2.403		10.57	0.04	0.0010		87.75	2.11		4.70	0.11		1M KOH	0.28	92.77
85	574	C	7	3	1707829	140.00	141.00	255.90	19.23444			-0.72	-118.40							1.68	1.08	2.224		2.411		10.49	0.05	0.0012		87.01	2.10		4.50	0.11		1M KOH		
85	574	C	7	4	1707832	40.00	41.00	256.40	19.25688			-0.73	-118.38							1.77	1.22	2.232		2.734		10.70	0.05	0.0014		88.76	2.43		4.50	0.12		1M KOH		
85	574	C	7	4	1707831	90.00	91.00	256.90	19.27924			-0.73	-118.35							1.66	1.05	2.240		2.358		10.65	0.03	0.0007		88.47	2.09		4.10	0.10		1M KOH		
85	574	C	7	4	1707830	140.00	141.00	257.40	19.30153			-0.74	-118.33	1205.01		35.52		227.15		1.66	1.05	2.248		2.366		10.77	0.04	0.0009		89.44	2.12		3.30	0.08		1M KOH	0.33	93.11
85	574	C	7	5	1707833	40.00	41.00	257.90	19.32373			-0.75	-118.30							1.76	1.21	2.255		2.727		10.70	0.04	0.0011		88.83	2.42		4.20	0.11		1M KOH		
85	574	C	7	5	1707834	90.00	91.00	258.40	19.34586			-0.76	-118.27							1.79	1.26	2.263		2.843		10.73	0.05	0.0014		89.04	2.53		4.20	0.12		1M KOH		
85	574	C	7	5	1707835	140.00	141.00	258.90	19.36792			-0.76	-118.25	1531.39		7.95		229.25		1.70	1.12	2.271		2.533		10.52	0.06	0.0015		87.23	2.21		5.50	0.14		1M KOH	0.07	92.86
85	574	C	7	6	1707838	40.00	41.00	259.40	19.38990			-0.77	-118.22							1.76	1.21	2.279		2.756		10.90	0.04	0.0011		90.52	2.49		4.10	0.11		1M KOH		
85	574	C	7	6	1707836	140.00	141.00	260.40	19.43363			-0.79	-118.17							1.72	1.15	2.294		2.631		10.69	0.05	0.0013		88.66	2.33		3.30	0.09		1M KOH		
85	574	C	7	7	1707845	40.00	41.00	260.90	19.45539			-0.79	-118.15	1373.69		23.88		254.20		1.60	0.96	2.302		2.207		10.91	0.06	0.0013		90.43	2.00		3.40	0.08		1M KOH	0.22	94.11
85	574	C	8	1	1707846	40.00	41.00	261.40	19.47708			-0.80	-118.12							1.62	0.99	2.309		2.286		10.81	0.04	0.0009		89.71	2.05		3.40	0.08		1M KOH		
85	574	C	8	1	1707847	90.00	91.00	261.90	19.49870	19.48	21.00	-0.80	-118.10		1902.52		58.81		169.26	1.72	1.15	2.317	2.32	2.657	2.61	10.52	0.05	0.0013	0.001188	87.21	2.32	2.31	4.90	0.13	0.11	1M KOH		
85	574	C	8	1	1707848	140.00	141.00	262.40	19.52024			-0.81	-118.08	3669.03		113.25		119.72		1.71	1.13	2.324		2.629		10.29	0.05	0.0013		85.33	2.24		5.10	0.13		1M KOH	1.06	91.54
85	574	C	8	2	1707851	40.00	41.00	262.90	19.54172			-0.82	-118.06							1.68	1.08	2.332		2.528		10.29	0.05	0.0013		85.37	2.16		5.80	0.15		1M KOH		
85	574	C	8	2	1707850	90.00	91.00	263.40	19.56313			-0.82	-118.04							1.74	1.18	2.339		2.755		10.47	0.04	0.0011		86.96	2.40		4.20	0.12		1M KOH		
85	574	C	8	2	1707849	140.00	141.00	263.90	19.58447			-0.83	-118.02	1621.05		53.47		64.85		1.71	1.13	2.346		2.654		10.59	0.04	0.0011		87.89	2.33		2.60	0.07		1M KOH	0.50	91.03
85	574	C	8	3	1707852	40.00	41.00	264.40	19.60575			-0.83	-118.00							1.70	1.12	2.354		2.625		10.33	0.04	0.0011		85.73	2.25		6.30	0.17		1M KOH		
85	574	C	8	3	1707853	90.00	91.00	264.90	19.62696			-0.84	-117.98	2905.57		118.78		120.36		1.69	1.10	2.361		2.596		10.59	0.04	0.0010		87.85	2.28		4.10	0.11		1M KOH	1.11	93.10
85	574	C	8	3	1707854	140.00	141.00	265.40	19.64811			-0.84	-117.96	1011.91						1.79	1.26	2.367		2.974		11.14	0.04	0.0012		92.49	2.75		2.10	0.06		1M KOH		
85	574	C	8	4	1707895	30.00	31.00	265.80	19.66498			-0.85	-117.95							1.71	1.13	2.404		2.719		10.74	0.06	0.0016		89.03	2.42		2.90	0.08		1M KOH		
85	574	C	9	1	1707896	40.00	41.00	270.90	19.87690			-0.91	-117.74							1.73	1.16	2.410		2.801		10.77	0.04	0.0011		89.37	2.50		3.70	0.10		1M KOH		
85	574	C	9	1	1707897	90.00	91.00	271.40	19.89739			-0.91	-117.73	2263.93		3.61		337.19		1.72	1.15	2.443		2.801		10.71	0.05	0.0014		88.88	2.49		3.00	0.08		1M KOH	0.03	91.96
85	574	C	9	1	1707898	140.00	141.00	271.90	19.91783			-0.92	-117.71							1.65	1.04	2.448		2.539		10.55	0.05	0.0013		87.52	2.22		3.40	0.09		1M KOH		
85	574	C	9	2	1707899	40.00	41.00	272.40	19.93823			-0.92	-117.69	2432.52		75.32		211.83		1.73	1.16	2.454		2.852		10.57	0.04	0.0011		87.73	2.50		4.00	0.11		1M KOH	0.70	92.47
85	574	C	9	2	1707900	90.00	91.00	272.90	19.95859			-0.93	-117.67							1.75	1.19	2.459		2.935		10.21	0.03	0.0009		84.84	2.49		5.30	0.16		1M KOH		
85	574	C	9	2	1707901	140.00	141.00	273.40	19.97891			-0.93	-117.65							1.76	1.21	2.463		2.979		10.23	0.05	0.0015		84.83	2.53		5.50	0.16		1M KOH		
85	574	C	9	3	1707902	40.00	41.00	273.90	19.99919			-0.94	-117.63							1.60	0.96	2.468		2.366		10.26	0.05	0.0012		85.10	2.01		5.00	0.12		1M KOH		
85	574	C	9	3	1707903	90.00	91.00	274.40	20.01943	20.01	10.00	-0.94	-117.61	2779.73	2869.09	81.73	64.38	119.51	198.11	1.70	1.12	2.490	2.46	2.778	2.77	10.25	0.04	0.0011	0.001227	85.06	2.36	2.40	5.10	0.14	0.12	1M KOH	0.76	90.96
85	574	C	10	1	1707904	40.00	41.00	280.40	20.26019			-1.01	-117.38							1.73	1.16	2.493		2.898		10.45	0.05	0.0014		86.63	2.51		4.20	0.12		1M KOH		
85	574	C	10	1	1707905	90.00	91.00	280.90	20.28013			-1.01	-117.36	3123.81		79.48		156.68		1.68	1.08	2.507		2.718		10.28	0.05	0.0014		85.25	2.32		4.50	0.12		1M KOH	0.74	90.54
85	574	C	10	1	1707906	140.00	141.00	281.40	20.30007			-1.02	-117.34							1.70	1.12	2.508		2.798		10.16	0.06	0.0017		84.16	2.35		4.40	0.12		1M KOH		
85	574	C	10	2	1707909	40.00	41.00	281.90	20.32000			-1.02	-117.33							1.63	1.01	2.509		2.523		9.84	0.05	0.0013		81.59	2.06		6.20	0.16		1M KOH		
85	574	C	10	2	1707908	90.00	91.00	282.40	20.33993			-1.03	-117.31	3745.47		81.73		165.36		1.71	1.13	2.509		2.838		10.27	0.06	0.0017		85.12	2.42		5.50	0.16		1M KOH	0.76	91.44
85	574	C	10	2	1707907	140.00	141.00	282.90	20.35985			-1.03	-117.29							1.69	1.10	2.509		2.759		10.06	0.06	0.0017		83.35	2.30		5.60	0.15		1M KOH		
85	574	C	10	3	1707910	40.00	41.00	283.40	20.37978			-1.04	-117.27	3956.68		27.24		219.29		1.73	1.16	2.509		2.916		10.09	0.04	0.0012		83.72	2.44		6.40	0.19		1M KOH	0.25	90.41
85	574	C	10	3	1707911	90.00	91.00	283.90	20.39971			-1.04	-117.26							1.74	1.18	2.508		2.955		10.40	0.04	0.0012		86.32	2.55		4.10	0.12		1M KOH		
85	574	C	10	3	1707912	140.00	141.00	284.40	20.41965			-1.05	-117.24							1.75	1.19	2.508		2.993		10.26	0.04	0.0012		85.14	2.55		4.70	0.14		1M KOH		
85	574	C	10	4	1707915	40.00	41.00	284.90	20.43959			-1.05	-117.22	2084.27		10.48		196.01		1.68	1.08	2.506		2.717		10.70	0.05	0.0014		88.84	2.41		3.80	0.10		1M KOH	0.10	92.79
85	574	C	10	4	1707914	90.00	91.00	285.40	20.45955			-1.06	-117.20							1.80	1.27	2.505		3.186		10.39	0.04	0.0013		86.14	2.74		5.40	0.17		1M KOH		
85	574	C	10	4	1707913	140.00	141.00	285.90	20.47951			-1.06	-117.19							1.73	1.16	2.503		2.909		9.76	0.04	0.0012		80.95	2.36		6.20	0.18		1M KOH		
85	574	C	10	5	1707943	40.00	41.00	286.40	20.49950	20.51	24.00	-1.07	-117.17		2536.56		29.64		160.61	1.79	1.26	2.501	2.49	3.142	2.94	10.07	0.04	0.0013	0.001305	83.62	2.63	2.54	6.10	0.19	0.14	1M KOH		
85	574	C	10	5	1707942	90.00	91.00	286.90	20.51950			-1.07	-117.15	2998.91		19.28		207.06		1.75	1.19	2.499		2.982		10.08	0.04	0.0012		83.64	2.49		6.30	0.19		1M KOH	0.18	90.16
85	574	C	10	5	1707941	140.00	141.00	287.40	20.53952			-1.07	-117.14							1.78	1.24	2.496		3.096		9.79	0.04	0.0012		81.23	2.52		5.10	0.16		1M KOH		
85	574	C	10	6	1707944	40.00	41.00	287.90	20.55956			-1.08	-117.12	1928.49		13.74		186.87		1.78	1.24	2.493		3.093		10.74	0.03	0.0009		89.24	2.76		3.60	0.11		1M KOH	0.13	93.00
85	574	C	10	6	1707945	90.00	91.00	288.40	20.57963			-1.08	-117.10							1.75	1.19	2.490		2.972		10.92	0.03	0.0009		90.71	2.70		2.60	0.08		1M KOH		
85	574	C	10	6	1707946	140.00	141.00	288.90	20.59973			-1.09	-117.08							1.79	1.26	2.486		3.123		10.91	0.03	0.0009		90.62	2.83		3.20	0.10		1M KOH		
85	574	C	10	7	1707959	40.00	41.00	289.40	20.61986			-1.09	-117.07	1616.99		11.44		111.18		1.73	1.16	2.482		2.885		10.78	0.06	0.0017		89.35	2.58		2.90	0.08		1M KOH	0.11	92.42
85	574	C	11	1	1707960	40.00	41.00	289.90	20.64002			-1.10	-117.05	1616.99		11.44		111.18		1.73	1.16	2.478		2.880		10.15	0.06	0.0017		84.12	2.42		6.60	0.19		1M KOH	0.11	90.89
85	574	C	11	1	1707961	90.00	91.00	290.40	20.66022			-1.10	-117.03							1.77	1.22	2.473		3.030		11.07	0.04	0.0012		91.88	2.78		2.80	0.08		1M KOH		
85	574	C	11	1	1707962	140.00	141.00	290.90	20.68045			-1.11	-117.01							1.82	1.30	2.468		3.217		10.37	0.06	0.0019		85.95	2.76		4.60	0.15		1M KOH		
85	574	C	11	2	1707967	40.00	41.00	291.40	20.70073			-1.11	-117.00							1.77	1.22	2.463		3.017		10.93	0.03	0.0009		90.80	2.74		3.40	0.10		1M KOH		
85	574	C	11	2	1707966	90.00	91.00	291.90	20.72105			-1.12	-116.98	1757.49		11.95		91.89		1.81	1.29	2.458		3.165		11.03	0.04	0.0013		91.59	2.90		3.60	0.11		1M KOH	0.11	95.34
85	574	C	11	2	1707965	140.00	141.00	292.40	20.74141			-1.12	-116.96							1.70	1.12	2.452		2.735		10.42	0.04	0.0011		86.51	2.37		4.20	0.11		1M KOH		
85	574	C	11	3	1707968	40.00	41.00	292.90	20.76183			-1.13	-116.94							1.74	1.18	2.446		2.881		10.34	0.04	0.0012		85.86	2.47		4.40	0.13		1M KOH		
85	574	C	11	3	1707969	90.00	91.00	293.40	20.78229			-1.13	-116.93							1.80	1.27	2.440		3.103		10.62	0.04	0.0012		88.15	2.74		3.50	0.11		1M KOH		
85	574	C	11	3	1707970	140.00	141.00	293.90	20.80281			-1.14	-116.91	1251.08						1.78	1.24	2.394		2.970		11.13	0.04	0.0012		92.37	2.74		2.00	0.06		1M KOH		

Leg	Site	Hole	Core	Section	Sample ID	Interval Top (cm)	Interval Bottom (cm)	mbsf Top	Age Ma: 9th Degree Polynomial	Binned Average Age: 0.5 My Increments	*n (Samples per Interval)*	Paleo LAT°N	Paleo LONG°E	Ba [ug/g]	Avg. Ba [ug/g]: Binned Interval	Th [ng/g]	Avg. Th [ng/g]: Binned Interval	U [ng/g]	Avg. U [ng/g]: Binned Interval	Wet Bulk Density g/cc	Dry Bulk Density g/cc	LSR [cm/kyr]	Avg LSR: Binned Interval	MAR [g/(cm2 *kyr)]	Avg MAR: Binned Interval	Avg. Total-Carbon Wt%	Corg Wt%	Corg MAR	Avg Corg MAR: Binned Interval	CaCO3 Wt%	CaCO3 MAR	Avg CaCO3 MAR: Binned Interval	Avg Bio-SiO2 Wt%	Bio-SiO2 MAR	Avg Bio-SiO2 MAR: Binned Interval	Bio-SiO2 Notes	Dust Wt% [Th/10.7]	Sum of Major Sediment Components Wt%
85	574	C	12	1	1707976	40.00	41.00	299.40	21.03289	21.06	14.00	-1.19	-116.71		1452.41		11.95		91.89	1.74	1.18	2.386	2.32	2.811	2.88	10.84	0.03	0.0008	0.001115	90.08	2.53	2.57	2.30	0.06	0.10	1M KOH		
85	574	C	12	1	1707975	90.00	91.00	299.90	21.05427			-1.20	-116.69							1.80	1.27	2.333		2.968		10.86	0.04	0.0012		90.20	2.68		2.30	0.07		1M KOH		
85	574	C	12	1	1707974	140.00	141.00	300.40	21.07574			-1.20	-116.67	1401.91						1.75	1.19	2.324		2.774		10.75	0.04	0.0011		89.23	2.47		2.90	0.08		1M KOH		
85	574	C	12	2	1707977	40.00	41.00	300.90	21.09731			-1.21	-116.65							1.79	1.26	2.314		2.906		10.88	0.05	0.0015		90.29	2.62		2.60	0.08		1M KOH		
85	574	C	12	2	1707978	90.00	91.00	301.40	21.11897			-1.21	-116.64							1.86	1.37	2.303		3.146		10.89	0.04	0.0013		90.38	2.84		2.70	0.08		1M KOH		
85	574	C	12	2	1707979	140.00	141.00	301.90	21.14072			-1.22	-116.63							1.80	1.27	2.293		2.916		10.75	0.04	0.0012		89.21	2.60		2.50	0.07		1M KOH		
85	574	C	12	3	1707989	40.00	41.00	302.40	21.16258			-1.22	-116.61							1.83	1.32	2.282		3.010		11.05	0.04	0.0012		91.79	2.76		2.10	0.06		1M KOH		
85	574	C	12	3	1707988	90.00	91.00	302.90	21.18454			-1.22	-116.60							1.74	1.18	2.271		2.676		11.01	0.02	0.0005		91.53	2.45		2.80	0.07		1M KOH		
85	574	C	12	3	1707987	140.00	141.00	303.40	21.20661			-1.23	-116.59	1222.89						1.82	1.30	2.260		2.946		11.11	0.04	0.0012		92.25	2.72		2.10	0.06		1M KOH		
85	574	C	12	4	1707990	40.00	41.00	303.90	21.22878			-1.23	-116.58	1628.70						1.69	1.10	2.249		2.473		9.32	0.04	0.0010		77.29	1.91		12.60	0.31		1M KOH		
85	574	C	12	4	1707991	90.00	91.00	304.40	21.25107			-1.23	-116.57							1.77	1.22	2.238		2.741		10.89	0.04	0.0011		90.42	2.48		3.00	0.08		1M KOH		
85	574	C	12	4	1707992	140.00	141.00	304.90	21.27347			-1.24	-116.56	1219.57						1.79	1.26	2.226		2.797		10.94	0.05	0.0014		90.80	2.54		2.30	0.06		1M KOH		
85	574	C	12	5	1707995	40.00	41.00	305.40	21.29598			-1.24	-116.54	1742.58						1.80	1.27	2.215		2.817		10.72	0.04	0.0011		88.98	2.51		2.10	0.06		1M KOH		
85	574	C	12	5	1707994	90.00	91.00	305.90	21.31862			-1.24	-116.53	1362.19		27.05				1.85	1.35	2.203		2.974		10.80	0.04	0.0012		89.68	2.67		3.50	0.10		1M KOH	0.25	93.47
85	574	C	12	5	1707993	140.00	141.00	306.40	21.34138			-1.25	-116.52							1.83	1.32	2.191		2.890		11.00	0.04	0.0012		91.35	2.64		3.80	0.11		1M KOH		
85	574	C	12	6	1707996	40.00	41.00	306.90	21.36426			-1.25	-116.51							1.83	1.32	2.179		2.874		11.27	0.04	0.0011		93.57	2.69		1.90	0.05		1M KOH		
85	574	C	12	6	1707997	90.00	91.00	307.40	21.38727			-1.25	-116.50							1.83	1.32	2.167		2.858		11.13	0.04	0.0011		92.45	2.64		2.30	0.07		1M KOH		
85	574	C	12	6	1707998	140.00	141.00	307.90	21.41040			-1.26	-116.48	743.11						1.93	1.48	2.156		3.181		11.35	0.03	0.0010		94.34	3.00		1.30	0.04		1M KOH		
85	574	C	12	7	1708295	33.00	34.00	308.33	21.43041			-1.26	-116.47							1.71	1.13	2.143		2.423		11.18	0.05	0.0012		92.70	2.25		2.70	0.07		1M KOH		
85	574	C	13	1	1708296	40.00	41.00	308.90	21.45708			-1.26	-116.46							1.76	1.21	2.131		2.577		11.01	0.05	0.0013		91.33	2.35		2.80	0.07		1M KOH		
85	574	C	13	1	1708297	90.00	91.00	309.40	21.48062			-1.27	-116.45							1.77	1.22	2.118		2.594		10.93	0.05	0.0013		90.66	2.35		3.10	0.08		1M KOH		
85	574	C	13	1	1708298	140.00	141.00	309.90	21.50430	21.49	22.00	-1.27	-116.43	1087.80	1333.34		27.05		0.00	1.77	1.22	2.105	2.10	2.579	2.71	11.29	0.04	0.0010	0.001167	93.72	2.42	2.49	2.00	0.05	0.07	1M KOH		
85	574	C	13	2	1708304	40.00	41.00	310.40	21.52812			-1.27	-116.42							1.89	1.41	2.092		2.956		11.20	0.04	0.0012		92.95	2.75		2.30	0.07		1M KOH		
85	574	C	13	2	1708305	90.00	91.00	310.90	21.55209			-1.28	-116.41							1.82	1.30	2.080		2.710		11.10	0.04	0.0011		92.14	2.50		3.10	0.08		1M KOH		
85	574	C	13	2	1708306	140.00	141.00	311.40	21.57620			-1.28	-116.40							1.74	1.18	2.067		2.435		11.15	0.04	0.0010		92.52	2.25		2.20	0.05		1M KOH		
85	574	C	13	3	1708310	40.00	41.00	311.90	21.60047			-1.28	-116.38	1341.75						1.76	1.21	2.054		2.484		11.28	0.03	0.0007		93.83	2.33		1.80	0.04		1M KOH		
85	574	C	13	3	1708311	90.00	91.00	312.40	21.62488			-1.29	-116.37							1.82	1.30	2.041		2.660		11.21	0.05	0.0013		92.94	2.47		1.70	0.05		1M KOH		
85	574	C	13	3	1708312	140.00	141.00	312.90	21.64945			-1.29	-116.36							1.88	1.40	2.029		2.834		11.04	0.04	0.0011		91.69	2.60		1.60	0.05		1M KOH		
85	574	C	13	4	1708313	40.00	41.00	313.40	21.67418			-1.29	-116.34							1.81	1.29	2.016		2.595		11.20	0.04	0.0010		92.99	2.41		1.70	0.04		1M KOH		
85	574	C	13	4	1708314	90.00	91.00	313.90	21.69906			-1.30	-116.33	1836.41						1.90	1.43	2.003		2.862		11.17	0.04	0.0011		92.71	2.65		1.50	0.04		1M KOH		
85	574	C	13	4	1708315	137.00	138.00	314.37	21.72260			-1.30	-116.32							1.78	1.24	1.991		2.470		11.01	0.06	0.0015		91.30	2.25		2.60	0.06		1M KOH		
85	574	C	13	5	1708320	35.00	36.00	314.85	21.74679			-1.30	-116.31							1.78	1.24	1.938		2.405		10.10	0.06	0.0014		83.63	2.01		6.50	0.16		1M KOH		
85	574	C	14	1	1708323	40.00	41.00	318.40	21.93051			-1.33	-116.21							1.92	1.46	1.926		2.811		11.13	0.06	0.0017		92.28	2.59		2.10	0.06		1M KOH		
85	574	C	14	1	1708324	90.00	91.00	318.90	21.95710			-1.33	-116.20	1673.98						1.78	1.24	1.874		2.325		10.40	0.05	0.0012		86.24	2.01		4.00	0.09		1M KOH		
85	574	C	14	1	1708325	140.00	141.00	319.40	21.98386			-1.34	-116.18							1.78	1.24	1.862		2.309		10.67	0.07	0.0016		88.33	2.04		4.90	0.11		1M KOH		
85	574	C	14	2	1708328	40.00	41.00	319.90	22.01082	21.98	8.00	-1.34	-116.17		2743.48					1.66	1.05	1.849	1.84	1.946	2.21	10.15	0.04	0.0008	0.001207	84.29	1.64	1.95	7.60	0.15	0.09	1M KOH		
85	574	C	14	2	1708329	90.00	91.00	320.40	22.03795			-1.35	-116.15							1.76	1.21	1.836		2.221		10.77	0.04	0.0009		89.46	1.99		3.80	0.08		1M KOH		
85	574	C	14	2	1708330	140.00	141.00	320.90	22.06527			-1.35	-116.14	3812.97						1.68	1.08	1.824		1.978		10.09	0.06	0.0012		83.59	1.65		6.10	0.12		1M KOH		
85	574	C	15	1	1708337	40.00	41.00	327.90	22.46820			-1.41	-115.93							1.76	1.21	1.725		2.087		10.96	0.05	0.0010		90.94	1.90		2.20	0.05		1M KOH		
85	574	C	15	1	1708338	94.00	95.00	328.44	22.50092	22.61	10.00	-1.41	-115.91	1572.40	2147.00	34.91	34.69	126.94	133.82	1.76	1.21	1.645	1.61	1.989	1.98	11.23	0.03	0.0006	0.000895	93.30	1.86	1.80	2.20	0.04	0.05	1M KOH	0.33	95.86
85	574	C	15	1	1708339	140.00	141.00	328.90	22.52898			-1.42	-115.89							1.82	1.30	1.633		2.129		10.95	0.05	0.0011		90.82	1.93		2.20	0.05		1M KOH		
85	574	C	15	2	1708340	42.00	43.00	329.42	22.56092			-1.42	-115.88							1.77	1.22	1.623		1.988		10.90	0.05	0.0010		90.43	1.80		2.80	0.06		1M KOH		
85	574	C	15	2	1708341	90.00	91.00	329.90	22.59060			-1.42	-115.86							1.72	1.15	1.612		1.848		10.97	0.04	0.0007		91.02	1.68		2.30	0.04		1M KOH		
85	574	C	15	2	1708342	140.00	141.00	330.40	22.62172			-1.43	-115.85	1521.98		37.11		143.54		1.76	1.21	1.601		1.936		10.90	0.05	0.0010		90.42	1.75		2.80	0.05		1M KOH	0.35	93.62
85	574	C	15	3	1708343	40.00	41.00	330.90	22.65305			-1.43	-115.84							1.77	1.22	1.591		1.948		10.96	0.05	0.0010		90.93	1.77		2.00	0.04		1M KOH		
85	574	C	15	3	1708344	90.00	91.00	331.40	22.68459			-1.43	-115.82							1.79	1.26	1.580		1.985		10.78	0.04	0.0008		89.43	1.78		2.30	0.05		1M KOH		
85	574	C	15	3	1708345	140.00	141.00	331.90	22.71634			-1.44	-115.81							1.80	1.27	1.570		1.996		10.63	0.05	0.0010		88.21	1.76		3.50	0.07		1M KOH		
85	574	C	15	4	1708346	40.00	41.00	332.40	22.74830			-1.44	-115.80	1680.65		32.04		130.97		1.78	1.24	1.559		1.934		10.99	0.04	0.0008		91.24	1.77		2.60	0.05		1M KOH	0.30	94.18
85	574	C	15	4	1708347	90.00	91.00	332.90	22.78047			-1.44	-115.78							1.68	1.08	1.549		1.679		10.84	0.04	0.0007		89.96	1.51		2.60	0.04		1M KOH		
85	574	C	15	4	1708348	140.00	141.00	333.40	22.81285			-1.45	-115.77							1.80	1.27	1.538		1.956		11.02	0.05	0.0010		91.46	1.79		2.40	0.05		1M KOH		
85	574	C	15	5	1708349	50.00	51.00	334.00	22.85198			-1.45	-115.75							1.80	1.27	1.529		1.945		10.94	0.05	0.0010		90.78	1.77		2.70	0.05		1M KOH		
85	574	C	15	5	1708350	90.00	91.00	334.40	22.87824			-1.46	-115.74	1043.22						1.81	1.29	1.518		1.955		10.93	0.04	0.0008		90.77	1.77		2.10	0.04		1M KOH		
85	574	C	15	5	1708351	140.00	141.00	334.90	22.91126			-1.46	-115.73							1.81	1.29	1.510		1.944		11.11	0.04	0.0008		92.21	1.79		2.50	0.05		1M KOH		
85	574	C	15	6	1708352	40.00	41.00	335.40	22.94448			-1.46	-115.71							1.77	1.22	1.499		1.836		11.09	0.04	0.0007		92.06	1.69		3.00	0.06		1M KOH		
85	574	C	15	6	1708353	105.00	106.00	336.05	22.98799			-1.47	-115.69							1.80	1.27	1.491		1.896		11.08	0.03	0.0006		92.16	1.75		2.30	0.04		1M KOH		
85	574	C	15	6	1708354	140.00	141.00	336.40	23.01156	23.00	16.00	-1.47	-115.68	1022.77	2257.53	25.68	55.21	130.48	114.11	1.55	0.88	1.481	1.48	1.304	1.73	10.84	0.05	0.0007	0.000737	89.93	1.17	1.56	2.50	0.03	0.05	1M KOH	0.24	92.72
85	574	C	15	7	1708355	30.00	31.00	336.80	23.03863			-1.47	-115.67							1.60	0.96	1.472		1.412		11.00	0.05	0.0007		91.28	1.29		1.90	0.03		1M KOH		
85	574	C	16	1	1708356	40.00	41.00	337.40	23.07949			-1.48	-115.66							1.76	1.21	1.464		1.771		11.06	0.05	0.0009		91.76	1.62		2.30	0.04		1M KOH		
85	574	C	16	1	1708357	90.00	91.00	337.90	23.11376			-1.48	-115.64	3485.94		82.29		97.18		1.74	1.18	1.454		1.713		10.63	0.05	0.0009		88.22	1.51		3.40	0.06		1M KOH	0.77	92.44
85	574	C	16	1	1708358	140.00	141.00	338.40	23.14824			-1.49	-115.63							1.75	1.19	1.446		1.726		10.69	0.04	0.0007		88.75	1.53		3.30	0.06		1M KOH		
85	574	C	16	2	1708359	40.00	41.00	338.90	23.18293			-1.49	-115.61							1.71	1.13	1.437		1.625		10.52	0.04	0.0007		87.26	1.42		n/a	n/a		1M KOH		
85	574	C	16	2	1708360	90.00	91.00	339.40	23.21783			-1.50	-115.60							1.72	1.15	1.429		1.638		10.38	0.04	0.0007		86.16	1.41		4.70	0.08		1M KOH		
85	574	C	16	2	1708361	137.00	138.00	339.87	23.25082			-1.50	-115.58	4055.10		80.84		97.82		1.71	1.13	1.420		1.606		10.44	0.03	0.0005		86.78	1.39		4.10	0.07		1M KOH	0.76	91.67
85	574	C	16	3	1708362	40.00	41.00	340.40	23.28824			-1.50	-115.57							1.68	1.08	1.412		1.531		9.73	0.04	0.0006		80.73	1.24		8.00	0.12		1M KOH		
85	574	C	16	3	1708363	90.00	91.00	340.90	23.32376			-1.51	-115.55							1.73	1.16	1.404		1.632		10.25	0.04	0.0007		85.09	1.39		3.90	0.06		1M KOH		
85	574	C	16	3	1708364	140.00	141.00	341.40	23.35947			-1.51	-115.54							1.78	1.24	1.396		1.732		9.85	0.03	0.0005		81.81	1.42		6.50	0.11		1M KOH		
85	574	C	16	4	1708365	34.00	35.00	341.84	23.39107	23.40	6.00	-1.52	-115.52	3818.18	3936.64	88.11	84.47	79.46	88.64	1.74	1.18	1.355	1.39	1.596	1.66	10.11	0.05	0.0008	0.000664	83.85	1.34	1.40	5.90	0.09	0.09	1M KOH	0.82	90.62
85	574	C	17	1	1708366	40.00	41.00	346.90	23.76535			-1.56	-115.36							1.86	1.37	1.348		1.842		10.67	0.05	0.0009		88.52	1.63		3.60	0.07		1M KOH		
85	574	C	17	1	1708367	90.00	91.00	347.40	23.80338			-1.56	-115.35							1.81	1.29	1.312		1.689		11.00	0.04	0.0007		91.36	1.54		2.20	0.04		1M KOH		
85	574	C	17	1	1708368	140.00	141.00	347.90	23.84160			-1.57	-115.33							1.79	1.26	1.305		1.640		10.88	0.04	0.0007		90.31	1.48		2.20	0.04		1M KOH		
85	574	C	17	2	1708369	40.00	41.00	348.40	23.87999			-1.57	-115.31							1.79	1.26	1.299		1.632		10.61	0.04	0.0007		88.12	1.44		3.60	0.06		1M KOH		
85	574	C	17	2	1708370	90.00	92.00	348.90	23.91856			-1.58	-115.30							1.82	1.30	1.294		1.686		10.61	0.04	0.0007		88.11	1.49		3.30	0.06		1M KOH		
85	574	C	17	2	1708371	140.00	141.00	349.40	23.95730			-1.58	-115.28	3017.20		40.09		78.56		1.83	1.32	1.288		1.698		10.52	0.04	0.0007		87.36	1.48		3.80	0.06		1M KOH	0.37	91.57
85	574	C	17	3	1708372	40.00	41.00	349.90	23.99621	24.02	14.00	-1.58	-115.26		3164.11		48.70		77.83	1.82	1.30	1.282		1.671		10.38	0.03	0.0005		86.24	1.44		4.00	0.07		1M KOH		
85	574	C	17	3	1708373	90.00	91.00	350.40	24.03529			-1.59	-115.25	3017.20		40.09		78.56		1.74	1.18	1.277	1.30	1.504	1.64	10.46	0.03	0.0005	0.000624	86.88	1.31	1.43	4.60	0.07	0.06	1M KOH	0.37	91.88
85	574	C	17	3	1708374	140.00	141.00	350.90	24.07453			-1.59	-115.23							1.78	1.24	1.271		1.577		10.31	0.04	0.0006		85.57	1.35		4.70	0.07		1M KOH		
85	574	C	17	4	1708375	40.00	41.00	351.40	24.11394			-1.60	-115.21							1.76	1.21	1.266		1.531		9.91	0.04	0.0006		82.23	1.26		5.70	0.09		1M KOH		
85	574	C	17	4	1708376	90.00	91.00	351.90	24.15350			-1.60	-115.20							1.70	1.12	1.261		1.407		10.18	0.03	0.0004		84.58	1.19		4.60	0.06		1M KOH		
85	574	C	17	4	1708377	140.00	141.00	352.40	24.19322			-1.61	-115.18	4173.64		81.58		88.10		1.79	1.26	1.256		1.578		10.30	0.03	0.0005		85.61	1.35		4.20	0.07		1M KOH	0.76	90.60
85	574	C	17	5	1708378	40.00	41.00	352.90	24.23309			-1.61	-115.16							1.76	1.21	1.252		1.514		10.39	0.04	0.0006		86.28	1.31		3.80	0.06		1M KOH		
85	574	C	17	5	1708379	90.00	91.00	353.40	24.27311			-1.62	-115.15	2448.40		33.04		66.07		1.85	1.35	1.456		1.966		10.69	0.04	0.0008		88.78	1.75		2.50	0.05		1M KOH	0.31	91.63

VITA

Name: Christine Marie Piela

Address: Department of Oceanography
MS 3146, Texas A&M University
College Station, Texas 77843-3146

Email Address: Leucas104@neo.tamu.edu

Education: B.S., Marine Science/Geology, The University of Miami, 2008
M.S., Geologic Oceanography, Texas A&M University, 2010